Title

THE THEORETICAL ANALYSIS OF NUCLEAR REACTIONS INVOLVING STRONGLY DEFORMED NUCLEI USING PHENOMENOLOGICAL MODELS

Author

Mackintosh, Raymond Stuart.

Publication Date

1970-03-01

UCRL-19529

c.2

THE THEORETICAL ANALYSIS OF NUCLEAR REACTIONS INVOLVING STRONGLY DEFORMED NUCLEI USING PHENOMENOLOGICAL MODELS

Raymond Stuart Mackintosh
(Ph. D. Thesis)

March 1970

AEC Contract No. W-7405-eng-48

LAWRENCE RADIATION LABORATORY
UNIVERSITY of CALIFORNIA BERKELEY

UCRL-19529

DISCLAIMER

Contents

The Theoretical Analysis of Nuclear Reactions Involving Strongly Deformed Nuclei Using Phenomenological Models

Raymond Stuart Mackintosh

Lawrence Radiation Laboratory
University of California
Berkeley, California

ABSTRACT

Stripping reactions, A(d,p) A+1, are studied for the case where A is a strongly deformed nucleus. In the standard treatment, using DWBA, the possibility that the projectiles d and p can set the nucleus in rotational motion is ignored. We have studied in detail the importance of these inelastic processes using the coupled channel source-term technique of Ascuitto and Glendenning. We have shown this to be equivalent to the coupled channel Born Approximation written down by Penny and Satchler. We have also generalized a formal derivation of DWBA given by Greider and Dodd. We have discovered that for A$\sim$25 and for 10 and 12 MeV deuterons, inelastic processes are of vital importance -- that relative strengths of levels may be greatly changed by their inclusion and that angular distributions may be significantly improved, although the detailed shape is still not reproduced for these light nuclei. This latter failing, therefore, seems to be characteristic of any generalization for zero range DWBA to include

rotational excitations. For 12 MeV deuterons in the deformed rare earth region, the inclusion of inelastic processes will, in general, lead to substantial differences in values, extracted by comparison with experiment, of the amplitudes with which particular angular momenta occur in the various Nilsson states. Angular distributions of weaker levels in a band are often changed substantially and the change in stripping strengths of various levels is quite comparable to that which is a result of coriolis mixing (not included in our calculations). Our calculations involve purely macroscopic rotational excitations and we further ignore transitions between members of different bands of the odd A residual nucleus.

I. INTRODUCTION

The usefulness of the deuteron stripping reaction

$$d + A \longrightarrow p + (A+1)$$

treated as a direct reaction is well established as a source of spectroscopic information. In particular, it has proven very useful[1] in elucidating the complex energy level structure of odd strongly deformed nuclei, an application which is the subject of the present work.

The level structure of the odd-A residual nuclei can often be resolved into a sometimes quite striking array of rotational bands, each based on a particular deformed intrinsic state. Each intrinsic single particle state is characterized by a set of amplitudes c_{jl} corresponding to angular momentum j.

In the customary treatment of stripping reactions, the stripping takes place without pre-excitation of the target nucleus by the deuteron, and without coupling between states of the residual nucleus induced by the interaction with the outgoing proton. In this case, for even target nuclei (spin zero), as was first pointed out by Satchler,[2] the excitation of a state of spin I of a given band can proceed only through the component of the intrinsic state of angular momentum I (amplitude c_{Il}), because the neutron must carry all the angular momentum transferred in the reaction. The cross section thus factors:

$$\sigma_I(\theta) \propto C_{Il}^2 \sigma_l(\theta) \qquad (2)$$

The cross sections for transitions to the various members of the band measure the amplitudes of the angular momenta that occur in the single particule state on which the band is built. Furthermore, as $\sigma_l(\theta)$ is independent of nuclear structure, eq(2) can be used to study and compare different bands in different nuclei -- perhaps to estimate quasiparticle occupation factors (U_ν^2) for the deformed single particle states. If the c_{jl} values for a given band are considered known, the band based on this intrinsic state can be identified by the characteristic pattern of stripping cross sections of its various members and traced from nucleus to nucleus throughout the deformed region. These reactions are reviewed somewhat more fully in Chapter VIII, section B.

It is important that bands can be unambiguously identified by the pattern of the intensities of the band members, and that c^2 can be reliably extracted from experiments. However, the collectivity of strongly deformed nuclei may invalidate eq(2).

The rotational states are coupled strongly by the interaction of a projectile with the deformation of the nuclear field, sufficiently strongly, in fact, for the higher order processes to be important in inelastic scattering. This is the motivation for the present work in which we study the extent to which

inelastic processes, i.e. pre-excitation and post excitation of rotational levels of the target and residual nuclei, invalidate or modify band identifications and c^2 measurements based on the no-scattering factorization, eq(2).

Although we use coupled channel techniques entirely, our calculation will be the equivalent of calculating an approximation to the true transition matrix T of the reaction, in the following form:

$$T_{model} \propto \langle \text{outgoing wave} | V_{int} | \text{incoming wave} \rangle \qquad (3)$$

As far as the stripping interaction, V_{int}, is concerned, this expression has the form of the first order term of a perturbation (Born) series. In the past, this form has been employed with the incoming and outgoing waves calculated according to a hierarchy of approximations: plane wave Born approximations (PWBA), coulomb wave approximations, distorted wave Born approximation (DWBA). For the case of rearrangement collisions, the next approximation, still with V_{int} taken to first order, is that employed herein: the coupled channel Born approximation, CCBA. In this, the entrance channel wavefunction contains not only the elastic channel components (as in DWBA; for an illustrated example, see the appendix to this chapter) but also components corresponding to target states excited by the deuteron before the stripping interaction takes place. Likewise, the outgoing wave is calculated with the states of the residual nucleus coupled together by the interaction between the proton

and the A+1 particles. In each case, the wavefunctions are calculated by means of the (infinite order) coupled channel method using purely macroscopic excitation. These will be modified not only by the inclusion of inelastic channels, but the elastic channel components will be modified by virtue of the change required for the optical potential and by the scattering back into this channel. In our calculations we ignore coupling between different bands of the residual nucleus on the grounds that the corresponding single particle transition is much weaker than the intraband collective transitions.

Any reaction on a complex nucleus is a many body problem which is, in a real sense, nonsolvable. Of course, we do perform calculations and obtain numbers that can be compared with experiments, and our scheme must be justified to the extent that it <u>works;</u> the difference between working and seeming to work is not always obvious, and the importance of the many approximations that remain is not entirely clear. Our replacement of the many body nuclear field by a one body local optical potential is only partially mitigated by the explicit inclusion of the strongly coupled nuclear states (excited by means of a deformation of this field) as far as our calculation of the projectile wavefunctions in the interaction region is concerned. The effect of the non-rigorous treatment of rearrangement processes, and the closely related problem of the neglect of other partitions is still largely unknown, although estimates

have been made of specific aspects of this: inclusion of the stripping interaction to higher order and the polarization of the deuteron. The customary zero range approximation which facilitates the calculation of certain integrals and which we use, is on a different footing and the extent of its validity is fairly well known. To sum up: this work is directed to the study of a single physical process that can affect the stripping reaction - the excitation of particularly strongly excited states of the target and residual nucleus; otherwise we make standard approximations.

The initial aim of this work was simply to discover how important these processes are and thus establish the validity of the many analyses of experimental data that have been made without regard to them. However, we demonstrate how, in some cases studied, spectroscopic information may be obtained. For a further discussion of the general procedure and of the importance of this work, see the last part of Chapter II.

We have discussed the various aspects of this work in turn and tie the threads together at the end according to the following scheme.

Mindful, in the first place, that we are studying a stripping reaction, we present in Chapter II the customary definitions and results of stripping theory that we shall draw upon later. We shall discuss the effects of the approximations that we have made that relate specifically to the stripping aspects of

the problem. We discuss in more detail the overall approach that is required to fully delineate the influence of inelastic processes on stripping reactions, and we shall give an account of the effects we expect to see.

In Chapter III we give a formal derivation of the CCBA.

The calculation of the nuclear wavefunction is discussed in Chapter IV together with an analysis of the various nuclides treated and tabulations of the wavefunctions employed. We shall show that a correct calculation of the bound neutron wavefunction is of more importance than is sometimes assumed. In this work we ignore coriolis mixing.

In Chapter V the formal results of Chapter III are expressed in coupled channel form adaptable to a numerical procedure which is briefly indicated. We discuss here the inelastic scattering of the deuterons and protons in model independent terms.

In Chapter VI the various interaction matrices which enter the scattering and stripping problems are evaluated in terms of the particular models used. In section D, we show how selection rules that apply to direct processes may be broken in the presence of inelastic transitions.

The procedure required to obtain the "correct" optical potential is discussed in Chapter VII together with a tabulation of the various optical potentials used.

The stripping calculations are presented and discussed in

Chapter VIII. Section B of this chapter also contains a brief review of stripping spectroscopy in the rare earth region.

Finally we discuss our conclusions in Chapter IX and discuss what we feel to be important experiments that should be carried out.

Previous discussions of various aspects of the method used herein have been presented by a number of authors.[3,4] The work of Ascuitto and Glendenning[4] introduced the source term approach to stripping.

Appendix

Deuteron Stripping on Magnesium: an Example

As an example of the physical processes which are included in our stripping calculations, we consider $^{24}Mg(d,p)^{25}Mg$ as illustrated in fig. I.1. The spectrum of ^{25}Mg is given in Chapter IV. As we ignore inter-band coupling in the product nucleus, we need show only one band, for example, the [211] 1/2+ band. The j=7/2+ component of the [211] 1/2+ state is zero as Nilsson calculates it (for a full discussion, see Chapter IV), but there will be small amplitudes present. The direct stripping amplitude to the 7/2+ level is very small in any case. The vertical arrows, up and down, signify the coupled-channel-calculated inelastic scattering. The more or less horizontal arrows, in one direction only, represent the stripping interaction which acts to first order. We note that there are amplitudes that lead to state Z which involve only one scattering. One of these $A \rightarrow W \rightarrow Z$ will be smaller than the others as the transition $W \rightarrow Z$ is not excited by a Y_2 deformation. Thus the stripping amplitude of state Z can be considered to be the sum, to first order in inelastic processes, of three amplitudes, and we shall find that they are comparable in magnitude. It is clear why the cross section for a state such as W,X,Y, or Z is no longer linear in c_W^2 etc., for <u>each</u> state depends on c^2 for <u>every</u> state to an extent that varies with the importance of the

inelastic processes.

Figure Captions for Chapter I

Fig. I.1 Stripping on ^{24}Mg. Illustrating the multiplicity of amplitudes which add coherently to give the total amplitude for state W,X,Y, or Z when inelastic scattering (vertical lines) is permitted among the states of the target and final nuclei. The double lines denote the DWBA paths. The DWBA amplitude for state Z is small enough to describe Z as "forbidden in DWBA."

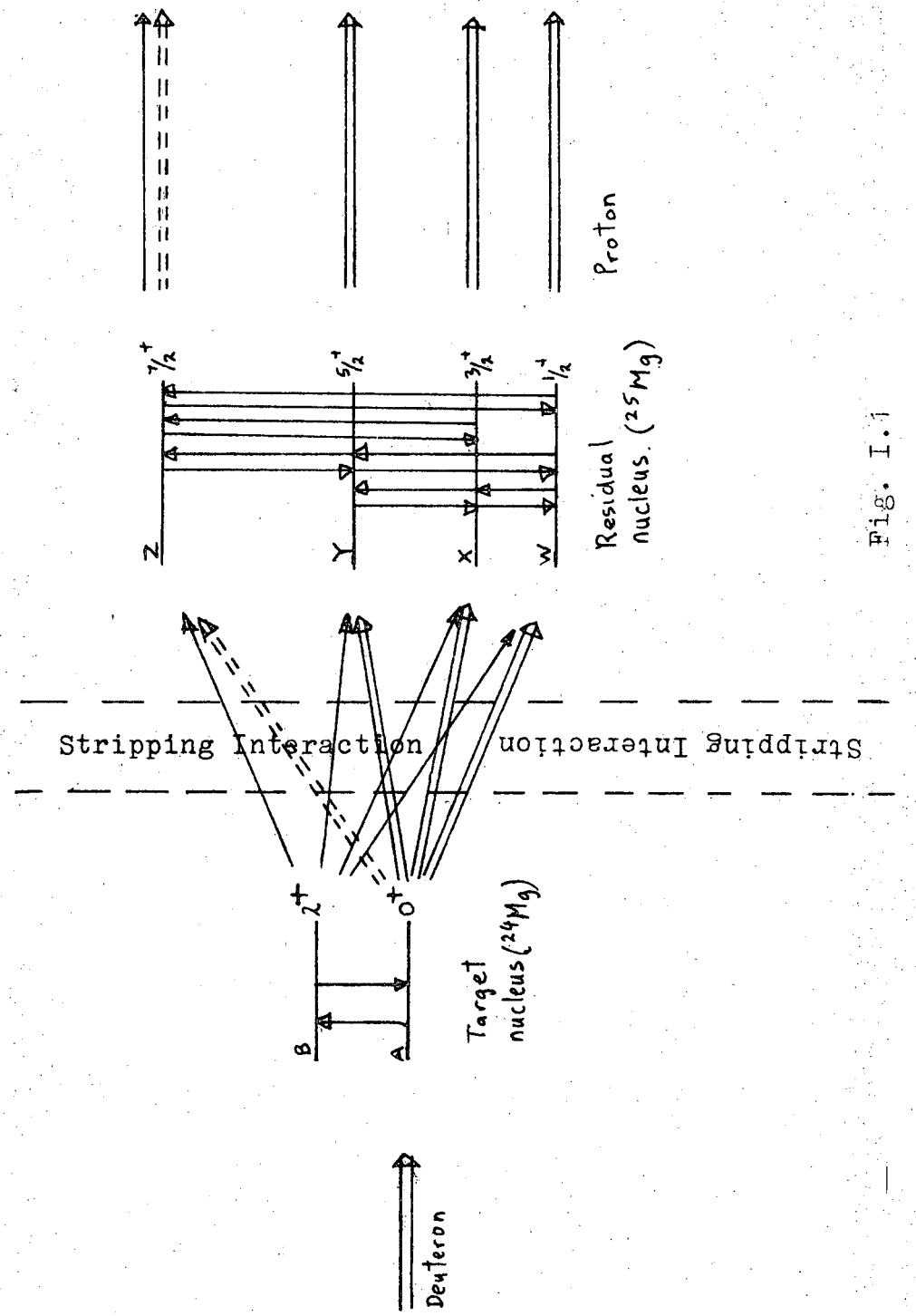
Proton
7/2+
5/2+
3/2+
1/2+
Z
Y
X
W
Residual nucleus. (25Mg)
Stripping Interaction
2+
0+
B
A
Target nucleus (24Mg)
Deuteron

Fig. I.1

II. STRIPPING REACTIONS

In the following, we give a brief account of the general properties of stripping reactions, and certain standard results and definitions will be given drawing in part on the review articles[5,6]. Many of the approximations which we make are shared with usual DWBA approach and are of quite well known ranges of validity. This is relevant if we wish to consider our study as more than a series of model calculations.

We then discuss the use of DWBA for light nuclei and find that it cannot be counted on to give good angular distributions for magnesium.

A consistent procedure is then set forth for studying the role of inelastic processes, and finally the earlier discussion is called upon in an expansion of the brief account given in the Introduction of the possible importance of inelastic processes.

A. Stripping Theory Definitions

The reaction under consideration is $d + A \longrightarrow p + (A+1)$. We treat it as a direct reaction, in other words, one that takes place in the short time characterizing the transit of a nucleon. This raises the possibility of a perturbation treatment. In the customary DWBA treatment (see Introduction) the neutron is dropped into the ground state of A to form some component of a particular state of (A+1). The spectroscopically significant feature of this treatment is what might be called

the "incoherent separability" of the proton angular distributions. The differential cross section leading to some state $\Phi_{J_f}(A+1)$ of the residual nucleus (A+1) may in general be written (neglecting spin-orbit interactions) as follows:[5]

$$\frac{d\sigma}{d\Omega} = [\text{Kinematic and Statistical Factors}] \times \sum_{j\ell} \beta_{j\ell}^2 \sum_{m} |B_{\ell j}^{m}|^2 \quad \ldots (1)$$

Here $B_{\ell j}^{m}$ (see equation (4) below) is a function of the scattering angle, distinctively characteristic of the orbital angular momentum, l, of the stripped neutron. It is the amplitude for the direct transfer of a neutron into a bound orbital of angular momentum, j, for a particular momentum transfer defined by the projectile energies and the scattering angle. The $\beta_{j\ell}$ expresses the parentage of the state $\Phi_{J_f}(A+1)$ of the residual nucleus on the coupled state $[\Phi_{J_i}(A), \varphi_j]_{J_f}$, where $\Phi_{J_i}(A)$ is the ground state of the target nucleus and φ_j is the neutron associated with $B_{\ell j}^{m}$. It turns out that even with spin-orbit coupling, the incoherency in J remains.[7] The factors $\beta_{j\ell}$ are commonly[8] expressed as reduced matrix elements of $a_j^{\dagger}$ as follows:

$$\langle J_2 \| a_j^{\dagger} \| J_1 \rangle = -(\hat{J}_2)^{1/2} \beta_{j\ell} \quad (2)$$

using Racah's notation[9] which is not that used by Bohr and Mottelson.[8] There are many variants of this definition in the literature, and the spectroscopic factor $\mathcal{S}$ is often used

$$\mathcal{S}_{j\ell} = \langle J_2 \| a_j^{\dagger} \| J_1 \rangle^2 . \quad (3)$$

The significance of the factorization property of the angular distribution is that if one or a small number of angular momentum transfers are present then these l's can be identified and their relative strengths determined. This would be difficult if there were interference between the various l's. In the case of an even-even target nucleus (spin zero), the quantum numbers of the transferred neutron are those of the residual nucleus. It is often possible, in this model, to treat a limited range of nuclei (say, the rare earths) as follows. Standard angular distributions for possible l values are calculated together with tables of Q-dependence and A-dependence. The spectroscopic factors, S_l, are now simply obtained as multiplicative constants for matching any particular angular distribution. The particular form S_{jl} takes in the case of deformed nuclei has been alluded to in the Introduction and will be derived in Chapter VI.

The incoherent separability of the angular distribution (1) no longer holds when inelastic processes are present: the stripping amplitude is a coherent sum of amplitudes corresponding to the stripping interaction taking place through different "routes." The quantum numbers of the transferred neutron are no longer those of the final state for a spin zero target. The amplitudes which may contribute to the cross section of a particular state have been shown for a particular case in the appendix to Chapter I.

B. Customary Stripping Approximations

Within the framework of the usual treatment of stripping reactions (i.e. DWBA and its present generalization CCBA) a number of approximations are widely employed. The errors which they engender are fairly well understood for the case of DWBA calculations, and we might suppose that these carry over, qualitatively at least, into CCBA calculations.

1. Zero Range Approximation

The factor B_ℓ^m which appears in eq(1) contains the following integral:

$$B_\ell^m(\vec{k}_d,\vec{k}_p) \propto \int \psi_p^{(-)*}(\vec{k}_p,\vec{r}_p')\,\phi_\ell^{m*}(r_n)\,V_{np}(r)\,\psi_d^{(+)}(\vec{k}_d,\vec{R})\,\phi_d(r)\,d\vec{r}_n\,d\vec{r}_p' \qquad (5)$$

This is a six-dimensional integral over the proton and neutron coordinates (for notation, see ref.[5]) and as such is very difficult to evaluate numerically (for a full discussion, see Austern et al[10]). In order to make stripping cross sections realistically calculable, it has been customary to make the zero range approximation in which the product $V_{np}(\vec{r}_{np})\,\phi_d(\vec{r}_{np}) = \mathcal{D}(\vec{r}_{np})$ is replaced by $D_0\,\delta(\vec{r}_{np})$, where D_0 can be given various plausible values depending on the mode of derivation[6] (e.g. from effective range theory). This approximation corresponds to overemphasizing the high momentum components of the linear momentum transferred between the deuteron and the proton. The effect can be calculated exactly in the plane wave approximation where it results in a multiplicative factor depending on the momentum transfer such that the back angle

cross section (corresponding to high momentum transfer) is attenuated. This attenuation will be less, however, when distorting potentials are introduced, for, in this case, back angle protons will be generated largely in a stripping interaction of relatively low momentum transfer.

The zero range approximation tends to overestimate the contribution of the interior regions to the source of protons. The difficult exact finite range calculations have been performed for some cases. Dickens et al[11] compare the results with those of "Local Energy Approximation" (LEA), which was introduced by Perey and Saxon.[12] Here the zero range "form factor" is multiplied by radial factor that depends on the energies of the particles involved at a given radius (Local Energy). It turns out that finite range effects are not negligable, that they are smallest for the most "physical" of the possible deuteron optical potentials (discussed in Chapter VII), and that the LEA is a remarkably good approximation to the exact calculation. Dickens et al[11] give a notably simple procedure for the incorporation of the LEA into stripping. Use is sometimes made of sharp radial cutoff as a rough means of simulating this effect although it is not as good as LEA. The calculations of Dickens et al suggest that with well chosen optical potentials, the overall normalization is the quantity most influenced by this approximation.

It has been suggested,[13] however, that LEA is less adequate

as a representation of finite range effects for light nuclei: a higher order approximation than LEA is appropriate for ^{25}Mg g.s., a case we consider in Chapter VIII. The effect is not large.

We must note that in an approximation similar to LEA, a finite range stripping interaction has been shown[14] to have a very small effect on the angular distribution of protons in ^{24}Mg(d,p) for l transfer of zero or two.

2. Effects Due to Non-locality of One Body Potentials

The most physical one body potential for either bound or scattering states is non-local. The antisymmetrization of the total wavefunction and the consequent exchange integrals, together with the need to account for the effect of virtual excitations in a one body model are responsible. It turns out (Perey effect) (see Austern[15]) that the wavefunction of an attractive non-local potential is always less within the nucleus than the wavefunction determined by the equivalent (energy dependent) local potential. This means that local optical potentials found by matching elastic scattering are bound to overemphasize the contribution from the nuclear interior. This is interesting from our point of view in that part of the non-locality in an elastic scattering optical potential is due to the excitation and deexcitation of the strongly coupled states. To some extent then, for reasons explained in Chapter VII, we expect that explicit inclusion

of such states would, other effects aside, reduce the back angle cross section by virtue of the changed elastic channel wavefunctions. This change is in the same direction as LEA. We might suppose that the effect of non-locality of the one body potential could, like the finite range effect, be simulated by a suitably chosen radial cutoff.

Our program has provision for an arbitrary radial cutoff, but this feature was seldom invoked. The extensive test of DWBA for ^{40}Ca(d,p) carried out by Lee, Schiffer et al[16] suggests that although some angular distribution shapes were improved by the use of a radial cutoff (possibly due to enforced neglect of unsatisfactory wavefunctions in the nuclear interior), the spectroscopic factors could not be consistently extracted. The proton angular distributions were fitted quite well for calcium.

3. Deuteron D-state

The consequences of the customary neglect of the deuteron d-state for stripping calculations has been studied by Johnson.[17] The numerical results[18] indicate that a contribution to the j-dependence occurs which is quite large for cases where the l transfer is as large as three. The effect on l=0 transitions is quite small. This calculation accounts for the tensor components in the stripping interaction, V_{np}, (the potential that binds the deuteron) simply by incorporating the correct d-state admixture; a property of the DWBA method (Johnson).

4. Exchange Effects

The effect of neglecting the exchange integrals increases with decreasing A,[19] but is probably small even for light nuclei[20] except perhaps for levels forbidden by some selection rule.

C. DWBA in Light Nuclei

Among the approximations made in the customary DWBA approach we might have listed the neglect of the polarizability of the deuteron. Some discussion of this phenomenon will be given in Chapter VII, but it seems that to give a full, consistent description of the role played by this and associated phenomena in stripping reactions it is probably necessary to go outside the framework of the DWBA altogether. For nuclei as light as carbon (see, for example, Schiffer et al[21]) or oxygen (see, for example, Alty et al[22]), the customary DWBA does not give good angular distributions in the backward hemisphere, nor even fit the shape of the stripping peak very well, and LEA does not seem to give a consistent improvement. We take this to imply that we should not expect perfect angular distributions for stripping on magnesium. The basic assumption that stripping may be adequately described by considering only the centre of mass motion of the deuteron tends to fail when the nucleus is of comparable dimensions to the large, loose deuteron. A quite different stripping theory[23] has been introduced in which the proton and neutron propagate independently in the field of the

nucleus; it has had considerable success in carbon, for example.

A somewhat different departure from the customary DWBA is embodied in the calculations of Rawitscher[24] who employs coupled channel techniques to include the stripping interaction to higher order. Significant changes are found in strongly excited levels of ^{41}Ca. Referring to the specific case of magnesium, we note that the d5/2 stripping amplitude, for example, is split among three 5/2+ levels: it is not altogether clear that one can argue from the relative weakness of the cross section of one of these states (compared with the very strong levels of calcium) to the smallness of the effect under discussion in stripping on magnesium. In fact, as we shall see in Chapter VII, the whole process of deuterons interacting with ^{24}Mg is poorly understood. One aspect of the general problem of applying DWBA to light nuclei is the difficulty of determining suitable optical potentials. Because of resonance phenomena that may occur, optical potentials averaged over a range of nuclei are often found necessary (for example, see ref.[21]). With these the angular distributions are, as mentioned above, often quite poor. In particular they are too low in the backward hemisphere. Accordingly, a number of stripping analyses[25,26,68] have been made in which the optical potential is adjusted to fit the stripping reaction itself, and it is found that the absorption required is usually considerably less. In fact, we have found that the deuteron optical potentials used in refs.[25,26]

gave a very bad representation of elastic scattering - the absorptive part was about half of what might have been expected. This is possibly related to the deuteron polarization phenomenon: the optical potential expresses the absorption of ground state deuterons from the beam. Some are absorbed into compound nucleus states, but some into excited deuteron states (which represent the fact that the deuteron becomes smaller in the nuclear interior) which may still undergo stripping.

D. Consistent Study of Inelastic Processes

It is perhaps remarkable that in spite of all the strictures that have been raised againt it, zero range DWBA sometimes works remarkably well. Certainly, there are many parameters involved, and it is true that often optical potential parameters are required which are not suitable for deuteron or proton scattering. As an example of a particularly successful zero range distorted wave (i.e. DWBA) calculation, we note the work of Bjorkholm, Haeberli and Mayer[27] who find rather good agreement between experiment and the customary DWBA theory for the angular distribution, analysing power and polarization of the (d,p) stripping reaction on the moderately[73] collective ^{52}Cr leading to the ground state of the residual nucleus. The point is that the deuterons and protons are treated consistently matching the (d,d) and (p,p) cross section and polarization data at the appropriate energies and thus fixing the optical potentials for the stripping calculation. This is a model of

what we would like to do when we have included the inelastic processes in the calculation; new optical potentials would be found which would reproduce all of the deuteron and proton elastic and inelastic data with cc calculations.

There remains the possibility that the agreement found in such calculations as the above, for one* state, at one energy is fortuitous. A stronger test of either DWBA or CCBA, then, would be that a similar agreement should be obtained over a range of energies with continuously varying optical parameters. The coupled channel stripping calculations should also be carried out for a series of energies. As the inelastic processes are expected to be energy dependent (we shall see that they might be expected to absorb some of the energy dependence of the optical potential), this is expected to provide a more rigorous test of the stripping mechanism common to both approaches.

The experimental data required for a program such as this is considerable; it is never available in all its detail for nuclei we may wish to study. What is available varies from case to case, but in general our calculations are model calculations. We shall discuss the optical potentials in

---

*Anticipating one of our findings: entrance channel inelastic effects in magnesium can alter the relative strength of two levels rather markedly with only a moderate change in angular distribution.

Chapter VII, but we mention that spin-orbit interactions are often chosen for physical reasonableness rather than from any fit to polarization data. Where we treat energy dependence, we must follow a model calculation by assuming an energy dependence for the optical potential. Cases of this are described in Chapter VII, and their use in particular stripping reactions is discussed in Chapter VIII.

E. Inelastic Processes in Stripping Reactions-Summary of Problems Raised

The foregoing discussion of stripping reactions allows us to enumerate in more detail what we hope to learn from this study.

1. We must be able to demonstrate the validity or otherwise of the customary measurements of the Nilsson factors c_j based on the factorization eq(2) of Chapter I which depends on the neglect of inelastic processes. That is, we should be able to determine the extent to which a calculated cross section is proportional to c^2 and the extent to which the proportionality constant can be reliably calculated from nucleus to nucleus.

2. We should determine the degree to which the poor angular distributions calculated for light nuclei using DWBA may be repaired by the inclusion of inelastic processes of the kind described here. To the extent that we fail, then DWBA and its predictions are in some doubt. We hope to settle the question of the need for radically different stripping and scattering

optical potentials.

3. Related to (1) and (2) is the question of the effect on the angular distributions of inelastic processes and the reliability of the common practise of determining c^2 in the rare earth region from measurements at, perhaps, four angles. Connected with but distinct from (1) above is the question of "j-dependence" which is not accounted for in Mg by the use of spin-orbit interactions.

4. We should hope to demonstrate the basis of the findings of Siemssen and Erskine[28] that the most satisfactory optical potentials for stripping onto tungsten were "average potentials" over the rare earths rather than potentials which optimally fit elastic scattering on tungsten.

5. It turns out that when coupled channel calculations of inelastic scattering are carried out, it is often possible to tell whether a process was populated directly from the ground state or whether a multistep process was involved in the excitation. A direct excitation has, as in the case of stripping, an angular distribution characteristic of the angular momentum transferred. If a state of known spin corresponds to an angular distribution which is markedly less forward peaked or markedly augmented at back angles than would be expected for a direct excitation, then we may suppose multistep processes to be important. This device has been used[29] to make deductions about certain gamma band states in Erbium, for example. Now,

the claim has been made[30] that some property of this kind holds for stripping also; the claim is that one may suppose inelastic processes to be significant where the angular distribution is distinctly augmented at back angles, in comparison with the DWBA result. It is important that we test this plausible hypothesis.

III. FORMAL THEORY OF NUCLEAR REACTIONS- APPLICATION TO STRIPPING

In order to justify the formal results that we employ in calculating stripping cross sections, we first give a brief account of some relevant aspects of reaction theory. In view of the special problems associated with rearrangement collisions- the ad hoc quality of the customary assumptions, for example- we have felt it necessary to point out some of the fundamental weaknesses of our approach which, as we shall show, is a generalization of the usual DWBA stripping theory. While not intended to be a full critical analysis of rearrangement collision theory, we hope the following makes clear the limitations of our calculation.

A. General Formulation

As a consequence of the finite range character of nuclear forces (and, in effect, of shielded e.m. forces) it is possible to divide a particular many body system into partitions such that an asymptotic region may be defined for each partition; the various components which define the partition are non-interacting. A partition is defined by the nucleons in each component, not by the states of the components.

In a time dependent picture, a nuclear reaction takes place when the components of a two-component partition come within range of the nuclear interaction. The nuclear interaction, in

general, couples the "incoming state" to all the states of the total hamiltonian. We may have a special interest in

$$A+a \longrightarrow B+b \tag{1a}$$

for example, but a whole series of reactions

$$\begin{aligned} &\longrightarrow C+c \\ &\longrightarrow D+d \qquad \text{etc.} \end{aligned} \tag{1b}$$

cannot be ignored in the complete solution.* Energy conservation will, of course, dictate that all the wavefunctions for many partitions will decay exponentially in the asymptotic region. However, all of these states are part of the complete solution Ψ of the total hamiltonian, H

$$(H-E)\Psi = 0 \tag{2}$$

We see that in stripping reactions where states of only two partitions are of interest, we are actually involved in a many body problem of overwhelming complexity. It turns out, however, that it is just certain aspects of this complexity that make it possible to give a phenomenological representation of many body effects through the use of such constructs as the optical potential (whose absorptive powers are well known!)

In view of the various partitions which potentially may

---

*The quantum mechanical 3-body problem was solved only when the importance was appreciated of incorporating all the communicating channels into the problem in a symmetric manner.

enter our discussion (see (1a), (1b)), we introduce the following notation. We shall speak of partition L, where L=1,2,3. . . Normally, 1 and 2 will correspond to the incoming and outgoing partitions of interest, respectively. As we can almost always speak (in two-component partitions) of a "particle" (in general, composite) and a "nucleus," we may label the components of partition L as p_L and n_L.

It is convenient to define an asymptotic hamiltonian, H_L for partition L in the following way:

$$H=H_L+T_L+V_L \tag{3}$$

where V_L is the interaction which vanishes asymptotically in L, and T_L is the c.m. relative kinetic energy of the components of L. The separation of the centres of mass of these components we label $\vec{r}_L$.

We also define the hamiltonians which correspond to the internal energy of the components of partition L, as follows:

$$H_L=H_L^P + H_L^N \tag{4a}$$

where H_L^P and H_L^N are the projectile and nucleus internal hamiltonians having eigenfunctions in the mnemonic notation:

$$(H_L^P - E_i^P)\,\pi_{iL} = 0 \tag{4b}$$

$$(H_L^N - E_j^N)\,\nu_{jL} = 0 \tag{4c}$$

where, for example, γ_i^L is the i^{th} eigenfunction of the "nucleus" in the L partition.

The complete sets π_i and γ_j contain states belonging to the continuum. We shall indicate below how the influence of the continuum states can be accounted for by means of an optical potential.

The eigenfunctions of H_L are given by

$$(H_L - \varepsilon_\alpha^{(L)})\psi_{\alpha L} = 0 \qquad (5)$$

where the channel label, α, subsumes i and j. We define plane waves $\Phi_{\alpha L}(\vec{r}_L)$ of momentum k_α, where

$$E = \varepsilon_\alpha^{(L)} + \frac{\hbar^2 k_\alpha^2}{2\mu_L}$$

where μ_L is the L partition reduced mass. They are solutions of the non-interaction equation:

$$(H_L + T_L - E)\,\Phi_{\alpha L}(\vec{r}_L) = 0 \qquad (6)$$

where

$$\Phi_{\alpha L}(\vec{r}_L) = \psi_{\alpha L}\, e^{i\vec{k}_\alpha \cdot \vec{r}_L}$$

Although the internal structure wavefunctions are properly orthonormal, $\langle \psi_{\alpha L} | \psi_{\beta L} \rangle = \delta_{\alpha\beta}$, it is important to observe that $\langle \Phi_{\alpha L} | \Phi_{\beta M} \rangle$ is never, in general, zero - a difficulty that propagates throughout reaction theory.

We can now write down the well known formal solution of eq(2) for Ψ, the total wavefunction:

$$\Psi_{\alpha L}^{(\pm)} = \Phi_{\alpha L} + \frac{1}{E^{\pm} - H_L} V_L \Psi_{\alpha L}^{(\pm)} \qquad (8)$$

Here, $\Psi_{\alpha L}^{(\pm)}$ is the solution with plane waves in channel of partition L, and outgoing (respectively, ingoing) waves in all other partitions, and $E^{\pm} = E \pm i\varepsilon$. The "post" and "prior" forms of the exact transition amplitude for channel β in partition 2 with incoming waves in channel α are, respectively (see, for example, Goldberger and Watson,[31] p.197)

$$T_{\beta\alpha}^{+} = \langle \Phi_{\beta 2} | V_2 | \Psi_{\alpha 1}^{(+)} \rangle \qquad (9a)$$

and

$$T_{\beta\alpha}^{-} = \langle \Psi_{\beta 2}^{-} | V_1 | \Phi_{\alpha 1} \rangle \qquad (9b)$$

Note that $T^{+} = T^{-}$ only on the energy shell where

$$\langle \Phi_1 | V_1 | \Phi_2 \rangle = \langle \Phi_1 | V_2 | \Phi_2 \rangle$$

furthermore eq(9a) involving Ψ_{α}^{+} derives its usefulness from the fact that $\Psi^{(+)}$ can never be known exactly - if it were, there would be no need for (9a), This equation, however, is the basis of the usual perturbation approximations, which leads us into our difficulties: the kernel for the perturbation series (in plane wave Born, or DWBA) is singular (see, for example, Greider and Dodd[32]). Moreover, the rearrangement form of the Lippmann-Schwinger equation, with the m-partition outgoing Green function

$$\Psi_L^{(+)} = \frac{1}{E^+ - H_m} V_M \Psi_L^{(+)} \qquad (10)$$

is homogeneous and does not have unique solutions. (For a discussion of these points, see Brezin[33] and Greider and Dodd). The same problem occurs in the simplest rearrangement process - the three body problem. What does this imply about stripping reactions? Clearly, the fact that they are vastly more complex in other respects may mask specific three body effects; yet, certain results of an exact three body treatment* should give us pause.

Numerical solutions are difficult but have been carried out with simple separable potentials. These calculations suggest (Brezin) the importance of the symmetric treatment involving all the physical partitions and that the simple approximation schemes involving only transitions between particular channels of interest are inadequate for n-d scattering and breakup: it would appear to be"more important to treat the three body mechanisms exactly than to have a very detailed two body force and to treat the three body dynamics approximately."(Brezin)

We shall follow the usual road in ignoring these fundamental difficulties.

---

*For a lucid account of the motivation, solution and properties of the Fadeev-Lovelace equations, see Brezin.

B. Approximate Transfer Amplitude

At this point we have quoted the formal expressions (eq(9a), (9b)) for the transition matrix, T, which could in principle be calculated.

Clearly, in the face of the absolute unattainability of Ψ, some approximation procedure will have to be involved if we are ever to calculate numbers to compare with a measured flux of protons at angle θ. Our program is to provide such a comparison through the use of a coupled-channel generalization of DWBA in which the"distorted waves" become solutions of an inelastic scattering problem containing excited states of the nuclei. We shall not discuss the coupled-channel theory of inelastic scattering here, and we shall use standard results from Feshbach's unified theory of nuclear reactions (Feshbach[34]). The technique has been presented in detail by Glendenning.[35] This article contains all the results we shall need and we shall quote results from it without proof.

In order to obtain solutions of equation(2), we may expand the total wavefunction in the states of the various partitions as follows (see(4b),(4c)):

$$\Psi = \sum_i \pi_{i_1} \nu_{i_1} f_{i_1}(R_1) \equiv \sum_i' \tilde{\varphi}_i \qquad (11a)$$

$$= \sum_i' \pi_{i_1} \nu_{i_1} f_{i_1}(R_2) \equiv \sum_i' \tilde{\varphi}_{i_1} \qquad (11b)$$

and similarly in other partitions; let us consider only partitions 1 and 2 explicitly. The expansion coefficients are the relative (centre of mass) radial wavefunctions for partition L with centre of mass separation R_L. Notice that we have alternative expansions of the wavefunction, so that the natural generalization of the derivation of the coupled-channel equations for inelastic scattering (using expansions (11a) and (11b) together with an ad hoc stripping interaction) will be incorrect to the extent that $\langle \tilde{\varphi}_i | \tilde{\varphi}_j \rangle \neq 0$ for i and j within whatever projected spaces might be appropriate.* In fact, it will be seen that this non-orthonormality problem reappears in our formal result.

The projection operators required are defined as follows for partition L:

$$P_L^{\pi} = |\pi_{oL}\rangle\langle\pi_{oL}| \qquad (12)$$

P_L^{π} projects onto the ground state of the projectile in L; for L=1 this is the ground state of the deuteron. For L=2 (proton) it is 1. These operators will be useful to us when we come to discuss the general problem of the composite particle optical potential. The nucleus projection operators are:

---

*We have an over-complete set. A rigorous coupled-channel derivation would involve a Schmidt orthogonalization procedure - and be prohibitive.

$$P_L^{\nu} = \sum_j |\nu_{jL}\rangle\langle\nu_{jL}| \qquad (13)$$

P_L^{ν} projects onto some subset, which we shall also refer to symbolically as P_L^{ν}, of the states of the nucleus in L. Using these, we define total projection operators

$$P_L = P_L^{\pi} P_L^{\nu} \qquad (14)$$

with

$$P_L + Q_L = 1 \qquad (14a)$$

It follows from Feshbach's theory (see Glendenning[35]) that those parts of the exact total wavefunction , that lie within the subspace P_L, i.e. $P_L\Psi$, can be calculated from the following effective interaction:

$$V_L = P_L\left(V_L + V_L Q_L \frac{1}{E^+ - Q_L H Q_L} Q_L V_L\right)P_L \qquad (15)$$

This is a formal result and V_L, a complex, non-local function involving all the nuclear coordinates, cannot be calculated exactly from it. However, the diagonal matrix elements (and non-diagonal, in a macroscopic collective model) are often represented by the optical potential. In the usual treatment[35] the second half is assumed negligable. Let us assume we have some V_L. We shall discuss our model for it in Chapter VI.

We can define the following Green functions in terms of V_1, V_2 :

$$g_1^{(+)} = \frac{1}{E^+ - H_1 - \bar{V}_1} \qquad (16)$$

$$g_2^{(-)} = \frac{1}{E^- - H_2 - \bar{V}_2^\dagger} \qquad (17)$$

Note that the incoming wave Green function, $g_2^{(-)}$, involves the complex interaction $\bar{V}_2^\dagger$.

From these, the projected wavefunctions with plane waves in channel α or β may be calculated using the Feshbach theory results (see Glendenning[35])

$$P_1 \psi^{(+)} \equiv \chi_{\alpha 1}^{(+)} = (1 + g_1^{(+)} V_1) \Phi_{\alpha 1} \equiv \omega_1^{(+)} \Phi_{\alpha 1} \qquad (18)$$

$$P_2 (\psi^{(+)})^* \equiv \chi_{\beta 2}^{(-)} = (1 + g_2^{(-)} V_2^\dagger) \Phi_{\beta 2} \equiv \omega_2^{(-)} \Phi_{\beta 2} \qquad (19)$$

These equations are exact. The tilde on $\tilde{\chi}_2^{(-)}$ draws attention to the fact that it has been calculated from the complex conjugate of the effective interaction. When we wish to indicate that we are calculating χ_L from a phenomenological representation of V_L (e.g. the optical potential, $\bar{V}_L$) we shall write them $\bar{\chi}_1^{(+)} \approx P_L \psi^{(+)}$, for example. We shall now show how a coupled-channel Born approximation can be derived by a generalization of the proof of the DWBA given by Greider and Dodd.[32]

The Green function for the entire system is given by

$$G^{(+)} = [E^+ - H]^{-1} \tag{20}$$

and the wave operators Ω_1^+ , Ω_2^- are defined in terms of the exact, many body potentials, V_1 and V_2 , as follows:

$$\Omega_1^{(+)} = 1 + G^+ V_1 \tag{21a}$$

$$\Omega_2^{(-)} = 1 + G^- V_2 \tag{21b}$$

They have the action

$$\Psi_L^{(\pm)} = \Omega_L^{(\pm)} \Phi_L \tag{22}$$

which is equivalent to eq(8).

From equations (8) and (9) we may write down the transition matrix element for a transition from channel α in partition 1 to channel β in partition 2 as follows:

$$T_{\alpha\beta}^{(+)} = \langle \Phi_{\beta 2} | V_2 + V_2 G^{(+)} V_1 | \Phi_{\alpha 1} \rangle$$

$$\equiv \langle \Phi_{\beta 2} | U_{21}^{(+)} | \Phi_{\alpha 1} \rangle \tag{23a}$$

$$T_{\alpha\beta}^{(-)} = \langle \Phi_{\beta 2} | V_1 + V_2 G^{(+)} V_1 | \Phi_{\alpha 1} \rangle$$

$$\equiv \langle \Phi_{\beta 2} | U_{21}^{(-)} | \Phi_{\alpha 1} \rangle \tag{23b}$$

These are the "post" and "prior" expressions for T, respectively. Consider the operator $U_{21}^{(-)}$ defined in eq(23b)

$$U_{21}^{(-)} = V_1 + V_2 G^{(+)} V_1 = \Omega_2^{(-)\dagger} V_1$$

$$= \Omega_2^{(-)\dagger}(V_1 - V_1)\omega_1^{(+)} + \Omega_2^{(-)\dagger}(1-(V_1-V_1)g_1^{(+)})V_1 \qquad (24)$$

This last form is an identity derived from the preceding, using the definition (eq(18)) of $\omega_1^{(+)}$ and rearranging terms - we shall show that the second half vanishes between plane waves. Using the identity

$$A^{-1} - B^{-1} = A^{-1}(B-A)B^{-1} \qquad (25)$$

we find that

$$G^{(+)} - g_L^{(+)} = G^{(+)}(V_L - V_L)g_L^{(+)} \qquad (26)$$

Using this, the second term of $U^{(-)}$ in eq(24) becomes

$$s.t. \equiv \Omega_2^{(-)\dagger}(1-(V_1-V_1))g_1^{(+)})V_1$$

$$= V_1 + V_1 g_1^{(+)} V_1 + (V_2 - V_1) g_1^{(+)} V_1$$

$$= V_1 \omega_1^{(+)} + (H_1 - H_2)(\omega_1^{(+)} - 1)$$

where we have used the definition of $\omega_1^{(+)}$. Now, using this again, together with the explicit form for $g_1^{(+)}$, we obtain:

$$s.t. = (E + i\epsilon - H_2)(\omega_1^{(+)} - 1)$$

Inserting the plane wave eigenvectors Φ_2 of H_2, we find that between plane wave states the following holds:

$$s.t. = i\epsilon(\omega_1^{(+)} - 1)$$

In all cases that will concern us, this expression vanishes in the limit $\varepsilon \longrightarrow 0$. We have defined V_1 to allow scattering only within P_1^{π}, in our particular case, the deuteron ground state. For this reason, it does not generate an outgoing flux in the "2" channels; that is to say, $|\omega_1^{(+)}|\Phi_1\rangle$ has outgoing flux in a finite number of channels for which $\langle\Phi_2|\omega_1^{(+)}|\Phi_1\rangle$ is finite. Hence

$$\lim_{\varepsilon \to 0} \; i\varepsilon \langle \Phi_2 | \omega_1^{(+)} | \Phi_1 \rangle = 0$$

(If V_1 did not have this property, $\omega_1^{(+)}$ could be rearranged to have a part with an outgoing Green function for "2" channels which would cancel ($E + i\varepsilon - H_2$)).

Finally, we have

$$U_{21}^{(-)} = \Omega_2^{(-)^+}(V_1 - V_1)\omega_1^{(+)} \qquad (27)$$

The well known relationship of Gell-Mann and Goldberger relating Green functions for partial potentials becomes, in this case, (using eq(17):

$$\Omega_2^{(-)} = \left[1 + G^{(-)}(V_2 - V_2^{+})\right]\omega_2^{(-)}$$

Inserting this in eq(27), we get

$$U_{21}^{(-)} = \omega_2^{(-)^+}\left[(V_1 - V_1) + (V_2 - V_2)G^{(+)}(V_1 - V_1)\omega_1^{(+)}\right] \qquad (28)$$

where V_1 and V_2 are complex; note that the conjugate of

appears in Greider and Dodd's version of eq(28) and of eq(30) below. This corresponds to the following transition matrix

$$T^{(-)}_{\alpha\beta} = \langle \tilde{\chi}^{(-)}_{\beta 2} | (V_1 - U_1) + (V_2 - U_2)\, G^{(+)}(V_1 - U_1) | \chi^{(+)}_{\alpha 1} \rangle \qquad (29)$$

Following the same procedure, we can derive the post-interaction

$$T^{(+)}_{\alpha\beta} = \langle \tilde{\chi}^{(-)}_{\beta 2} | (V_2 - U_2) + (V_2 - U_2) G^{(+)}(V_1 - U_1) | \chi^{(+)}_{\alpha 1} \rangle \qquad (30)$$

Equations (28) and (30) can be used for real calculations only after a number of further approximations have been made. In the first place, the term involving $G^{(+)}$ is dropped, being computationally intractable. This amounts to recognizing that V_1 and V_2 have two actions: they cause inelastic excitations in the appropriate partition, and they cause rearrangement, i.e. transitions, between partitions. Roughly speaking, dropping the $G^{(+)}$ term in (30) involves keeping V_2 in its inelastic excitation capacity to all orders, and to first order as a stripping interaction. Rawitscher[24] has carried out calculations in which the stripping interaction is included to higher orders and the effect is appreciable. We should note also that Rawitscher's calculation involved stripping reactions in which the first order term (and so, cross section) was signifcantly larger than in the cases we consider. However, in Chapter II we argued in general terms that this does not necessarily imply that for Mg, at least, the higher order terms are negligable. Greider and

Dodd show that equation (27) can be rearranged into the form of an integral equation:

$$U_{21}^{(-)} = \omega_2^{(-)\dagger}(V_1 - \bar{V}_1)\omega_1^{(+)} + \omega_2^{(-)\dagger}(V_2 - \bar{V}_2)G_2^{(+)}U_{21}^{(-)} \qquad (31)$$

(where $G_2^{(+)} = [E^+ - H_2]^{-1}$), for which the kernel is divergent. (It is a reemergence of the divergence which necessitated Fadeev's treatment.) Thus our statement that we have treated stripping to first order must be qualified: we are not taking the first order term of a convergent expansion. Just what this means is unclear though Dodd and Greider[36] claim* to have reformulated the series in a convergent form.

We shall choose eq(30) as the basis for our calculations, our criteria being calculational tractability and physically reasonable results in the analogous DWBA calculations. We further approximate by replacing χ_L by $\bar{\chi}_L$ calculated using phenomenological potential $\bar{V}_L$,

$$T_{\alpha\beta} = \langle \bar{\tilde{\chi}}_{\beta 2}^{(-)} | (V_2 - \bar{V}_2) | \bar{\chi}_{\alpha 1}^{(+)} \rangle \qquad (32)$$

We shall refer to this as the coupled-channel Born approximation, CCBA, expression for T.

C. Stripping Reactions

The particular reaction to which we shall apply this general

*This writer has not studied their solution. As seems inevitable, their solution is a special case of the Fadeev-Lovelace equations. A calculable form of this work is due to Rihan.[37]

result is deuteron stripping:

$$d + A \longrightarrow p + (A+1) \tag{33}$$

Replacing our 1 and 2 suffixes by d and p, respectively, we have

$$V_d = \sum_{i=1}^{A} \left[V(\vec{r}_p - \vec{r}_i) + V(\vec{r}_n - r_i) \right] \tag{34a}$$

$$\equiv V^p + V^n \tag{34b}$$

$$V_p = V(\vec{r}_p - \vec{r}_n) + V^p \tag{35a}$$

$$\equiv V_{np} + V^p \tag{35b}$$

The stripping interaction $V_{str} \equiv V_2 - \bar{V}_2$, becomes

$$V_{str} = V_{np} + V^p - \bar{V}_2 \tag{36}$$

It is customary to retain only the V_{np} term. The neglect of the $V^p - \bar{V}_2$ term has been a matter of pragmatics as it is rather difficult to calculate and it has seemed that reasonable results are obtained without it. Recent calculations by Smith[89] suggest that this term, in particular the imaginary part (see below), may be important for nuclei as light as silicon. It is possible, however, to argue that in general its effect is small. Consider $\bar{V}_2$. While it is an optical potential, it is, after all, an approximation to an effective

interaction, and, as such, must be constrained to have the same property, viz. $\bar{V}_2 = P_2 \bar{V}_2 P_2$. Hence, to the extent that $P_1 P_2 \approx 0$, $\langle \chi_p^{(-)} | \bar{V}_2 | \chi_d^{(+)} \rangle = 0$ (remember, P_1 includes a projection onto the ground state of the deuteron). Note also that $\bar{V}_2$ is an A+1 particle operator, or a one particle approximation to it (in the diagonal matrix elements, or in a macroscopic model). On the other hand, V^p is an A particle (real) operator and does not contain a projection operator which projects onto the proton plus the low lying states of the A+1 particle system. In spite of this, consideration of V^p suggests that its action will be small for much the same reason that that of $\bar{V}_2$ is small: there is still need for an overlap between a neutron bound in a deuteron and a neutron bound in a nucleus, as the neutron coordinate does not enter this term of V_{str} . In a particular nuclear model, then, it can usually be argued that V^p and $\bar{V}_2$ will have very similar actions, and that the difference can be ignored, although it is quite conceivable that the difference could have the same order of magnitude as either term. The cancellation will never be perfect;* the whole question is clouded by our dubious

---

*Within the collective model, consider the following decomposition (see Chapter IV) of a state in a band of the (A+1) particle nucleus.

$$|J, M, K_1\rangle \approx 2 \sum_{j \ell m J} \left(\frac{\hat{J}}{\hat{J}_1}\right)^{1/2} C^{J j J_1}_{0 K_1 K_1} C^{J j J_1}_{m M M_1} D^{J}_{M 0} |0\rangle \, C_{j\ell}(k_1) \phi_{j \ell m}(r_n)$$

Clearly, this contains several states $D^J_{M_0}|0\rangle$ belonging to P_1;

procedure of regarding the scattering interaction and stripping interactions separately, and including the one to all orders and the other to first order, and subtracting them. As we have suggested, a rigorous solution to this problem can only be obtained when a complete orthogonalized basis is employed. We can state, however, that the effect of $(V^P - \bar{V}_2)$ depends on the nuclear model and on P_1 and P_2, and it is possible that it is more important for CCBA than for DWBA.[89] We calculate the stripping transition matrix:

$$T_{dp} = \langle \tilde{\chi}_p^{(-)} | V_{np} | \chi_d^{(+)} \rangle \qquad (37)$$

having simplified our notation. It looks much like DWBA and, in fact, was written down by analogy to DWBA.[3]

D. Coupled Channel Procedure for Stripping Amplitude

The calculation of the transition matrix T from eq(37) is still a difficult technical problem. A purely coupled channel method of calculating stripping amplitudes has been devised by Ascuitto and Glendenning.[4] We shall show formally that it

---

so may $|J_2 M_2 K_2\rangle$ based on a different intrinsic state, K_2. Now, it can be easily shown that exciting only the core of this, i.e. $D^J_{N0}|0\rangle \longrightarrow \sum a_{J'} D^{J'}_{M0}|0\rangle$, that we can excite states of the K_2 band, and, in principle, many bands. This, then, is a clear difference between V^P which operates only on the core by definition and $\bar{V}_2$ which acts only within a band by definition.

gives precisely the stripping amplitude of eq(37).

In outline, the deuteron coupled channel wavefunctions $\chi_d^{(+)}$ are calculated and then incorporated in the "source" term of an inhomogeneous coupled channel equation for protons. This latter calculation requires little more effort than the calculation of $\tilde{\chi}_p^-$, yet the transition matrix can be extracted directly without the complication of evaluating T by integrating eq(37).

Consider the set of coupled inhomogeneous equations implied by the following ansatz:

$$(T_p + \bar{V}_p - E)\chi_p^I = -V_{np}\chi_d^{(+)} \qquad (38)$$

The superscript I emphasises that we have the solution to an inhomogeneous equation. The deuteron wavefunctions, $\chi_d^{(+)}$, are solutions of the coupled homogeneous equations:

$$(T_d + \bar{V}_d - E)\chi_d^{(+)} = 0$$

The boundary condition is that $\chi_d^{(+)}$ contains a plane wave of deuterons in the target ground state channels, and outgoing waves only in other channels. The effective interaction will be taken to operate only within some subset of the nuclear states. These will normally be the states which couple most strongly to the ground state of the target nucleus. The relative motion wavefunction of a deuteron in its ground state and the strongly coupled target states given schematically

(for details of angular momentum coupling, see Chapter VI) by:

$$\chi_d^{(+)} = \sum_\alpha{}' \varphi_\alpha(A)\, U_\alpha(R_d) \tag{40}$$

Similarly, V_p is defined within some specified set P_p of target states which are strongly coupled together (not necessarily to the ground state). A formal solution of equation (38) may be written down as the following homogeneous integral equation

$$\chi_p^{I(+)} = \frac{1}{E^+ - H_p - V_p} V_{np} \chi_d^{(+)} \tag{41}$$

There is no plane wave component in χ_p^I. This can be rearranged, using identity, eq(25), into the form

$$\chi_p^{I(+)} = -\frac{1}{E^+ - H_p}\left[1 + V_p \frac{1}{E^+ - H_p - V_p}\right] V_{np} \chi_d^{(+)} \tag{42}$$

We notice that $[E^+ - H_p]^{-1}$ is the bare Green function with the outgoing wave boundary condition (compare usual derivation of eq(9a) starting from eq(10)) which leads by a stardard procedure to the following expression for T:

$$T_{dp} = \langle \phi_p | \left[1 + V_p \frac{1}{E^+ - H_p - V_p}\right] V_{np} | \chi_d^{(+)} \rangle$$

$$= \langle \tilde{\chi}_p^{(-)} | \, V_{np} \, | \chi_d^{(+)} \rangle \tag{43}$$

where we define $\langle \tilde{\chi}_p^{(-)} |$ as the conjugate of

$$\tilde{\chi}_p^{(-)} = \phi_p + \frac{1}{E^- - H_p - V_p^\dagger} V_p^\dagger \phi_p \tag{44}$$

This is precisely the wavefunction defined in eq(19) and appearing in eq(32) and eq(37) involving the conjugated effective interaction. Thus we see that the T-matrix extracted from the solution of eq(38) with outgoing proton boundary conditions is just that of eq(37) which we called the CCBA approximation to T.

It has been shown by Ascuitto and Glendenning[4] that in the DWBA limit, the simple coordinate space representation of the Green function

$$\frac{1}{E^+ - H_p - V_p}$$

where V_p corresponds to a space of one nuclear state, can be used to prove our formal result explicitly. This proof would apply also to the case of coupled incoming channels leading to the hybrid cc-dw calculations of Iano, Penny and Drisko.[3]

E. Summary

We have derived a plausible generalization of the DWBA stripping amplitude in which no assumptions beyond those which are customary are made. However, it does include the effects of inelastic transitions which have been previously neglected. It is well known that the conventional treatment of stripping reactions has defects which are quite independent of any consideration of inelastic effects. This will be particularly true when we make additional simplifications such as the zero range approximation. Thus in fitting experiments there is a limit to what we can expect, particularly at backwards angles. Our theory includes nothing of antisymmetrization effects.

APPENDIX

Use of Source Term for Inelastic Scattering

Comment should be made that source term methods might well be useful for a large class of non-rearrangement inelastic scattering reactions. The time necessary for a coupled channel inelastic scattering calculation increases almost exponentially with the number of channels included. There is, furthermore, a natural limitation to the number of channels that can be included. Under certain circumstances the source term procedure is a suitable technique for alleviating this problem. It may occur that the states of a nucleus fall into two subsets: one group being strongly excited and the other relatively weakly. While transitions between states within a set are important, the influence of the weak group upon the strong group may be negligable. Such a circumstance occurs, for instance, when the inelastic excitation of the ground band and gamma band of a deformed nucleus are calculated together. In this case, we calculate the ground band wavefunctions

$$(H-E)\Psi^{(+)}_{STRONG} = 0 \qquad (45)$$

and then the weakly excited levels

$$(H-E)\Psi^{(+)}_{WEAK} = -V\Psi_{STRONG} \qquad (46)$$

If a search for certain parameters describing the weak levels is to be made, Ψ_{STRONG} could be stored and reused with considerable computational savings.

IV. NUCLEAR WAVEFUNCTIONS

A. Introduction

This study is concerned with deformed nuclei which can be set into rotation in some scattering process. It is now believed that nuclear non-sphericity occurs in a wider* range of nuclei than those nuclei the spectra of which are clearly rotational (with A~25, A=150-190, and many actinide nuclei). However, we shall confine ourselves to strongly deformed nuclei because these nuclei will not only exhibit most strongly the phenomena which we are studying, but the model commonly employed for their description is most likely to be valid for large deformations.

In the first place, the large deformation is reflected in a large quadrupole moment of the intrinsic structure, which within the framework of the rotational model results in large values of B(E2) for intraband gamma transitions. This in turn means that the low lying levels of the ground band may be very strongly excited by inelastic scattering and it is this which may prove to be important for stripping reactions.

---

*The phase transition from spherical to deformed at N=90 is by no means as sharp as the spectra might suggest; Hartree-Fock calculations predict considerable deformation throughout the p and s-d shells; ^{8}Be reveals a rotational spectrum in α-α scattering and even the ground state of the closed shell nucleus ^{16}O has definite rotational properties in the coexistence model. The "ideal" shell model nucleus ^{18}O has rotational properties underlying its spectrum.

A large deformation is necessary in order for the model we use to be valid. We define an intrinsic state χ, (calculated perhaps using some deformed potential well) so that our total wavefunction factors into a product $D\chi$, where D is a rotational wavefunction. Underlying this separation is the adiabatic picture: a nucleus with a large deformation i.e., a large moment of inertia, will rotate sufficiently slowly, compared to the velocities of the single particle motion, that the effect of the coriolis interaction can be treated in perturbation theory. It can be shown that the product wavefunction D is a good approximation if the intrinsic wavefunction is nearly orthogonal to the same intrinsic wavefunction at a small angular displacement. The extent to which this holds will depend on the deformation. We should note that a given deformation for a nucleus of A~25 will not mean the same as it does for A~160. Ripka[38] has recently called into question the adiabatic model for the s-d shell, although ^{24}Mg, for example, has a very large deformation indeed. The extent to which the collective transitions are enhanced is also smaller in this region.

The nuclei we consider should have a well-defined equilibrium shape, thus excluding such possibly deformed nuclei as ^{150}Sm (which is so soft that the zero-point motion is comparable to the mean deformation) and ^{152}Sm for which an added neutron may change the deformation.

Ideally, we should have available deformation parameters which can account, in terms of some self consistent theory, for both inelastic scattering as well as the level ordering of odd nuclei and the equilibrium shape of even nuclei. In practice, we shall have to use deformations obtained from scattering experiments when we wish to describe the scattering process, and deformations that account for level ordering and neutron separation energies when we wish to calculate the neutron wavefunction. A typical even-even rotational spectrum is that of ^{166}Er. The 2+ level at .787 MeV is the bandhead of a rotational gamma band (see fig. IV.2). Figures IV.1, IV.3 and IV.4 show odd nucleus rotational spectra.

B. Rotational Wavefunctions

The use of adiabatic wavefunctions for rotational nuclei is standard and we merely set out our conventions and definitions here. They are similar to those used in the review articles of Nilsson.[39]

The symmetrized rotational wavefunction of a state of spin J, based on an axially symmetric intrinsic state for which J_3 (the projection of angular momentum on the 3 (intrinsic) axis) has eigenvalue K, is

$$\psi^J_{MK} = \frac{1}{\sqrt{2}} \sqrt{\frac{2J+1}{8\pi^2}} \left(1 + R_i R_e^{-1}\right) \chi_K D^J_{MK} \qquad (1)$$

The intrinsic wavefunction, χ_K will be discussed in detail below.

We define (following Nilsson: this is not universal)

$$\chi_{-K} \equiv R_i \chi_K = e^{i\pi J_2} \chi_K \tag{2}$$

where R_i represents a rotation of π about the intrinsic 2-axis which, with a suitable phase convention, is equivalent to time reversal; R_e^{-1} acts on the rotation operator:

$$R_e^{-1} D^J_{MK} = (-)^{J+K} D^J_{MK} \tag{3}$$

The symmetrized wavefunction thus becomes:

$$\psi^J_{MK} = \sqrt{\frac{2J+1}{16\pi^2}} \left\{ \chi_K D^J_{MK} + (-)^{J+K} \chi_{-K} D^J_{M-K} \right\} \tag{4}$$

For the case of K=0, the normalized rotational wavefunction is

$$\psi^J_M = \sqrt{\frac{2J+1}{8\pi^2}} \chi_0 D^J_{M0} \tag{5}$$

These wavefunctions would have to be modified in the case of a nucleus that was not axially symmetric; χ_K would be replaced by a sum over χ_Ω such that $\Omega \leqslant J$ of the state in question.

In the present calculations, we use a single particle or single quasiparticle model for the odd nucleus of the stripping reaction; the target nucleus states considered will have the form (5) which we now write

$$|JM0\rangle = \sqrt{\frac{2J+1}{8\pi^2}} |0\rangle D^J_{M0} \tag{5'}$$

and the product nucleus will have the odd-neutron wavefunction,

$$|JMK\rangle = \sqrt{\frac{2J+1}{16\pi^2}}\left\{ a_K^\dagger |\hat{o}\rangle D^J_{MK} + (-)^{J+K} a^\dagger_{-K} |\hat{o}\rangle D^J_{M,-K} \right\} \quad (4')$$

where $|o\rangle$ and $|\tilde{o}\rangle$ represent the intrinsic state of the core nucleons in the target nuclei, and a_K creates a (quasi-) neutron with $\langle J_3 \rangle = K$. Other quantum numbers are implicit. If the intrinsic state $|o\rangle$ is sufficiently "soft", (as for example, ^{152}Sm is soft in the Y_{20} degree of freedom) the addition of another nucleon can change the equilibrium deformation, or, through "blocking" effects, etc. alter $|\hat{o}\rangle$ sufficiently for $\langle \hat{o}|o\rangle$ to be markedly less than unity. Although $\langle \hat{o}|o\rangle$ is an input parameter for our calculations, and may be interesting in the samarium transition region, we usually assume that it is 1.0. In fact this will turn out to be a good assumption even for magnesium where the probable deformation may be changed by as much as from $\beta_2 = .4$ to $\beta_2 = .3$ by the 25^{th} particle. In this case $\langle \tilde{o}|o\rangle$ still turns out to be greater than 0.9.

One exception to wavefunction (4') will be considered, namely an odd nucleus gamma band. The general odd-nucleus gamma band has an intrinsic state, $J_3 = \Omega$, coupled to a gamma phonon excitation of the core for total $K = \Omega + 2$, $|\Omega - 2|$. For the case $K = \Omega - 2$, for example

$$|JMK\rangle = \sqrt{\frac{2J+1}{16\pi^2}} \left\{ a^{\dagger}_{\Omega} \,|\, \text{Gamma phonon}, k=-2\rangle \, D^{J}_{MK} \right.$$

$$\left. + (-)^{J+K} a^{\dagger}_{-\Omega} \,|\, \text{Gamma phonon}, k=2\rangle \, D^{J}_{M-K} \right\} \qquad (6)$$

As an example of this, we shall carry out a model calculation in which we treat the K=3/2+ band at 532 KeV in ^{167}Er as being purely a gamma band; it is possibly largely of this character.[40] In this case, we shall consider the excitation of this band by way of the excitation of the K=2 gamma bandhead at 787 KeV in ^{166}Er.

Our calculations ignore the presence of coriolis admixed impurities in these wavefunctions. In order to study the importance of inelastic effects, we avoid the complication and the ambiguities of band mixing. Most cases we treat are those in which this mixing should be small: we try to avoid cases where there are nearby bands with K differing by unity, for example. There is no real problem in extending this work to include band mixing. We remark that the drastic effects that the coriolis interaction can have on the level ordering of bands with K=1/2 should not affect the purity of the states within these bands.

C. The Single Particle Intrinsic Wavefunctions

The single particle intrinsic wavefunctions, being the

eigenfunctions of a hamiltonian that does not have spherical symmetry, have components of various angular momenta.

For many purposes Nilsson's[41] wavefunctions for a deformed harmonic oscillator are adequate:

$$\chi_\Omega = \sum_{j\ell}{}' c_{j\ell}(\Omega)\,\chi_{j\ell\Omega} \tag{7a}$$

$$= \sum_{\ell\Lambda}{}' a_{\ell\Lambda}(\Omega)\,\chi_{\ell\Lambda\Omega} \tag{7b}$$

where, using standard notation,

$$c_{j\ell\Omega} = \sum_{\Lambda}{}' C^{\ell\,\frac{1}{2}\,j}_{\Lambda\,\Sigma\,\Omega}\; a_{\ell\Lambda}(\Omega) \tag{8}$$

We have omitted here any label on χ_Ω based on asymptotic quantum numbers. The $c(\Omega)$ and $a(\Omega)$ are expansion coefficients of spherical oscillator wavefunctions with a given oscillator constant and within some subspace of fixed total quantum number $N=2(n-1)+l$. We shall use the result (cf. equation (2))

$$\chi_{-\Omega} \equiv R_i \chi_\Omega = \sum_{j\ell} (-)^{j+\Omega}\, c_{j\ell}(\Omega)\,\chi_{j\ell,-\Omega} \tag{9}$$

in the calculation of the form factor ($\chi_{-\Omega}$ is sometimes defined differently).

These wavefunctions are clearly unsatisfactory for stripping reactions for two reasons. The characteristic asymptotic radial form of the oscillator wavefunctions makes

them inadequate for a reaction such as stripping which is very sensitive to the wavefunction at the nuclear surface. We prefer not to use the method of matching to a Hankel function tail determined by the intrinsic neutron separation energy because of ambiguities that arise in separating out the rotational energy. As Nilsson points out, for example, for an s1/2 particle added to a rotor, a=1 and all the rotational energy is in the core.

The other reason for seeking more realistic intrinsic wavefunctions is that $\Delta N=2$ admixtures (discussed in section E below), while ignored in Nilsson's calculations, can not necessarily be neglected in certain cases where selection rules are involved. For example, l=4 admixtures in the low lying bands of ^{25}Mg would provide alternative modes of excitation of the two "forbidden" 7/2+ levels, the excitation of which by means of inelastic scattering processes will be of particular interest to us.

D. Energy of the Intrinsic Single Particle States

In order to calculate appropriate intrinsic single particle wavefunctions, we must know the separation energy of the neutron from the deformed well. We can calculate this from the Q value of the (d,p) reaction, for example, together with the following relationship between the experimental energies, E_J, within a band, K, and the intrinsic energies, ϵ_K :

$$E_J = \varepsilon_K + \left(\frac{\hbar^2}{2\mathcal{J}}\right)\left[J(J+1) - 2K^2 + \delta_{K,1/2}\, a\,(-)^{J+1/2}(J+1/2)\right] \qquad (10)$$

The moment of inertia, $\mathcal{J}$, and the decoupling constant, a, for a given band, may be determined by using this result to fit the energies within the band.

Unfortunately, the resulting energies are quasiparticle energies and will not be those of the single particle wavefunctions that determine the radial shape. If pairing is important, the low lying energies are "compressed" around the fermi energy.

E. Calculation of the Single Particle Wavefunctions

Two programs have been made available to us which calculate the eigenfunctions of a single particle moving in a deformed Woods-Saxon potential. In order to use these to determine the correct wavefunctions, we must determine the deformation and potential parameters. We should not regard deformation parameters measured by inelastic scattering experiments, for example, as necessarily appropriate for this problem. Ideally we should determine all of these parameters by demanding that all the energies ε_K, (corrected for the energy displacement of low lying levels arising from pairing effects) and, for the case of K=1/2 bands, the decoupling parameters can be fitted simultaneously. It may be necessary to use a range of deformations for various bands in order to do this. When we discuss the details, we shall see that our

form factor calculations fall short of this ideal.

Both programs finally give wavefunctions of the following form:

$$\chi_{\Omega} = \sum_{njl}{}' C_{njl}(\Omega)\, R_{nl}(\nu r^2) \left[Y_l\, S_{1/2} \right]^{\Omega}_{j} \qquad (11)$$

where R_{nl} are the radial solutions of a 3-dimensional harmonic oscillator defined in an appendix. This form is very convenient for computational purposes, and we have tabulated c_{njl} for all the cases we have treated.

Because the particular characteristics of the deformed Woods-Saxon programs have materially affected the course of this work, we shall discuss them briefly.

1. Faessler and Sheline[42] first expand the wavefunctions of a spherical Woods-Saxon potential in terms of spherical harmonic oscillator (h.o.) wavefunctions. The eigenfunctions are then identified by the radial quantum number n of the spherical h.o. component with the largest amplitude. Wavefunctions of fixed N=2n+l are then used as a basis for a calculation of the intrinsic wavefunctions of given deformation. This follows the procedure of Nilsson's original calculations where the truncated space was also confined to a fixed total oscillator quantum number N=2n+l. As l must change by two, four, . . . by virtue of parity conservation, then oscillator components, N', which could be admixed with the levels under consideration, must have N-N' =2, 4, . . . etc. Nilsson argued that the corresponding $2\hbar\omega$ energy denominators would make the mixing small, and he had the freedom to redefine the deformation

parameters such that within this new representation this mixing actually vanishes. No such freedom exists for the Woods-Saxon potential. Moreover, our primary concern is not the energy which is insensitive to such admixtures; but the wavefunction itself and $\Delta N=2$ components are potentially important for our calculations. The energy denominator argument is not convincing for large deformations where particular levels coming down from a higher major shell can exchange their identity with a level rising from a shell $\Delta N=2$ lower. The Faessler program, as it stands, does not include provision for a Y_4 deformation, although the existence of deformations with this multipolarity is well established in the rare earths[43] and even ^{20}Ne.[44] The modification needed to include this would be quite straightforward.

The program calculates the wavefunctions, energies and the $K=1/2$ band decoupling constants for all the levels of a given major shell for a series of values of β, the Y_{20} deformation: $\beta = .1,.2,.3,.4$. For a precise definition of β and of their surface parameterization see ref.[42] and Appendix II of this chapter. We employ only their "B" parameterization as it seems more closely related to the optical potential. The program has been updated since the published account of it: the more expanded radial basis is actually essential for meaningful angular distribution calculations. The added center of mass correction changes the energies but not the wavefunctions

(significantly) in the A ~25 region.

The program has one great advantage: it is rapid enough to carry out a search over many sets of well parameters. Unfortunately, the components missing from their basis are of potential importance precisely for our calculation. Moreover, levels which are weakly bound for a spherical well (for example, the d3/2 level for A ~25) carry excessive large n components into strongly deformed wavefunctions. This shortcoming seems to be fatal in some cases: important components of the 7/2+[633] state in ^{167}Er are unbound and this intrinsic state cannot be calculated by the program as it stands.

2. A much more inclusive set of basis states and a far more flexibly defined nuclear deformation are the features of the program SAXOND written by N.K. Glendenning. It has provided wavefunctions where Faessler's program failed. Because the more sophisticated calculation takes much longer, it is not possible to search for parameters which accurately reproduce the empirically determined intrinsic energies, ε_κ. Our procedure has been to choose an ""optical-model-plausible" set of parameters that works reasonably well in the particular cases discussed below. The spin-orbit strength was found to be optimally a little less than that employed by Blomquist and Wahlborn.[45]

Throughout this work, we shall continue to refer to levels by their Nilsson asymptotic quantum numbers. There are few

cases of mistaken identity that might arise. SAXOND calculates $a_{n\ell\Lambda}$ from which we calculate c_{nlj}. We shall give these together with c_{jl} calculated from

$$C_{j\ell} = \left(\sum_n C_{nj\ell}^2\right)^{1/2} \times (\text{sign of largest } C_{nj\ell}) \qquad (12)$$

This is the amplitude for the component of the wavefunction with quantum numbers jl.

It is often useful to compare these with the tabulation of c_{jl} prepared by Vergnes and Sheline[46] using equation (8) above together with Nilsson's[41] tabulation of $a_{l\Lambda}$.

In the following section we should bear in mind the result (demonstrated in chapter VI) that the strength of the direct transition to the state j of some band of the odd neutron residual nucleus is proportional to the square of the amplitude, c_j^2 for the appropriate intrinsic state.

F. Wavefunctions for the Various Nuclides Studied

1. ^{25}Mg

The low lying spectrum of ^{25}Mg can be well described in terms of three rotational bands based on the [202]5/2+, [211]1/2+ and [200]1/2+ Nilsson states; this is illustrated in fig. IV.1. The absence of a low lying K=3/2+ band suggests that first order coriolis induced admixtures are small. This spectrum readily yields the data (we make use, in part, of the analysis of Mottelson and Nilsson) which is presented in Table IV.1. It is known[47] that T=0 pairing plays a role in ^{24}Mg;

the possible role that pairing may play in deflecting the single particle levels of ^{25}Mg is more obscure. We shall ignore this factor and attempt to fit the separation energies given in this table. In Table IV.2 and Table IV.3 we present the wavefunctions for the single neutron deformed states [211] 1/2+ and [202]5/2+ respectively. The parameters are listed in Table IV.13, but we comment that these wavefunctions were calculated at a single deformation that fitted best the energies of the three intrinsic states considered. However, the varied moments of inertia, the strong dependance of the [202]5/2+ level on deformation,[85] and, as we shall see, the stripping results themselves all suggest that these bands in fact have different deformations. It must be regarded probable that the [211] 1/2+ wavefunction, at least, which was used for stripping calculations corresponds to an excessively small deformation and that $c_{3/2+}$ is too large.

Other wavefunctions have been used for ^{25}Mg stripping calculations. They were calculated using SAXOND and are given in Tables IV.4 and IV.5. It is clear that the l=4 components have small amplitudes and we shall find reason to ask if they may not in fact be larger. Recently de Swiniarski et al[44] have interpreted inelastic scattering experiments in terms of a small (small, that is, for the s-d shell), negative deformation in ^{24}Mg: β_4 =-.05. We found that by increasing β_2 and introducing reasonable β_4 deformations that the l=4

amplitudes could be at most doubled. For the effect of increasing β_2, compare Table IV.4 with Table IV.6 discussed below. This is relevant because it will turn out that the j=7/2+ states of ^{25}Mg are considerably underpopulated by our stripping theory. We found that the introduction of axial asymmetry tends to depress l=4 amplitudes and comment that the very interesting question of such asymmetry could well be explored using SAXOND wavefunctions and a "sufficient" stripping theory.

Finally, the [211] 1/2+ wavefunction has been calculated with β_2 =.4, probably appropriate for this band, and a stronger spin orbit interaction. After subtracting the c.m. energy correction estimated by F.S. with and without it, this wavefunction corresponds to the correct separation energy, 6.8 MeV and is given in Table IV.6a. Other wavefunctions were used for isolated calculations. We give only one, shown in Table IV.6. The parameters for these last two wavefunctions differ only by a difference in the real well depth of 1.2 MeV, yet there is a considerable difference in the admixture of components with large n. We shall later find that this can lead to an appreciable effect on the cross section. This should alert us to the possible errors that might be present (see Appendix I to this chapter) should we have chosen various potential and deformation parameters unwisely. We note, for instance, that Hartree-Fock solutions can be found that have a matter distribution

that is certainly not describable as purely quadrupole-deformed; in fact, the matter deformation in the centre may be oblate while the nucleus as a whole is prolate.[48]

2. ^{167}Er

The low lying spectrum of ^{167}Er is shown in Fig. IV.3. The interpretation of the levels shown is due to Harlan and Sheline.[40]

The [633] 7/2+ Band

The ground band based on the Nilsson level [633] 7/2+ is particularly interesting to us. The absence of nearby bands of K=5/2+ or K=9/2+ should, in the first place, ensure relatively small amplitudes for coriolis admixed impurities. More importantly, however, the ground state is expected to be weakly populated by the direct stripping reaction because of the small amplitude of the j=7/2 component in the [633] 7/2+ state. Thus the relatively large cross section of this level must be a consequence of inelastic processes together perhaps with a relatively long tail on the radial wavefunction.*

The Faessler-Sheline code was unable to provide a solution for this band. The wavefunction used appears in Table IV.7 and was calculated by SAXOND using parameter set D. The calculated intrinsic energy was -5.95 compared with that obtained from (eq. 10) (using Q=4.209) of -6.397. The

*We shall see that both factors are indeed important.

difference is roughly comparable to the pairing energy displacement. Most of the strength is in the 9/2+ and 13/2+ levels. The 7/2+ component has a recurrent property of weak components and one that may not appear in Faessler-Sheline calculations: the relatively large amplitude of at least one radial component of "large" n. The n=3 $c_{7/2+}$ component, although it raises the total $c_{7/2+}$ relatively slightly, could have a quite disproportionate effect in a stripping reaction. The proportionality of the cross-section to c_{jl}^2 for a given l does not hold if the radial wavefunctions are very different, and this is the basis of our comment above. Thus, although the c_{jl} calculated from eq (11) should be comparable to that of Vergnes and Sheline (because many properties are independent of the radial details of the wavefunction) we expect that very weak components, by virtue of relatively large amplitudes at the nuclear surface, may give cross sections in DWBA much larger than expected from c_j^2. This is independent of inelastic effects. We remark that these components are probably quite sensitive to the separation energy.

The [512]5/2- Band

The wavefunction, as calculated by SAXOND with the same parameters as above, is given in Table IV.8. The intrinsic energy $\varepsilon_{5/2}$=-5.57 compared with the empirical -6.074.

The 3/2- Gamma Band at 532 KeV

The 3/2- band a 532 KeV is treated as a gamma band consisting

of a K=2 phonon coupled to the [633]7/2+ Nilsson state. The relevant wavefunction is discussed above.

3. ^{155}Sm

The level structure of the odd-A isotopes of samarium has been studied by Kenefick and Sheline;[49] their interpretation of the low lying levels of ^{155}Sm in terms of Nilsson orbitals is given in fig. IV.4. The A=154 core can probably be regarded as outside the very narrow transition region and the overlap $\langle \hat{o}' | o \rangle$ is probably large in this nucleus. This overlap is conceivably lower for ^{152}Sm(d,p), though the effect on stripping may be obscured by changing quasiparticle population factors (u^2). The [521]3/2- and [523]5/2- bands must be mixed by the coriolis interaction. We shall, however, study the [521] 3/2- band, treating it as pure, commenting firstly that most of the levels are more strongly populated in stripping than those of the [523]5/2- band and secondly that in view of the stripping strength of the 5/2- level of the [523] band, the weakness of the 5/2- level of the [521] band suggests that the mixing between these bands may not be great. A search was conducted using Faessler's code to fit the neutron separation energies for the single neutron Nilsson states [521]3/2-, [523]5/2-, and [521]1/2- which are respectively -5.786, -5.4245 and -4.984. The decoupling parameter for the last level is a=.35. The parameter set D gives respectively -5.72, -5.416, -4.63 together with a=.485 for the [521]1/2- level. The

parameters R_0 and a_0 were not varied in the search. The corresponding wavefunction is listed in Table IV.9. The value of V_{so} (=10.) used by Faessler and Sheline is too great. The value of $c_{5/2-}$ is very sensitive to this parameter; V_{so}=10. would imply a value of $c_{5/2-}$ so great as to imply serious disagreement with the Kenefick and Sheline stripping results. V_{so}=8 is compatible with the value used by Blomquist and Wahlborn[45] but various optical model analyses[50] suggest that it is somewhat large, as does the $c_{5/2-}$ listed in the tabulation which is large enough to account for the cross section of this level without inelastic effects contributing. In Tables IV.10, IV.11 we give the wavefunction calculated by SAXOND firstly with the same parameters and then with V_{so} changed to 7.0. Notice that the n=1 component for l=3 j=5/2 is halved as V_{so} is reduced from 8 to 7. We shall use both these sets of wavefunctions for our stripping calculations.

The deformation β_2=.3 does not include the well established Y_4 deformation; these SAXOND wavefunctions were calculated in the first place for comparison with the Faessler wavefunctions where no Y_4 deformation can be included. The Y_{40} deformation was included for the case of the very similar nuclide ^{157}Gd.

4. ^{157}Gd

The low energy spectrum of ^{157}Gd shown in fig. IV.5 has been elucidated by Tjøm and Elbek.[51] It is rather similar to that of ^{155}Sm; in this region adding a pair of protons has a

smaller effect on the nuclear structure than adding a pair of neutrons.

The wavefunction for the [521]3/2- level in ^{157}Gd is given in Table IV.12. The parameters used in SAXOND to obtain this were set F of Table IV.12. These are the same as those used for ^{155}Sm but for the addition of a Y_4 deformation. Apart from the slight change in radius $R_0'/R_0=(157/155)^{1/3}$, the difference apparent in this wavefunction as compared with that of Table IV.11, $c_{5/2-}$ has been halved, must be due to the Y_{40} deformation.

G. Conclusion

In many cases our calculated wavefunctions contain components for which c_{jl} is small but for which the amplitude in the surface region may be comparable to the surface amplitude of components of large c_{jl}. These components correspond to levels that are weakly bound for a spherical potential. We shall show in the appendix which follows that the truncation of the radial wavefunction, when represented as a sum of components with different numbers of radial oscillator quanta, has a strong effect on the stripping cross section. Thus we must expect that j components with large surface amplitudes (that is, relatively large amplitudes of the high n components) will have direct transition cross sections considerably greater than suggested by the overall c_{jl}. An actual case is discussed in Chapter VIII where the large n=3 j=7/2+ component of the [633]7/2+ wavefunction

(see Table IV.7) of ^{167}Er is found to result in a cross section three times that predicted by proportionality to c_j^2.

Appendix I

Truncation of the Radial Wavefunction

In most of the examples of radial wavefunctions that we have been presented above, there is for each (jl) one predominating radial quantum number, the others having much smaller amplitudes in general. Nevertheless the amplitudes of these components do not usually appear to converge very well before about the eighth component. The number of radial components to be included in the calculation is an important planning consideration for the programming as each radial component requires the provision of considerable memory space. We considered it important to test the effect of varied truncations using the DWBA program TRANS.* The angular distribution of protons corresponding to the ground state of ^{25}Mg resulting from the stripping of 10.1 MeV deuterons was calculated using a Faessler wavefunction. The amplitudes of the radial components of the appropriate l=2 wavefunction are taken to be (for n=0,1,. . . 5)

-.9915 .0933 -.0682 .0538 -.0156 .0154

The calculation was carried out with respectively the first four, the first five, and finally all of the components included. The angular distributions for these three cases are shown

* I am grateful to N.K. Glendenning for the use of this program.

in fig. IV.6 with arbitrary but constant normalization. The increase in forward angle cross section as the small amplitude large-n components are added to the calculation is rather striking, as is the apparent lack of convergence. This forward angle enhancement corresponds to a reaction involving deuterons with large impact parameters undergoing stripping at the nuclear surface. In most of our calculations we have used seven (a check on our program with inelastic processes "switched off" by comparing with TRANS is possible for a maximum of seven components) or eight (the maximum for our program) components. We have found an appreciable difference, especially for the l=0 state in ^{25}Mg at small , as the number of radial components is increased from seven to eight.

The sensitivity of the cross section to the radial wavefunction is revealed in a comparison of the 12.3 MeV DWBA stripping cross sections for the two low lying 5/2+ levels in Mg. With the form factors given in Tables IV.4 and IV.5, the ratio of the cross sections normalized to the same c_{jl}^2 is about 2:1 in favour of the [202]5/2+ level. This result is due to the much longer tail of the more weakly bound 5/2+ ground state j=5/2 component (cf. eq(11) and Table IV.1). Although, as can be seen from these tables, the amplitude of the principal component for the ground state is about twice that for the excited 5/2+ state, the amplitudes

of the components of higher n are three to four times greater. (This difference in the wavefunctions may no longer be true if the [211] 1/2+ level were calculated with a more realistic $\beta_2 = .4.$)

As long as our primary object is an understanding of the importance of inelastic processes in stripping, eight radial components yield a meaningful model calculation. We bear in mind, of course, that in any case the form factor is not exactly the wavefunction of a Woods-Saxon well. We remark that as long as uncertainties in the nuclear model make the neutron separation energy uncertain, then the cross section is uncertain to a greater degree than one might gather from the literature.

Appendix II

Parameterization for the Potentials

We have employed wavefunctions calculated using a Woods-Saxon potential and we have quoted the corresponding values of the parameters which define this potential. For reference we show how these parameters are defined. Faessler and Sheline define the following real potential

$$V(r) = -V_0 f(r) + C_0 (1.4)^2 \frac{1}{r} \frac{\partial}{\partial r} f(r)\, 2\, \underset{\sim}{l} \cdot \underset{\sim}{s}$$

Equations (1) and (7) of Faessler and Sheline[42] do not agree; (7) appears to correspond to the program.* We have used $V_{so} \equiv C_0$.

$$f(r) = \left[1 + \exp\left[(r - R_0 A^{1/3})/a_0\right]\right]^{-1}$$

The deformation of the nuclear surface is parameterized according to F. and S. method B as

$$R = R_0\left[1 - \sum_{\lambda} \beta_{\lambda 0}^2/(4\pi) + \sum_{\lambda} \beta_{\lambda 0} Y_{\lambda 0}(\theta)\right]$$

This includes volume conservation, but their expansion of the surface is carried out only to second order. The parameterization used by SAXOND is similar apart from slightly different values of, for example, the spin orbit constant. We take advantage of the provision for the expansion of the surface to be carried to much higher order.

---

*We are grateful to Professor Sheline for forwarding this program to us.

Appendix III

Harmonic Oscillator Wavefunctions

We use the sign convention of Talmi quoted in de-Shalit and Talmi;[52] the wavefunctions have the same sign at the origin. This is contrary to the Nilsson convention in which the solutions have the same sign at infinity. Our radial quantum numbers start at zero so that the energy

$$E_{n\ell} = [2n+\ell+3/2]\hbar\omega = [N+3/2]\hbar\omega$$

where n=number of nodes excluding those at the origin and at infinity. We shall always use $\hbar\omega = 41A^{-1/3}$ MeV. With these conventions, together with the radial normalization

$$\int |R_{n\ell}(r)|^2 r^2 dr = 1$$

and the definition $\nu = m\omega/\hbar$ (twice that defined by Talmi) we have

$$R_{n\ell} = \left[\frac{2^{\ell-n+2}\,\nu^{\ell+3/2}\,(2\ell+2n+1)!!}{\sqrt{\pi}\,[(2\ell+1)!!]^2\,n!}\right]^{1/2} r^\ell e^{-\frac{\nu}{2}r^2} V_{n\ell}(\nu r^2)$$

where $V_{n\ell}$ is the polynomial

$$V_{n\ell}(x) = \sum_{k=0}^{n} (-)^k 2^k \binom{n}{k} \frac{(2\ell+1)!!}{(2\ell+2k+1)!!} x^k$$

Our R_{nl} thus differs by a factor of r from that of Talmi.

Table IV.1. Neutron separation energies E^s_κ for the three lowest intrinsic states of ^{25}Mg. The first four columns are taken from Mottelson and Nilsson,[85] and the fifth is calculated using eq (10). The sixth is calculated on the basis of a ground state to ground state neutron separation energy of 7.331 MeV.

Orbital	$E_{J=K}$	$\hbar^2/2\mathcal{J}$	a	ϵ_κ	E^s_K
[202] 5/2+	0.0	.23	0	.862	-6.469
[211] 1/2+	0.58	.165	-.2	.5057	-6.8253
[200] 1/2+	2.56	.15	-.42	2.4445	-4.8865

Table IV.2. Single neutron wavefunctions expressed in terms of c_{njl} for the [211] 1/2+ band of ^{25}Mg. Calculated using the F.-S. program using parameter set A of Table IV.13. These parameters were found after many trials, and the deformation was found by graphical extrapolation. This wavefunction was used for a series of model calculations but is criticized in the text. Note the slow convergence (i.e. c_{njl} does not rapidly become small for large n, as far as stripping is concerned) characteristic of l=0 wavefunctions, and the fact that the 3/2+ component, which is nearly unbound for $\beta_2 = 0$, is more slowly convergent than the 5/2+ component.

n \ j	1/2+	3/2+	5/2+
0	-.033973	-.70383	-.45113
1	-.508747	.08642	.04245
2	.108067	-.07797	-.03103
3	-.070755	.05019	.02448
4	.053742	-.02306	-.007098
5	-.02528	.01969	.007007
6	.01982	-.01181	-.003958
7	-.013091	.00852	.002184
8	.00858	-.00456	-.001865
c_j	-.530	.716	.455
c_j^2	.2809	.5126	.2070

Table IV.3. Wavefunction for the single neutron level [202]5/2+ for ^{25}Mg. Calculated using parameter set A of Table IV.13 and F.-S. program. (See caption to Table IV.2.)

n \ j	5/2+
0	-.9915
1	.0933
2	-.0682
3	.0538
4	-.0156
5	.0154
6	-.0087
$c_{5/2}$	-1.
$c^2_{5/2}$	1.

Table IV.4. Neutron wavefunction for [211] 1/2+ level in ^{25}Mg. Calculated by SAXOND using parameter set B. The l=4 components, though giving rise to small direct stripping amplitudes can have a significant effect when the direct amplitudes are added coherently to indirect amplitudes.

n \ j	1/2+	3/2+	5/2+	7/2+	9/2+
0	.04408	.7496	.4532	.0838	.0641
1	.4260	-.1242	-.0269	.00026	.00607
2	-.09678	.06134	.03087	.00369	.00341
3	.05116	-.04387	-.02358	-.00411	-.00313
4	-.03909	.01821	.00595	.000096	-.00081
5	.01752	-.01262	-.00681	-.00092	-.00112
6	-.01230	.00741	.00344	.00036	-.00005
7	.00756	-.00382	-.00158	.00007	.00004
c_j	.4444	.7639	.4558	.0839	.0646
c_j^2	.19749	.58358	.20772	.00705	.00417

Table IV.5. Neutron state [202]5/2+ calculated by SAXOND using parameter set B. (See caption to Table IV.4.)

n \ j	5/2+	7/2+	9/2+
0	-.98321	.03645	-.08713
1	.10896	.00308	-.00742
2	-.08834	.00272	-.00608
3	.05943	-.01496	.00384
4	-.02268	-.00012	.00047
5	-.01952	-.00063	.00153
6	-.01034	.00001	-.00002
7	.00573	-.00005	.00007
c_j	.9955	.0367	.0877
c_j^2	.99095	.00135	.00770

Table IV.6. Wavefunction for [211] 1/2+ level in ^{25}Mg. Calculated by SAXOND using parameter set C.

n \ j	1/2+	3/2+	5/2+	7/2+	9/2+
0	-.05296	-.67461	-.44307	-.09696	-.08797
1	-.51501	.15404	.01888	.00656	-.00788
2	.14136	-.06976	-.03005	-.00017	-.00077
3	-.07549	.04623	.02398	.00512	.00466
4	-.05423	-.02294	-.00576	-.00112	.00110
5	-.02718	.01412	.00668	.00096	.00165
6	.01784	-.00777	-.00307	-.00072	-.000002
7	-.01002	.00347	.00077	0.	0.

Table IV.6a. Wavefunction for [211] 1/2+ level in ^{25}Mg. Calculated by SAXOND using parameter set Cx.

n \ j	1/2+	3/2+	5/2+	7/2+	9/2+
0	.04945	.68838	.44232	.09972	.08891
1	.50643	-.14501	-.01236	-.00513	.00907
2	-.12809	.06510	.02814	.00433	.00468
3	.06765	-.04333	-.02232	-.00501	-.00449
4	-.04877	.02057	.00455	.00091	-.00125
5	.02330	-.01271	-.00606	-.00093	-.00165
6	-.01539	.00690	.00262	.00068	-.00005
7	.00852	-.00306	-.00057	0.	0.
c_j^2	.2831	.5016	.1971	.010	.008

Table IV.7. Neutron [633] 7/2+ state for A=167. Calculated by SAXOND with parameter set D.

n \ j	7/2+	9/2+	11/2+	13/2+
0	-.01057	-.21947	-.081689	.921002
1	.021815	-.29894	.0084057	.033239
2	-.004832	-.012672	.003687	-.034945
3	-.018951	.023293	.002841	-.052152
4	-.001935	.031126	-.001737	-.001732
5	.0011135	.0028593	.00071303	-.005644
6	.000635	-.00317	.0003314	-.008598
c_j	.031	-.3731	-.0823	.923
c_j^2	.000961	.1392	.00677	.8519

Table IV.8. Neutron state [512]5/2- for A=167. Calculated by SAXOND using parameter set D. The c_{nlj} shown were calculated and normalized by the stripping program from A_{nlj}. The c's shown were normalized without the l=7 components, and the l=3 and l=5 components shown are about 1% larger than used in the calculation with the complete wavefunction. We quote for reference the c_j values tabulated by Vergnes and Sheline.[46]

n \ j	5/2-	7/2-	9/2-	11/2-	13/2-	15/2-
0	-.016067	-.01695	.37247	-.25568	.08464	-.10656
1	.08101	-.8700	.08396	-.13232	.01886	-.02961
2	-.01277	.01360	.01089	-.01048	-.000958	.001528
3	.00061	-.00722	-.01973	.02028	-.007102	.01106
4	-.006299	.07329	-.00968	.01688	-.00334	.00585
5	.00252	-.00486	-.00332	-.00332	-.00109	.00187
6	-.000022	.00484	.00136	-.001598	.002014	-.00219
c_j	.083	-.873	.383	-.289	.087	-.111
c_j^2	.0069	.762	.147	.0835	.0076	.0123
c(V&S)	.1	-.8867	.376	-.25		

Table IV.9. Neutron wavefunction [521] 3/2- calculated by F-S using parameters D. Note the large value of $c_{5/2^-}$ compared with the Vergnes and Sheline value also shown. A=155.

n \ j	3/2-	5/2-	7/2-	9/2-	11/2-
0	.0214	.0011	-.0509	.5689	-.3263
1	..0221	.1638	-.6512	.0894	-.0228
2	.3119	-.0015	.0085	.0184	.0134
3	-.0362	-.0106	.0033	-.0287	.0183
4	.0186	.01725	.0588	-.0099	.0029
5	-.0423	-.0019	-.0034	-.0058	-.0016
6	.0121	.0041	.0022	-.0029	-.0031
7	-.0085	-.0037	-.0113	.0018	-.0012
c_j	.3194	.1652	.6560	.577	-.3279
c_j^2	.1018	.0273	.4303	.3529	.1076
c_j(V&S)	.3234	-.001	.7271	.5045	-.3349

Table IV.10. Neutron state [521] 3/2-. Calculated for A=155 by SAXOND using parameters D. They are truncated with $N=2n+l \leqslant 13$ according to the capacity of the stripping program at the time of calculation.

n \ j	3/2-	5/2-	7/2-	9/2-	11/2-
0	.01872	-.06601	-.02644	.55926	-.2728
1	.11053	-.1658	-.66526	.03143	-.10994
2	.31720	-.02244	.06989	.00260	.001522
3	-.02697	.00403	.00658	-.02317	.02214
4	-.00749	.01599	.04966	-.00366	.01389
5	-.03311	.00445	-.01129	0.	0.
6	.00403	0.	0.	0.	0.

Table IV.11. Neutron state [521] 3/2-. See Table IV.10 for comment. Parameters E.

n \ j	3/2-	5/2-	7/2-	9/2-	11/2-
0	.02177	-.05323	-.02479	.48819	-.3094
1	.12254	-.07953	-.69447	.03796	-.11743
2	.3600	-.02829	.07759	.000929	.00230
3	-.03215	.00367	.00598	-.02156	.02440
4	-.00817	.00959	.05111	-.00415	.01452
5	-.0374	.00507	-.0124	0.	0.
6	.00484	0.	0.	0.	0.

Table IV.12. Neutron wavefunction [521] 3/2- for A=157. SAXOND was used with parameters F.

n \ j	3/2-	5/2-	7/2-	9/2-	11/2-	13/2-	15/2-
0	-.02148	.04376	.02096	-.47416	.3238	-.1133	.08916
1	-.09099	.03827	.70259	-.05374	.1386	-.01624	.03418
2	-.32581	.02974	-.07396	-.00142	-.00407	.00464	-.00126
3	.03286	-.00380	-.00218	.02268	-.02733	.00874	-.01095
4	.00485	-.00620	-.05279	.00507	-.01597	.00252	-.00629
5	.03429	-.00491	.01293	.00164	-.00036	.00008	-.00169
6	-.00617	.00033	-.00189	-.00212	.00370	-.00182	.00286
7	.00080	.00099	.00859	0.	0.	0.	0.
c_j^2	.1172	.00434	.5026	.2283	.1251	.0132	.0093

Table IV.13. Parameters used in various calculations of the neutron bound state wavefunctions.

Identifier	V	R_0	a_0	V_{so}	R_{so}	a_{so}	β_2	β_4
A	-48.7	1.25	.65	-4.5	1.25	.65	.24	0.
B	-48.7	1.25	.65	-4.5	1.25	.65	.3	0.
C	-47.0	1.25	.65	-7.0	1.25	.65	.4	0.
Cx	-48.2	1.25	.65	-7.0	1.25	.65	.4	0.
D	-45.5	1.25	.65	-8.0	1.25	.65	.3	0.
E	-45.5	1.25	.65	-7.0	1.25	.65	.3	0.
F	-45.5	1.25	.65	-7.0	1.25	.65	.3	.05

Figure Captions for Chapter IV

Fig. IV.1 Low lying levels of ^{25}Mg.

Fig. IV.2 Low lying spectrum of ^{166}Er showing the ground band and the gamma band. The ground band follows the I(I+1) energy spacing about as well as that of most nuclei. The gamma band, however, follows this spacing extraordinarily closely (see Mackintosh[29]).

Fig. IV.3 Partial level diagram for ^{167}Er. The 3/2- band at 532 KeV has been interpreted as a K-2 γ-band coupled to the [633]7/2+ single particle state and mixed with [651]3/2+ and [402]3/2+.

Fig. IV.4 The low lying spectrum of ^{155}Sm. The assignment of Nilsson asymptotic quantum numbers, shown beneath each bandhead, is that of Kenefick and Sheline.[49] There is a 1/2- band at .824 MeV and many unassigned levels, some strongly fed in (d,p) reactions, beginning at .364 MeV. The relative stripping intensity at 65° is shown in parentheses.

Fig. IV.5 Part of the low energy spectrum of ^{157}Gd. The separation between the [521]3/2- and the [523]5/2- bands is somewhat greater than is the case for ^{155}Sm and suggests somewhat less coriolis mixing (see Tjom and Elbek[51]). The large cross section[51] to the .435 MeV level is, however, somewhat anomalous when compared with the results of Kenefick and Sheline. This level is not (ref.[46]) unusually sensitive to deformation.

Fig. IV.6 A study of the effect of varying the number of radial harmonic oscillator components in the formfactor of the l=2 neutron on the stripping of 10.1 MeV deuterons leading to the ground state of ^{25}Mg.

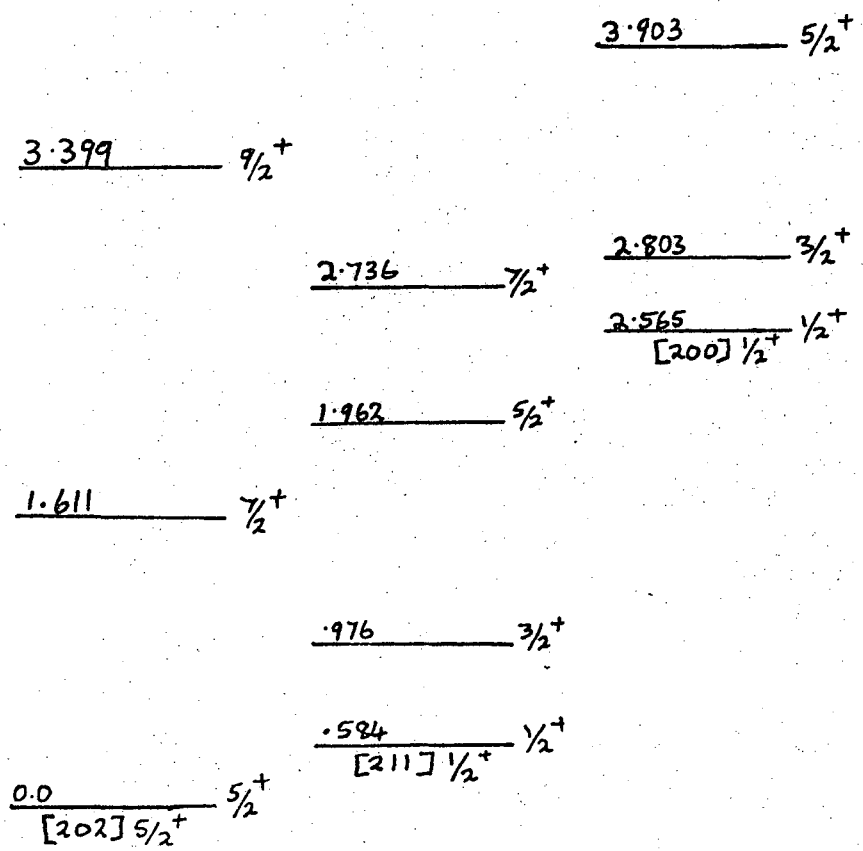
3·903 5/2+
3·399 9/2+
2·803 3/2+
2·736 7/2+
2·565 1/2+
[200] 1/2+
1·962 5/2+
1·611 7/2+
·976 3/2+
·584 1/2+
[211] 1/2+
0·0 5/2+
[202] 5/2+

Fig. IV.1

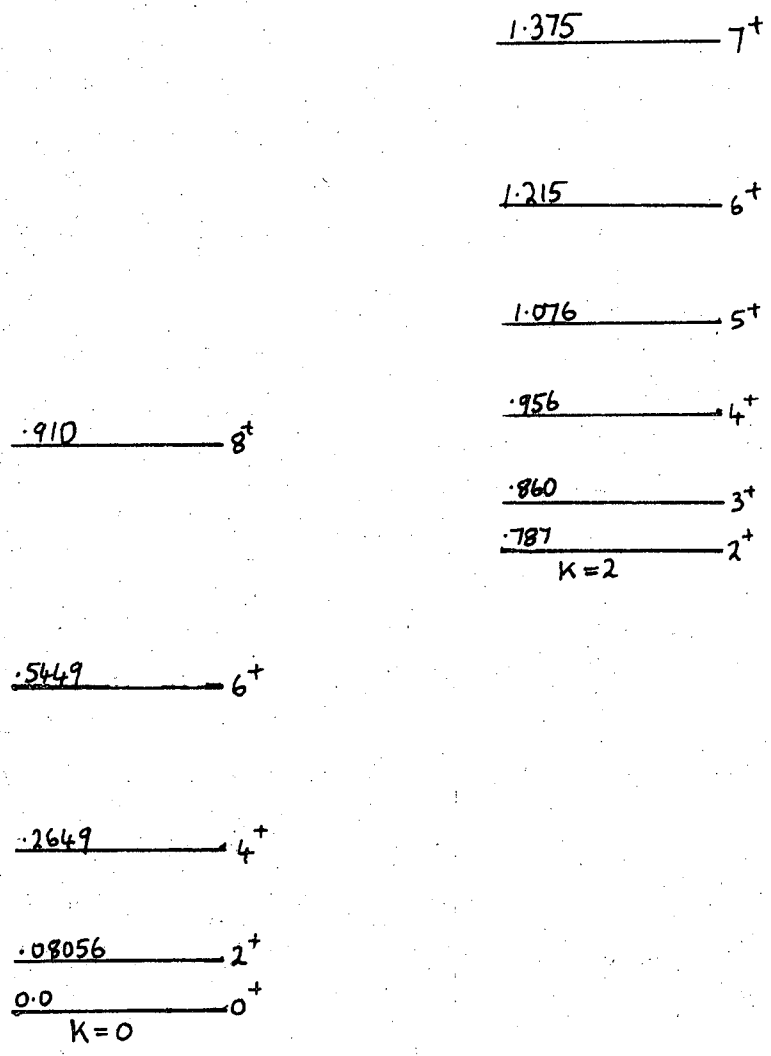
1·375 7+
1·215 6+
1·076 5+
·956 4+
·910 8+
·860 3+
·787 2+
K=2
·5449 6+
·2649 4+
·08056 2+
0·0 0+
K=0

Fig. IV.2

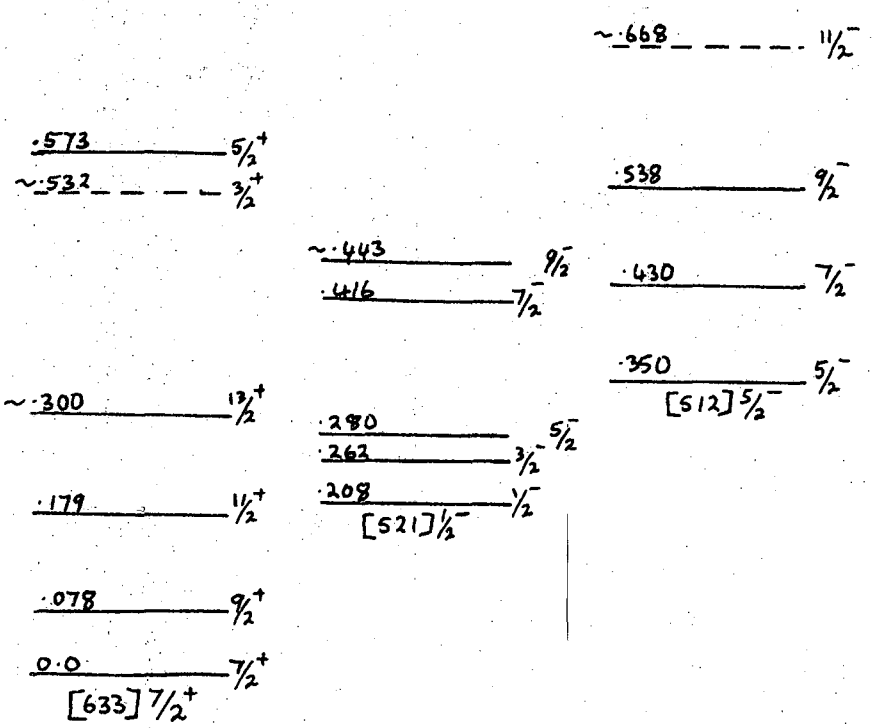
~.668 11/2⁻
.573 5/2⁺
~.532 3/2⁺
.538 9/2⁻
~.443 9/2⁻
.416 7/2⁻
.430 7/2⁻
.350 5/2⁻
[512] 5/2⁻
~.300 13/2⁺
.280 5/2⁻
.263 3/2⁻
.208 1/2⁻
[521] 1/2⁻
.179 11/2⁺
.078 9/2⁺
0.0 7/2⁺
[633] 7/2⁺

Fig. IV.3

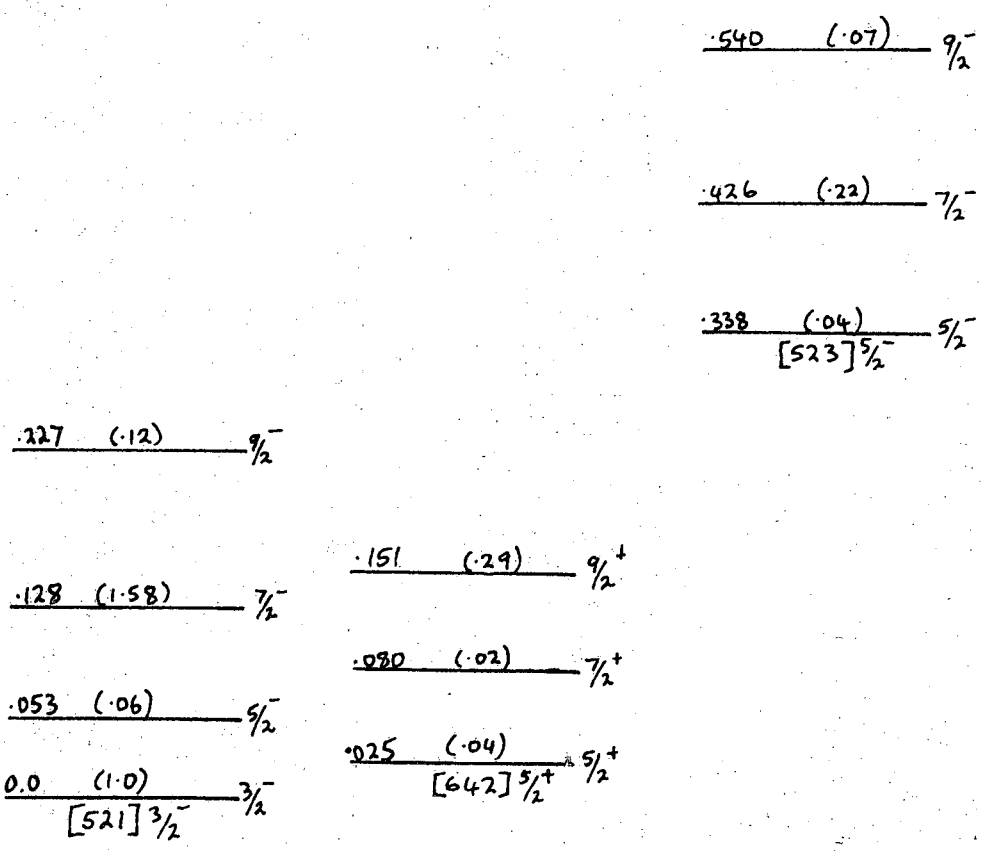
.540 (.07) 9/2⁻
.426 (.22) 7/2⁻
.338 (.04) 5/2⁻
[523] 5/2⁻
.227 (.12) 9/2⁻
.151 (.29) 9/2⁺
.128 (1.58) 7/2⁻
.080 (.02) 7/2⁺
.053 (.06) 5/2⁻
.025 (.04) 5/2⁺
0.0 (1.0) 3/2⁻
[521] 3/2⁻
[642] 5/2⁺

Fig. IV.4

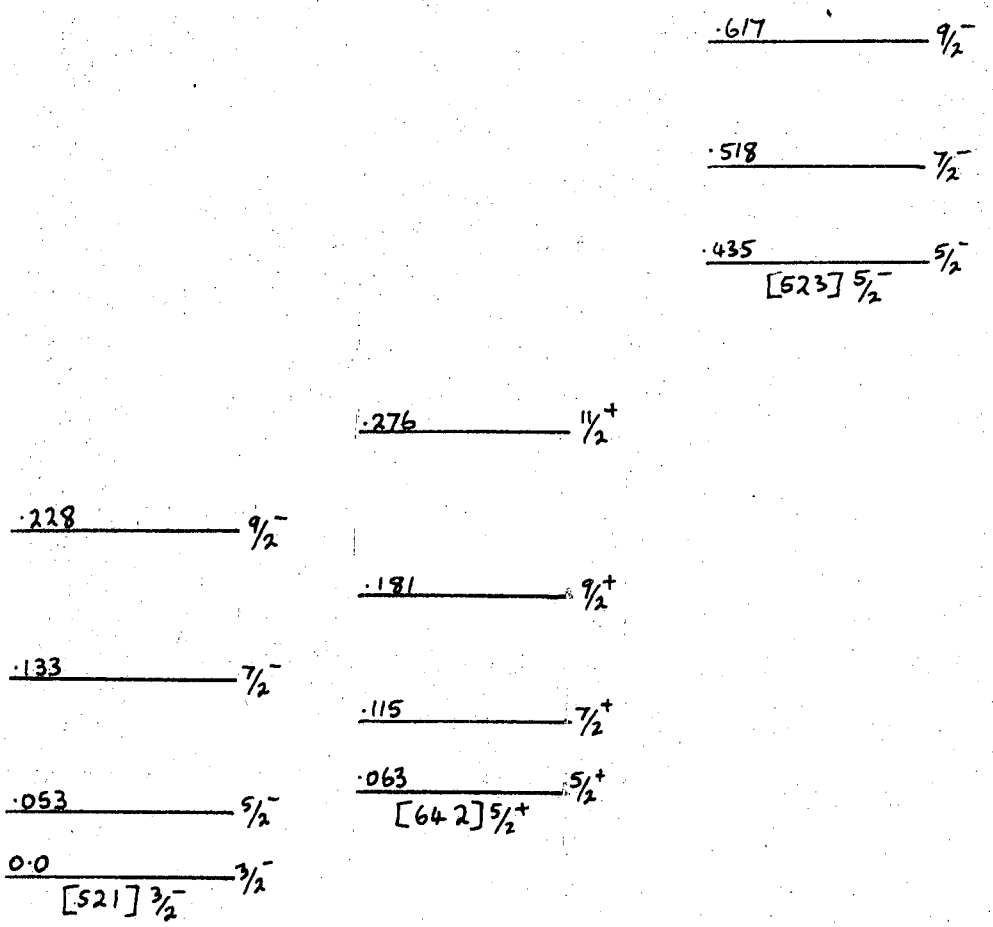
·617 9/2⁻
·518 7/2⁻
·435 5/2⁻
[523] 5/2⁻
·276 11/2⁺
·228 9/2⁻
·181 9/2⁺
·133 7/2⁻
·115 7/2⁺
·063 5/2⁺
·053 5/2⁻
[642] 5/2⁺
0·0 3/2⁻
[521] 3/2⁻

Fig. IV.5

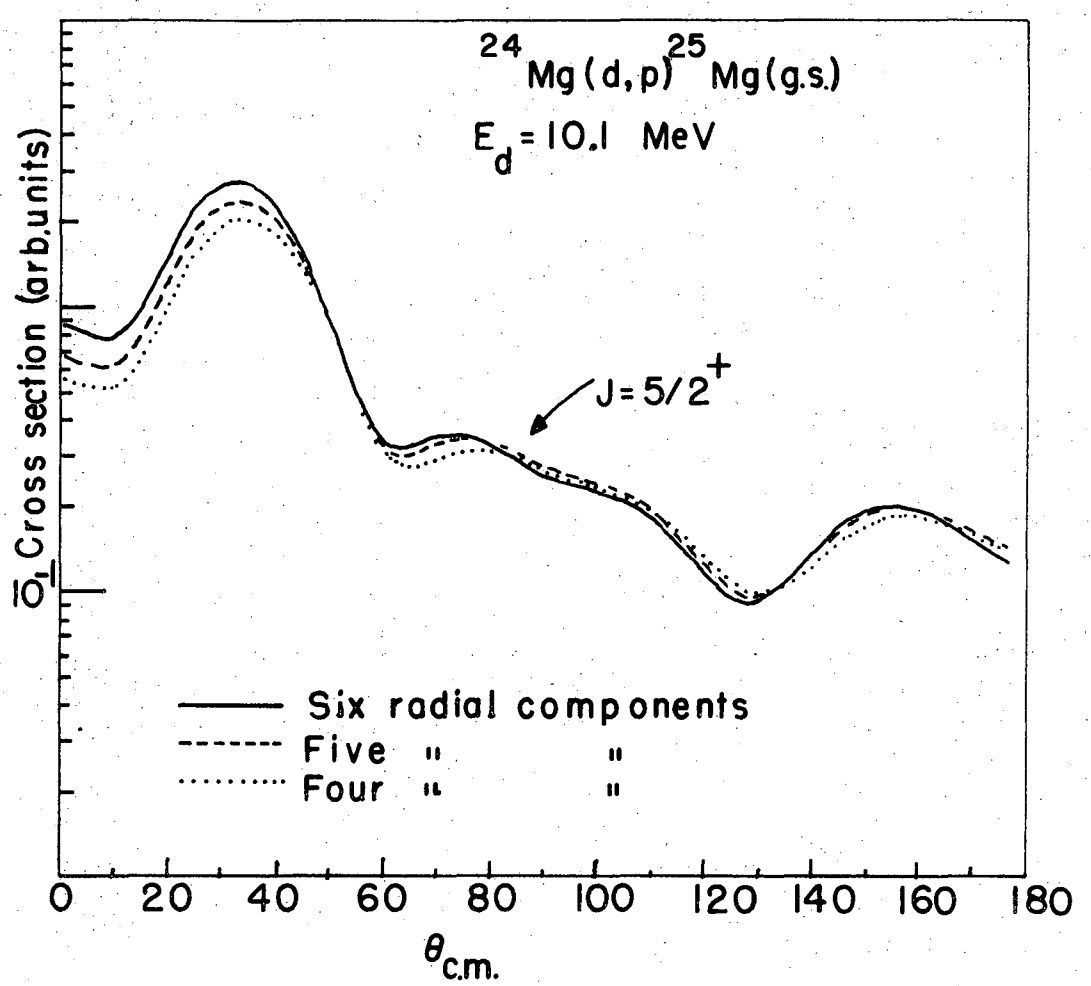

XBL 701-213

Fig. IV.6

V. COUPLED CHANNEL CALCULATIONS OF STRIPPING CROSS SECTION

In chapter III it was shown how inelastic transitions could be incorporated into the description of stripping reactions by solving the problem defined by the equations

$$(H_A + T_d + V_d - E)\chi_d^{(+)} = 0 \qquad (1)$$

$$(H_{A+1} + T_p + V_p - E)\chi_p^{(+)} = -V_{np}\chi_d^{(+)} \qquad (2)$$

subject to the boundary condition that $\chi_d^{(+)}$ contains incoming waves in the target channel, whereas $\chi_p^{(+)}$ contains only outgoing waves. In this chapter we show how these can be solved. The discussion in this chapter is independent of the details of the nuclear models. Although V_d and V_p are model interactions we omit the tilde introduced in Chapter III to distinguish model quantities. The reaction A(d,p)A+1 is understood throughout.

A. Deuteron Channels

The channel enumeration could be given for spin s particles, but certain features of the deuteron case warrant special attention. In our calculations we consider only the ground state of the deuteron, and the motion of its center of mass. The model hamiltonian of the target nucleus we denote by H_A and its eigenstates by $\Phi_{\alpha J_\alpha}(A)$. The label α sufficiently

labels the state, but we may append the spin of the state, J_α . Thus we write

$$(H_A - E_\alpha)\,\Phi_{I_\alpha} = 0 \qquad (3)$$

The parity of Φ_α we denote by π_α . In general, the wavefunction $\Phi_\alpha(A)$ involves the coordinates of the A nucleons; in the case where H_A is some collective hamiltonian, only the appropriate collective coordinates appear. The total model hamiltonian of the system may be written, appropriately to the "asymptotic deuterons" partition, as

$$H = H_A + T_d + V_d \qquad (4)$$

where T_d is the deuteron-nucleus c.m. kinetic energy, and V_d is the asymptotically vanishing model interaction representing the effective interaction. In our case, it is a deformed optical potential involving the coordinates of the deuteron c.m., r_d, and the nuclear collective coordinates. The total wavefunction of this system is thus the solution of

$$(H - E)\,\Psi(r_d, A) = 0,$$

i.e. equation (1) above.

The interaction V_d contains within its definition a specification of a truncated basis P_d. Given the nuclear states belonging to P, we must now enumerate all of the channels corresponding to the same values of the conserved quantum numbers I and π , where I is the total angular momentum of the system and π , the parity. The number of these states we

shall refer to as N_d and will depend on (I,π). In order to facilitate the use of a spin-orbit interaction for the projectile, we couple the angular momenta as follows. First the spin and the orbital angular momentum, l_c, of the deuteron in channel "c" are coupled to total orbital angular momentum j_c:

$$\mathcal{Y}^{m_c}_{l_c 1 j_c} = \left[Y_{l_c}(\hat{r}_d), \chi_1(d) \right]^{m_c}_{j_c} \qquad (5)$$

The 1 subscript refers to the deuteron spin; we denote by $\chi_1(d)$ the spin-one deuteron wavefunction. The bracket denotes angular momentum coupling in the usual way. These spin-orbit functions, $\mathcal{Y}$, are coupled to the nuclear state to form wavefunctions of total angular momentum I and parity π:

$$\varphi^{m}_{c\pi I}(\hat{r}_d, A) = \left[\mathcal{Y}_{l_c 1 j_c}, \Phi_{\alpha_c J_c} \right]^{m}_{I} \qquad (6)$$

Thus we have coupled according to $\vec{I} = \vec{j}_c + \vec{J}_c = (\vec{l}_c + \vec{1}) + \vec{J}_c$. The parity, $\pi = (-)^{l_c} \pi_d$, and I define those channels which must be considered together as a solution of the coupled equations. The label c which labels φ in eq(6) is used to summarize the set of quantum numbers appearing on the r.h.s. We use $\bar{c}$ to denote any set which contains the ground state of the target.

The total wavefunction for given (I,π) is now

$$\Psi^{\bar{c} I \pi}_{m} = \frac{1}{r} \sum_{c'} u^{\bar{c}\,\pi I}_{c'}(r_d)\, \varphi^{m}_{c'\pi I}(\hat{r}_d, A) \qquad (7)$$

In this equation, the wavefunction is labelled by $\bar{c}$ corresponding to the fact that the coupled system of equations that the u's satisfy is solved according to the boundary condition that only g.s. channels c have incoming waves. In the case of deuterons, (I, π) do not determine the channel parameters for the incoming waves, as they would for protons incident on a spin zero target. For nuclear state α_c, with spin J_c, we have

$$J_c = |I - j_c| \quad \ldots \quad I + j_c$$

$$l_c = |j_c - 1|, \; j_c, \; j_c + 1$$

Of these three values of l_c, the value $l_c = j_c$ has parity opposite to that of the other two so that l_c may have either one or two values for specified (I, π) consistent with $\pi = (-)^{l_c} \pi_\alpha$. In this work we shall always have deuterons incident on even targets so that the entrance channels always have nuclear spin and parity 0^+. In this case l_c defines the parity of the channel and $I = j_c$ the total angular momentum of the deuteron. For a given I, the channels divide into two groups of opposite parity, viz., those with $\pi = (-)^I$, for which $l_c = j_c = I$ in the entrance channel, and those with $\pi = (-)^{I+1}$ for which we have entrance channels of $l_c = I-1$ and $I+1$, so that the entrance channel is no longer specified, in general, by (I, π). This results in considerable complication not only for the (d,d') calculation, but for the entire stripping problem.

Just how we handle this is discussed later in this chapter.

B. Proton Channels

Given I and π of the system, we must specify the coupling of the proton channels, N_p in number. The coupling scheme is the same:

$$\mathcal{Y}_{\ell_c \frac{1}{2} j_c} = \left[Y_{\ell_c}(\hat{r}_p), \chi_{1/2}(p) \right]^{m_c}_{j_c} \tag{8}$$

$$\varphi^{M}_{c\pi I}(\hat{r}_p, A+1) = \left[\mathcal{Y}_{\ell_c \frac{1}{2} j_c}, \Phi^{(A+1)}_{\alpha_c J_c} \right]^{M}_{I} \tag{9}$$

$$\left.\begin{aligned} j_c &= |I - J_c| \ldots\ldots I + j_c \\ \ell_c &= j_c - \tfrac{1}{2}, \; j_c + \tfrac{1}{2} \geq 0 \end{aligned}\right\}$$

$$\pi = \pi_\alpha (-)^{\ell_c}$$

For stripping calculated according to our method, we need not consider incoming waves of protons. Although a (p,p') calculation involving even nuclei is more straightforward than (d,d'), we would be involved with (p,p') on odd nuclei, if the most consistent procedure was being followed. In this case, the calculation would entail an obvious extension of the procedure employed for (d,d') that is described below.

C. Coupled Channel Solution of Stripping

The following is a general formulation of the coupled channel method of calculating stripping reaction cross sections. Programming details are not given here though the block diagram of the arrangement of the programs, (fig.V.1) and its caption might clarify what follows.

In order to calculate the proton wavefunctions from the stripping equation (c.f., eq.(2))

$$(E - H)\psi_p^{(+)} = V_{np}\psi_d^{(+)} \qquad (10)$$

we must first calculate the deuteron wavefunctions $\psi_d^{(+)}$. (These are calculated by the program SCATERD, together with the (d,d') S-matrix elements which may, if desired, be used to calculate the appropriate (d,d') cross section in program CROSSD.)

The program SCATERD solves the following coupled differential equations, defined for given values of the conserved quantities, I, the total angular momentum of the system, and π , the parity.

$$\left\{ -\frac{\hbar^2}{2\mu_d}\left(\frac{\partial^2}{\partial r_d^2} + \frac{l_c(l_c+1)}{r_d^2}\right) + V_{cc}^{I,\pi} - E_c \right\} U_c^{I\pi\bar{c}}(r_d)$$

$$= -\sum_{c' \neq c} V_{cc'}^{I\pi}(r_d)\, U_{c'}^{I\pi\bar{c}}(r_d) \qquad (11)$$

Where $E_c = E - E_a$.

The notation is similar to that found in ref.[35] Equation(11) is a partial wave decomposition of eq(1).

We shall need

$$V_{cc'}^{I\pi} = \left\langle \varphi_{c\pi i}(\hat{r}_d, A) \middle| V(\vec{r}_a, A) \middle| \varphi_{c'\pi I}(\hat{r}_a, A) \right\rangle \qquad (12)$$

and the channel momentum

$$k_c^2 = \frac{2\mu}{\hbar^2} E_c$$

It is important, in our case, to retain the $\bar{c}$ label on $U_c^{I\pi\bar{c}}$, as the incoming channel, $\bar{c}$, is not specified by I, π as explained above.

In the asymptotic region, the solution of equation(6) in channel c becomes

$$u_c^{I\pi\bar{c}} \rightarrow \delta_{c\bar{c}} I_{\bar{c}}(k_{\bar{c}} r_d) - \left(\frac{k_c}{k_{\bar{c}}}\right)^{1/2} U_{\bar{c}c}^{I\pi} O_c(k_c r_d)$$

$$= \delta_{c\bar{c}} I_{\bar{c}}(k_{\bar{c}} r_d) - \left(\frac{v_c}{v_{\bar{c}}}\right)^{1/2} U_{\bar{c}c}^{I\pi} O_c(k_c r_d) \qquad (13)$$

where

$$I_\ell^* = O_\ell = G_\ell + i F_\ell \rightarrow \exp\left[i\left(kr - \eta \ln(2kr) - \ell\pi/2 + \sigma_\ell\right)\right] \qquad (14)$$

where F and G are the regular and irregular (real) coulomb wavefunctions, $\eta = \mu_a Z Z' e^2 / \hbar k_c$ and σ is the coulomb phase shift. This boundary condition may be applied to eq(11) according to the method described in ref.[4] For the case of $\pi = (-)^{I+1}$, SCATERD stores the matrix of trial

solutions and applies the boundary condition eq(13) for the two channels c successively. The matrix inversion that provides us with the (d,d') matrix $U_{\bar{c}c'}$ also specifies the appropriate boundary condition at the origin which permits equation (11) to be reintegrated so that the wavefunctions $u_c^{I\pi\bar{c}}(r_d)$ with asymptotic form eq(13) may be obtained for r_d from near zero to the external region. The proton wavefunctions, $\chi^{(+)}$, corresponding to our particular model are solutions of the inhomogeneous Schroedinger equation, eq(2) above, where V_p is the model effective interaction (in our case, a deformed complex optical potential) similar to V_d. We can make a partial wave decomposition of equation (2) and obtain for the radial channel wavefunctions of $\chi_p^{(+)}$ (see eq(9)) the following set of inhomogeneous coupled differential equations:

$$\left\{ -\frac{\hbar^2}{2\mu_p}\left(\frac{d^2}{dr_p'^2} + \frac{\ell_{c'}(\ell_{c'}+1)}{r_p'^2}\right) + V_{c'c'}^{I,\pi} - E_{c'} \right\} u_{c'}^{I\pi\bar{c}}(r_p')$$

$$+ \sum_{c''\neq c'}{}' V_{c'c''}^{I\pi}(r_p')\, u_{c''}^{I\pi\bar{c}}(r_p') = -\sum_{c'''=1\cdots N_d} S_{c'c'''}^{I\pi}\, u_{c'''}^{I\pi\bar{c}}(r_d)$$

$$\equiv S \qquad (15)$$

The sum on the r.h.s. is over the N_d deuteron channels. The $\bar{c}$ superscript on the proton wavefunction is defined by the

incoming deuteron channel corresponding to the deuteron wavefunctions which appear in the "source term", S. We shall refer to $S^{I\pi}_{c'c'''}$ as the "source term factors."

As for a given I and π, there are alternately one or two incoming channels c; for half the (I, π) duals, eq(15) must be solved twice, though the time consuming homogeneous integration need only be carried out once. By imposing the boundary condition

$$u^{I\pi\bar{c}}_{c'} \longrightarrow - \left(\frac{V_{\bar{c}}(d)}{V_{c'}(p)}\right)^{1/2} O_{c'}(k_{c'} r_{p'}) U^{I\pi}_{\bar{c}\,c'} \qquad (16)$$

on the solutions of eq(15) we are able to extract all of the scattering matrix elements, $U^{I\pi}$, required to calculate the cross section. The momentum in the deuteron channels is given by

$$k_{c'}^2 = \frac{2M_d}{\hbar^2} E_{c'}$$

We notice that radial coordinate r_p' appears in eq(15). This is defined by

$$\vec{r}_{p'} = \vec{r}_p - \frac{M_p}{M_{A+1}} \vec{r}_n \qquad (17)$$

In the zero range approximation where

$$V(\vec{r}_p - \vec{r}_n)\, \varphi_d(\vec{r}_p - \vec{r}_n) = D_0\, \delta(\vec{r}_p - \vec{r}_n)$$

we find from eq(13) that

$$r_{p'} = r_p \left(\frac{A}{A+1}\right) = r_d \left(\frac{A}{A+1}\right) \qquad (18)$$

The source term factors appearing in eq(11) are given by

$$S^{I\pi}_{c'c''} =$$

$$= \int \varphi^{\dagger}_{c'\pi I}(\hat{r}_{\rho'}, \sigma, A+1)\, V_{\rho n}\, \frac{r_{\rho'}}{r_d}\, \varphi_{c''\pi I}(r_d, A)\, d\Omega_{\rho'}\, d\vec{r}^{\,3A}_{n}\, d^3 r_n \qquad (19)$$

The matrix $S^{I\pi}$ is independent of c. The particular form of S for our model will be discussed in Chapter VI.

D. General Expression for Reaction Cross Section

The S-matrix elements $U^{I\pi}_{\bar{c}c'}$ are sufficient to calculate the reaction angular distribution, polarization or any of the depolarization functions associated with possible deuteron polarization. We shall derive the angular distribution and polarization for any reaction, including inelastic scattering.

The central physical property involved in the basic superposition principle of quantum mechanics: given a solution of the Schroedinger equation with, for example, incoming waves in some particular channel, then any superposition of such solutions is also a solution.

The asymptotic wavefunction eq(7) may be written in the form

$$\Psi^{\bar{c}I\pi}_{M} \longrightarrow \frac{1}{r} \sum_{c'} \varphi^{M}_{c'\pi I}(\hat{r}) \left[\delta_{c'\bar{c}}\, I_{\bar{c}}(k_{\bar{c}} r) - \left(\frac{V_{\bar{c}}}{V_{c'}}\right)^{\frac{1}{2}} U^{I\pi}_{\bar{c}c'}\, O_{c'}(k_{c'} r) \right] \qquad (20)$$

$$= \frac{1}{r} \sum_{c'} \varphi^{M}_{c'\pi I}(\hat{r}) \Big[\delta_{c'c} \left(I_{\bar{c}} - O_{\bar{c}}\right) + \left(\frac{V_{\bar{c}}}{V_{c'}}\right)^{\frac{1}{2}} \left(\delta_{c'\bar{c}} - U^{I\pi}_{\bar{c}c'}\right) O_{c'}(k_{c'} r) \Big] \qquad (21)$$

where the c' channels will include the proton channels. We must now determine the superposition coefficients, A, in the expansion of the total wavefunction

$$\Psi = \sum_{\bar{c}\pi I}' A_{\bar{c}\pi I}^{\;M} \Psi_M^{\bar{c} I \pi} \qquad (22)$$

in such a way that there is a plane, or coulomb distorted plane wave in the target (nuclear ground state) channels . Let the incoming particles, having spin s, be represented by the spinor $\chi_{s,}^{m}$. Consider the coulomb distorted wave

$$\Psi_{coul}^{M,m} = \Phi_{\alpha J}^{M}(A)\, \chi_{s,}^{m} \sum_{\ell}' (4\pi\hat{\ell})^{1/2} i^{\ell}\, e^{i\sigma_\ell}\, \frac{O_\ell - I_\ell}{2ikr}\, Y_\ell^0 \qquad (23)$$

$$= \sum_{\ell j I}' C_{0mm}^{\ell s j}\; C_{MM\,M+m}^{jJI}\; (4\pi\hat{\ell})^{1/2} i^{\ell} e^{i\sigma_\ell}\, \frac{O_\ell - I_\ell}{2ikr}\, \mathcal{Y}_{c\pi I}^{m+M} \qquad (24)$$

(see eq(5) and (6)) $c \equiv \alpha_0 \ell j I$ where α_0 is the target gound state. Substituting eq(21) and (22) and comparing with (24) we determine the superposition amplitudes, A:

$$A_{\bar{c}\pi I}^{M+m} = -\frac{1}{2ik_c}\; C_{0mm}^{\ell s j}\; C_{MM\,M+m}^{jJI}\; (4\pi\hat{\ell})^{1/2}\, i^{\ell}\, e^{i\sigma_\ell} \qquad (25)$$

With the help of equations (25),(8) and (9) (though we consider outgoing particles here of spin S_2) we find that the scattered wave part of (21) becomes

$$\Psi^{M,m} = \frac{1}{r} \sum_{\substack{\alpha' s_2 J' \\ M' m'}}' \exp\left[i\left(k'r - \eta' \ln(2k'r)\right)\right] \times$$

$$\times f_{\alpha J s M m, \alpha' J' M' m' s_2} \Phi^{M'}_{\alpha' J'} \chi^{m'}_{(s_2)} \qquad (26)$$

where the scattering amplitude, f, is given by

$$f_{\alpha J M m s_1, \alpha' J' M' m' s_2} = -\frac{1}{2ik_c} \sum_{\substack{l_c j_c \\ l' j' \\ I\pi}}' i^{l-l'} \exp\left[i(\sigma_l + \sigma_{l'})\right] \left(\frac{V_c}{V_{c'}}\right)^{\frac{1}{2}} \times$$

$$\times \left(\delta_{c'c} - U^{I\pi}_{c'c}\right) Y^{M+m-M'-m'}_{l'} (4\pi\hat{l})^{\frac{1}{2}} C^{(4)} \qquad (27)$$

where we define

$$C^{(4)} = C^{l\ s\ j}_{0\ m\ m}\ C^{j\ J\ I}_{m\ M\ M+m}\ C^{l'\ s'\ j'}_{\mu\ m'\ \mu+m'}\ C^{j'\ J'\ I}_{\mu+m'\ M'\ M+\mu} \qquad (28)$$

and $\mu = M + m - M' - m'$

For the case of elastic scattering, we must add the analytically known coulomb amplitude. The sum over $l_c j_c$ extends to all channels of given I, π corresponding to the ground state α, J_α. These equations apply to (d,d') and (d,p) using the appropriate part of $U^{I\pi}$ as calculated by SCATERD or STRIPDP. The cross section may be calculated in the usual way

$$\left(\frac{d\sigma}{d\Omega}\right)_{\alpha S J_\alpha \to \alpha' S' J_{\alpha'}} = \frac{1}{(2S+1)(2I_\alpha+1)} \sum_{\substack{M m \\ M' m'}} |\tilde{f}|^2 \qquad (29)$$

where $\tilde{f} = \left(\frac{V_{c'}}{V_c}\right) f$.

The method we have followed in calculating the cross section is a little different, as it enables us to calculate the polarization of the outgoing (protons) with no real cost in computing time.

Using the spherical harmonic addition theorem, we can replace Y_ℓ^0 in eq(17) by $\sum_{\bar{m}}' \left(\frac{4\pi}{\hat{\ell}}\right)^{1/2} Y_{\ell \bar{m}}(\pi/2,\theta) Y_{\ell \bar{m}}^*(\pi/2,0)$. The spin quantization axis is here taken to be perpendicular to the scattering plane. We may rewrite the scattering amplitude in the following form:

$$f = \frac{2\pi i}{k_c} \sum_{\substack{\ell j \\ \ell' j' \\ I\pi \bar{m}}}' i^{\ell-\ell'} \exp i(\sigma_\ell + \sigma_{\ell'}) \left(\frac{V_c}{V_{c'}}\right)^{1/2} \left(\delta_{c'c} - U^{I\pi}_{c'c}\right) \times$$

$$\times Y_{\ell'}^{\mu}(\pi/2\,\theta)\; Y_\ell^{\bar{m}}(\pi/2,0)\; C^{(4)}_{(\bar{m})} \qquad (30)$$

where we now define the product $C^{(4)}$ by

$$C^{(4)}_{(\bar{m})} = C^{\ell\, s\, j}_{\bar{m}\, m\, \bar{\bar{m}}}\; C^{j\, J\, I}_{\bar{\bar{m}}\, M\, M+\bar{\bar{m}}}\; C^{\ell' s' j'}_{\mu\, m'\, \mu+m'}\; C^{j' J' I}_{\mu+m'\, M'\, M+\bar{\bar{m}}} \qquad (31)$$

where $\bar{\bar{m}} = m+\bar{m}$, $\mu = M+\bar{\bar{m}} - M' - m'$. (32)

The calculation of the cross section is the same; the polarization, $P(\alpha', \theta)$ of protons corresponding to final state α' is for outgoing protons, simply

$$P(\alpha', \theta) = \frac{\sum'_{M m' M'} \left\{ \left| f_{\alpha M m \alpha' M' \frac{1}{2}} \right|^2 - \left| f_{\alpha M m \alpha' M' -\frac{1}{2}} \right|^2 \right\}}{\sum'_{M m M' m'} \left| f_{\alpha M m \alpha' M' m'} \right|^2} \quad . \quad (33)$$

Figure Caption for Chapter V

Fig. V.1 Three programs communicating by tape or disk file are used to calculate a stripping cross section according to the following scheme. File T46, output from SCATERD contains first the parameters of the (d,d') calculation, then successively

(a) I, π and the quantum numbers of incoming wave, $\bar{c}$	3 sets for each I
(b) The enumerated deuteron channels	
(c) The deuteron wavefunction in each of these	

(a) New set of I, π, $\bar{c}$
(b) Deuteron channels corresponding to (I, π, $\bar{c}$)
(c) Wavefunctions corresponding to (I, π, $\bar{c}$)

(a)
(b)
(c)

and so on

As STRIPDP reads (a), it enumerates the proton channels, as it reads (b), it calculates the relevant source term factors. As it reads (c), it calculates the (d,p) S-matrix elements $U_{\bar{c}c'}$. These, together with the enumeration of the channels, are employed by CROSSDP to calculate the cross section.

The (d,d') cross section may be calculated by program CROSSD if desired.

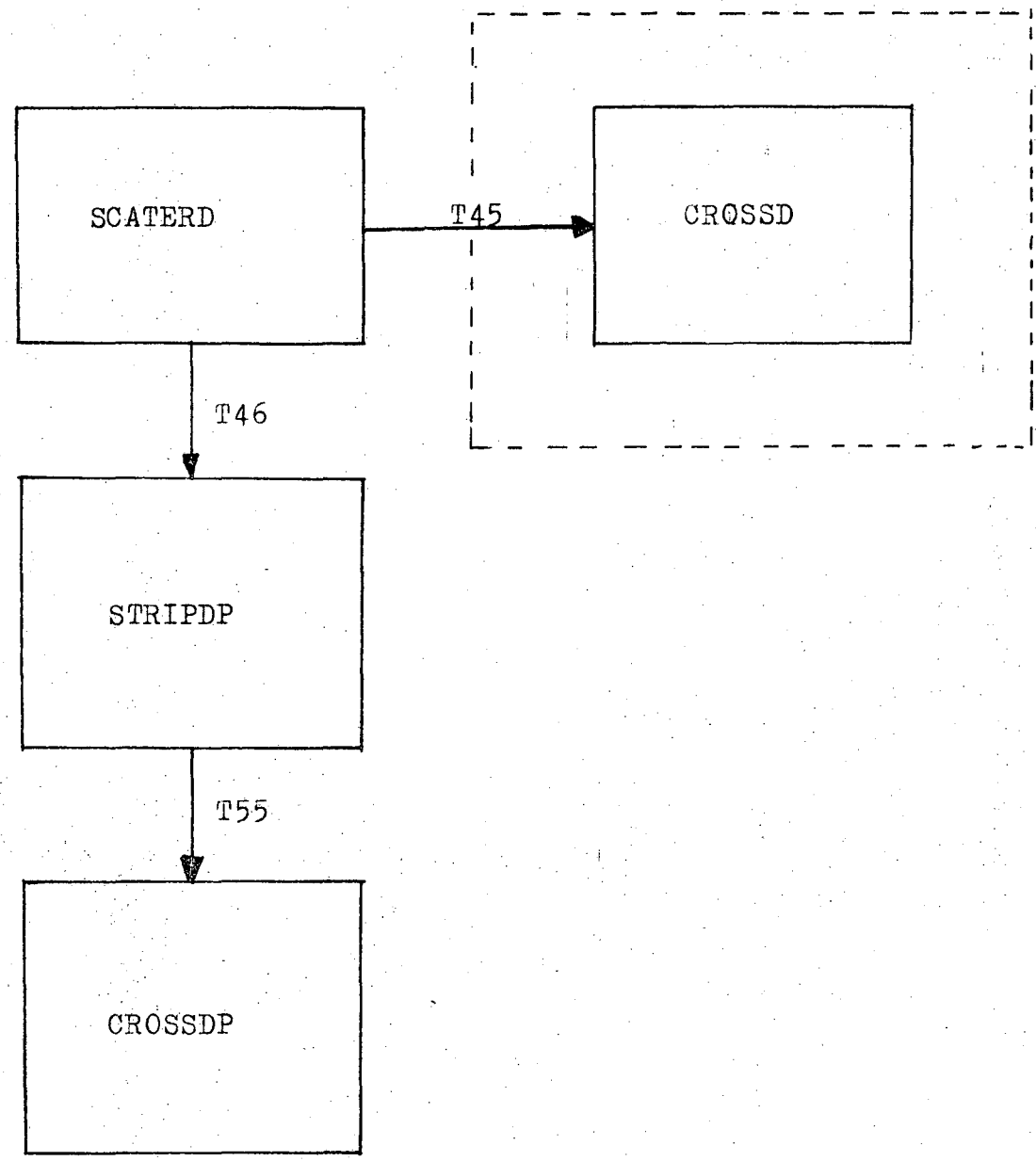

Fig.V.1

VI. FORMULATION OF SPECIFIC MODELS

The coupled-channel equations presented in the previous chaper were independent of any particular nuclear model. In this chaper we shall calculate the source term explicitly using the zero range approximation and the rotational model of Chapter IV. From the explicit form of the source term, we can show how selection rules arise and how they can be broken by inelastic scattering processes. In order to calculate the matrix elements $V_{cc'}^{I\pi}$ in eq(12) of Chapter V, we discuss first the general problem of scattering from a collective field and then the particular problem of scattering from an odd nucleus.

A. Zero Range Source Term

We wish to calculate

$$S_{c'c''}^{I\pi} = \int \varphi^{*}_{c'\pi I}(\hat{r}_p, \sigma, A+1)\, V_{pn}\, \frac{r_{p'}}{r_d}\, \varphi_{c''\pi I}(r_d, A)\, d\Omega_{p'}\, d^{3A}\, d^3 r_n \qquad (1)$$

using the zero range approximation

$$V_{pn}(\vec{r}_p - \vec{r}_n)\, \varphi_d(\vec{r}_p - \vec{r}_n) = D_0\, \delta(\vec{r}_p - \vec{r}_n) \qquad (2)$$

where φ_d is the s-state component of the internal deuteron wave function.

Let us make a general parentage expansion of the (A+1) particle nucleus in the form (see Chapter II):

$$\Phi_{\alpha' J_c'}(A+1) = \sum_{\alpha j \ell}{}' B(\alpha', \alpha j \ell) \left[\Phi_{\alpha}(A)_{J_c}, \varphi_{\ell_n j_n} \right]_{J_c'} \tag{3}$$

so that

$$\varphi^{M}_{c' \pi I} = \left[Y_{\ell' s' j'}, \Phi_{\alpha' J_c'}(A+1) \right]^{M}_{I} \tag{4}$$

$$= \sum_{\alpha j \ell}{}' B(\alpha', \alpha j \ell) \left[Y_{\ell' s' j'}, \left[\Phi_{\alpha J_c}(A), \varphi_{\ell_n j_n} \right]_{J_c'} \right]^{M}_{I} \tag{5}$$

Similarly, the deuteron wavefunctions can be written

$$\varphi^{M}_{c'' \pi I}(\hat{r}_d) = \left[\left[Y_{\ell_{c''}}(\hat{r}_d) \chi_1(d) \right]_{j_{c''}}, \Phi_{\alpha J_{c''}} \right]^{M}_{I}$$

$$= \left[\left[Y_{\ell_{c''}}(\hat{r}_d), \left[Y_0(\hat{r}_{pn}), \left[S_p, S_n \right]_1 \right]_1 \right]_{j_{c''}}, \Phi_{\alpha'' J_{c''}}(A) \right]^{M}_{I} \phi_n(r_{pn}) \tag{6}$$

where S_p and S_n are the spinors for the proton and neutron respectively, and we have written the deuteron wavefunction

$$\chi_1(d) = \left[Y_0(\hat{r}_{pn}, \left[S_p, S_n \right]_1 \right]_1 \phi_n(r_{pn}) = \frac{1}{\sqrt{4\pi}} \left[S_p, S_n \right]_1 \phi_n(r_{pn}) \equiv \left[S_p, S_n \right]_1 \varphi_n(r_{pn})$$

where φ is the wavefunction appearing in eq(2). We now observe that the proton-channel wavefunction (4) may be rearranged as follows:

$$\Phi^{M}_{c'\pi I}(\hat{r}_p) = \sum_{\alpha j \ell} B(\alpha_{c'}, \alpha j \ell) \Big[\Big[Y_{\ell_{c'}}(\hat{r}_{p'}), S_p \Big]_{j_{c'}}, \Big[\Phi_{\alpha J}, \varphi_{\ell n j_n}(\hat{r}_n) \Big]_{J_{c'}} \Big]^{M}_{I}$$

$$= \sum_{\alpha j \ell} B(\alpha_{c'}, \alpha j \ell) \Big[\Big[Y_{\ell_{c'}}(\hat{r}_{p'}), S_p \Big]_{j_{c'}}, \Big[\Phi_{\alpha J}, \Big[Y_{\ell}(\hat{r}_n), S_n \Big]_{j_n} \Big]_{J_{c'}} \Big]^{M}_{I} f_{j\ell}(r_n)$$

where $f_{j\ell}(r_n)$ is the neutron radial wavefunction

$$= \sum_{\alpha j \ell} B(\alpha_{c'}, \alpha j \ell) \sum_{\mathcal{J}} (\hat{J}_{c'} \hat{\mathcal{J}}) (-)^{j_{c'} + I + J_{c'}} \begin{Bmatrix} j_{c'} & j & \mathcal{J} \\ J & I & J_{c'} \end{Bmatrix} \times$$

$$\times \Big[\Big[\Big[Y_{\ell_{c'}}(\hat{r}_{p'}), S_p \Big]_{j_{c'}}, \Big[Y_{\ell}(\hat{r}_n), S_n \Big]_{j_n} \Big]_{\mathcal{J}}, \Phi_{\alpha J} \Big]^{M}_{I} f_{j\ell}(r_n)$$

$$= \sum_{\alpha j \ell} B(\alpha_{c'}, \alpha j \ell) \sum_{\mathcal{J} \ell_{c''}} (\hat{J}_{c'} \hat{\mathcal{J}}) (-)^{j_{c'} + I + J_{c'}} \begin{Bmatrix} j_{c'} & j & \mathcal{J} \\ J & I & J_{c'} \end{Bmatrix} \begin{bmatrix} \ell_{c'} & \frac{1}{2} & j_{c'} \\ \ell & \frac{1}{2} & j \\ \ell_{c''} & 1 & \mathcal{J} \end{bmatrix} \times$$

$$\times \Big[\Big[\Big[Y_{\ell_{c'}}(\hat{r}_p) \, Y_{\ell}(\hat{r}_n) \Big]_{\ell_{c''}}, \Big[S_p, S_n \Big]_1 \Big]_{j_{c''}}, \Phi_{\alpha J} \Big]^{M}_{I} f_{j\ell}(r_n) \qquad (7)$$

Substituting (5) and (7) into the integral (1), using eq(V.18)

in (2) and various orthogonality relationships, we find that the source term factor coupling deuteron channel c'' to proton channel c' is

$$S^{I\pi}_{c'c''} = \frac{A}{A+1} D_0 \sum_{jl} B(\alpha_{c'}, \alpha'' jl) \left[\frac{\hat{J}_{c'} \hat{J}_{c''} \hat{l}_{c'} \hat{l}}{4\pi \, \hat{l}_{c''}} \right]^{1/2} C^{l_{c'} \, l \, l_{c''}}_{0 \; 0 \; 0} (-)^{j_{c'}+I+J_{c'}} \times$$

$$\times \begin{Bmatrix} j_{c'} & j & j_{c''} \\ J_{c''} & I & J_{c'} \end{Bmatrix} \begin{bmatrix} l_{c'} & \frac{1}{2} & j_{c'} \\ l & \frac{1}{2} & j \\ l_{c''} & 1 & j_{c''} \end{bmatrix} f_{jl}\left(\frac{A+1}{A} r_{p'}\right) \tag{8}$$

and we observe that the complete source term is, in terms of the final state proton coordinate, $r_{p'}$, given by

$$S^{I\pi\bar{c}}_{c'}(r_{p'}) = \sum_{c''}{}' S^{I\pi}_{c'c''}\left(\frac{A+1}{A} r_{p'}\right) u_{c''}\left(\frac{A+1}{A} r_{p'}\right) \tag{9}$$

Care must be taken to ensure that the deuteron program and the stripping program which reads the deuteron wavefunctions employ radial meshes which bear the correct $\frac{A+1}{A}$ scaling relationship to each other.

B. Rotational Model Spectroscopic Factor

The original derivations of the spectroscopic factors for single nucleon stripping on deformed nuclei were due to Satchler[2] and Sawicki.[58] We shall derive the explicit results we need including the terms involving stripping into an excited state (ground band or gamma band) of the target nucleus.

We want to calculate the reduced matrix elements $\langle J_2 k_2 \| a^\dagger_{j\ell} \| J_1 k_1 \rangle$ where J_2 is the spin of some state in a band of intrinsic $m_3 = k_2$ of the residual nucleus, and J_1 is the spin of a state of the target nucleus. Usually we have $k_1 = 0$ except in the case in which we excite the gamma band of the target nucleus, in which case $k_1 = 2$.

Consider then the case of $k_1 = 0$. We employ equations (4') and (9) of Chapter IV.

$$\langle J_2 k_2 M_2 \mid a^\dagger_{j\ell,\mu} \mid J_1 k_1 M_1 \rangle$$

$$= \left(\frac{\hat{J}_2\,\hat{J}_1}{2}\right)^{1/2} \frac{1}{8\pi^2} \int \left\{ D^{*J_2}_{M_2 k_2} \sum_{j\ell} C_{j\ell} \langle a_{j k_2} \mid - D^{*J_2}_{M_2,-k_2} \sum_{j\ell} (-)^{I_2+j} C_{j\ell} \langle a_{j,-k_2} \mid \right\} \times$$

$$\times \sum_{\tilde{k}} D^{j}_{\mu \tilde{k}}\, \tilde{a}^\dagger_{j\ell\tilde{k}} \mid 0 \rangle\, D^{J_1}_{M_1,0}\, d^3\Lambda \qquad (10)$$

We denote* by Λ the argument of the rotation matrices and $\mid a_{j k_2} \rangle = \tilde{a}^\dagger_{j\ell k_2} \mid \tilde{0} \rangle$, ($\tilde{a}^\dagger$ acts in the body-fixed frame) and $a^\dagger_{j\ell,\mu}$ (lab. frame) $= \sum_{\tilde{k}} D^{j}_{\mu\tilde{k}}\, \tilde{a}^\dagger_{j\ell,\tilde{k}}$.

We have used the fact that $J_2 + j$ is integral.

The right hand side of eq(10) becomes

---

*The digamma, Λ , had fallen from use as a Greek letter by the classical period. It can often be seen on seventh century BC Corinthian vases.

(where $\langle\tilde{\sigma}|0\rangle$ is the overlap of the cores)

$$\left(\frac{\hat{J}_2\hat{J}_1}{2}\right)^{\frac{1}{2}}\frac{1}{8\pi^2}C_{j\ell}\langle\tilde{\sigma}|0\rangle\int d^3\Lambda\left\{\mathcal{D}^{*J_2}_{M_2,K_2}\mathcal{D}^{j}_{\mu,k_2}\mathcal{D}^{J_1}_{M_1,0}-(-)^{J_2+j}\mathcal{D}^{*J_2}_{M_2,-K_2}\mathcal{D}^{j}_{\mu,-k_2}\mathcal{D}^{J_1}_{M_1,0}\right\}$$

$$=\left(\frac{\hat{J}_2\hat{J}_1}{2}\right)^{\frac{1}{2}}\frac{1}{8\pi^2}C_{j\ell}\langle\tilde{\sigma}|0\rangle\left\{\begin{pmatrix}J_2 & j & J_1\\ -M_2 & \mu & M_1\end{pmatrix}\begin{pmatrix}J_2 & j & J_1\\ -K & K & 0\end{pmatrix}(-)^{M_2-K}-(-)^{J_2+j+M_2+K}\begin{pmatrix}J_2 & j & J_1\\ -M_2 & \mu & M_1\end{pmatrix}\times\right.$$

$$\left.\times\begin{pmatrix}J_2 & j & J_1\\ K & -K & 0\end{pmatrix}\right\} \qquad (11)$$

Hence, after some manipulation, we arrive at the following form for the reduced matrix element

$$\langle J_2\|a^{\dagger}_{j\ell}\|J_1\rangle=-\sqrt{2}\left(\frac{\hat{J}_1}{\hat{J}_2}\right)^{\frac{1}{2}}C_{j\ell}\langle\tilde{\sigma}|0\rangle C^{J_1\ j\ J_2}_{0\ K\ K}=-\beta_{j\ell}(\hat{J}_2)^{\frac{1}{2}} \qquad (12)$$

Using the definition and conventions of Chapter II, section A, we obtain, using eq(3) above

$$B(\alpha',\alpha j\ell)=\sqrt{2}\left(\frac{\hat{J}_1}{\hat{J}_2}\right)^{\frac{1}{2}}C_{j\ell}\langle\tilde{\sigma}|0\rangle C^{J_1\ j\ J_2}_{0\ K\ K} \qquad (13)$$

By a similar procedure, one may obtain the expression for the case of a neutron being stripped into the states of a (gamma) band to form a band K_2. We find

$$B(\alpha',\alpha j\ell)=\left(\frac{\hat{J}_1}{\hat{J}_2}\right)^{\frac{1}{2}}C_{j\ell}(k)\langle\tilde{2}|2\rangle C^{J_1\ \ j\ \ J_2}_{\mp 2\ \ K_2\pm 2\ \ K_2} \qquad (14)$$

where $k=|K_2\pm 2|$

Finally, we write the radial "form factor" in (8) (for the case of $K_1=0$) in the form

$$B(\alpha_{c'}, \alpha'' j\ell)\, f_{j\ell}(r)$$

$$= \sqrt{2}\left(\frac{\hat{J}_{c''}}{\hat{J}_{c'}}\right)^{1/2} C\begin{matrix} J_{c''} & j & J_{c'} \\ 0 & K & K \end{matrix} \langle \tilde{o} | o \rangle \sum_n{}' C_{nj\ell}(k)\, R_{n\ell}(r) \qquad (15)$$

The amplitudes $C_{nj\ell}(k)$ are explained and tabulated in Chapter IV and $R_{n\ell}$, the oscillator radial wavefunctions are defined in Appendix 3 of Chapter IV. This gives us the following form for the source term factors

$$S^{I\pi}_{c'c''} = \frac{A}{A+1} D_0 \sqrt{2} \langle \tilde{o} | o \rangle (-)^{j_{c'}+I+J_{c'}} \sum_{j\ell}{}' \left[\frac{\hat{J}_{c''}\hat{j}_{c''}\hat{\ell}_{c'}\hat{\ell}}{4\pi\,\hat{\ell}_{c''}}\right]^{1/2} C\begin{matrix} \ell_{c'} & \ell & \ell_{c''} \\ 0 & 0 & 0 \end{matrix} \times$$

$$\times C\begin{matrix} J_{c''} & j & J_{c'} \\ 0 & K & K \end{matrix} \begin{Bmatrix} j_{c'} & j & j_{c''} \\ J_{c''} & I & J_{c'} \end{Bmatrix} \begin{bmatrix} \ell_{c'} & 1/2 & j_{c'} \\ \ell & 1/2 & j \\ \ell_{c''} & 1 & j_{c''} \end{bmatrix} \sum_n{}' C_{nj\ell}(k)\, R_{n\ell}(r) \qquad (16)$$

The square bracket denotes the usual LS-JJ coupling coefficient. In practice, we expand $R_{n\ell}$ as a polynomial $A r^{\ell}(B + Cr^2 + \cdots r^{2(n-1)})$ to form a 3-dimensional array for each $I\pi$:

$$S^{I\pi}_{c'c''} \equiv \sum_{\nu}{}' G^{I\pi}_{c'c''\nu}\, r^{\nu} \qquad (17)$$

C. Selection Rules for Stripping and Inelastic Processes

We can see from eq(13) above that in the absence of inelastic processes selection rules might arise. The spectroscopic factor for stripping from the ground state of an even-even nuclues to members of a rotational band, of intrinsic spin projection, k, is for neutron spin j,

$$B(J_2, 0j\ell) = \sqrt{2}\,(\hat{J}_2)^{-1/2}\, C_{j\ell}(k)\, \delta_{jJ_2} \qquad (18)$$

This simply expresses the obvious fact, stated in Chapter II, that where there are no inelastic processes and the target is spin zero, the angular momentum of the transferred neutron is that of the state of the residual nucleus under consideration. Selection rules may arise if particular values of C_{jl} are very small. For example, in the usual Nilsson model, the intrinsic states of the three lowest lying bands are composed entirely of l=0 or l=2 components. Thus the 7/2+ and 9/2+ levels cannot be excited directly unless there are small l=4 components not included in the Nilsson calculation. We see that such selection rules may be broken by inelastic processes. If the 2+ state of ^{24}Mg is excited by the deuteron before stripping takes place, then the non-vanishing of the amplitude

$$B(J_2, 2jl) = \sqrt{2}\left(5/\hat{J}_2\right)^{1/2} C_{jl}(4)\, C^{2\ j\ J_2}_{0\ k\ k}$$

for j=5/2 and J_2=7/2, 9/2 assures that the 7/2+ and 9/2+ levels in ^{25}Mg can be populated. Additional amplitudes for these states will occur as a result of the scattering of the proton as it leaves the residual nucleus.

A similar selection rule is exemplified by the 7/2+ <u>ground state</u> of ^{167}Er (see Chapter IV for numerical details). It turns out that $c_{7/2+}$ for the ground band is extremely weak- to the extent that it would lead to an almost unmeasurable population of the ground state of ^{167}Er in the absence of

inelastic effects. In fact, we shall find in this case, that this statement needs to be qualified owing to the relative strength of the j=7/2+ radial wavefunction in the nuclear surface.

It should be observed that inelastic processes have the potentiality to change angular distributions of states corresponding to smaller $C_{j\ell}$ as amplitudes corresponding to the transfer of different angular momenta become important.

D. Macroscopic Approach to Inelastic Scattering

The most direct approach to inelastic scattering between states of a rotational band, i.e. states which have essentially the same intrinsic structure, is to deform the optical potential. The interaction between this non-spherical optical potential and the projectile will induce rotational excitations in the nucleus. The underlying concept is the self consistency between the nuclear shape and the nuclear field. The method can also be extended to collective vibrations where the self consistent field approach has been successful (see Baranger and Kumar[53]).

As the method is based on the optical potential using empirically determined parameters, many effects which are not explicitly taken account of, such as exchange effects, are to some extent allowed for implicitly. Be this as it may, we believe that macroscopically derived coupled-channel wavefunctions which

fit the inelastic scattering data must be "better" than those where no inelastic effects are included. How much "better" remains to be seen. The details of the parameterization of the surface expansion of the deformed optical potential have been reviewed by Glendenning[35] and the extension to vibrational wavefunctions of deformed nuclei by Glendenning and Mackintosh.[54] Some account of it will be given when we discuss the optical potential in a later chapter.

If the nuclear field is deformed, then one can write

$$V(\vec{r}) = V(r) + \sum_{L\geq 2} V_{Lk}(r)\, Y_{Lk}(\theta',\varphi')$$

in the intrinsic frame. The transformation to the lab frame gives

$$V(r,\theta,\varphi,\Lambda) = V(r) + \sum_{LM} Y_{LM}(\theta,\varphi) \sum_{k\geq 0} V_{Lk}(r)\, \frac{D^{*L}_{Mk} + (-)^k D^{*L}_{M-k}}{1+\delta_{k0}} \qquad (19)$$

where $V(r)$ is spherically symmetric. There will, in general, be an L=0 spherically symmetric component in the second term of eq(19) associated with the change in geometric parameters required for an optical potential when the elastic scattering is calculated with a deformed potential. This form embodies the usual collective model convention for the rotation matrices and differs somewhat from that in ref.[35] by the conjugated

rotation matrix. It also differs in the $(-)^k$ factor which arises from $V_{L-k} = (-)^k V_{Lk}$ which we can show always holds. The possibility of odd k (e.g. for vibrations with L=3, k=3) cannot definitely be excluded.[55] The spherical coordinates of the projectile are (θ, φ) in space fixed axes, and the orientation of the nucleus is represented by Λ , the argument of the rotation matrices. We observe that (19) may be rewritten:

$$V(r,\theta,\varphi,\Lambda) = V(r) + \sum_{\substack{LM \\ k\geq 0}} Y_{LM}(\theta,\varphi)\, V_{Lk}(r)\, (-)^k (-)^{-M} \frac{D^L_{-M,-k} + (-)^k D^L_{-M,k}}{1+\delta_{k0}} \qquad (20)$$

Note: L will be integral. In nearly any case of interest k will be even, as will M, but the $(-)^M$ allows us to write eq(20) as follows for the case of even k:

$$V(r,\theta,\varphi,\Lambda) = V(r) + \sum_{\substack{L \\ k\geq 0}} V_{Lk}(r)\; Y_L \cdot \left(\frac{D^L_{,k} + D^L_{,-k}}{1+\delta_{k0}} \right) \qquad (21)$$

This scalar product form (we remind the reader that it differs by a multiplicative factor from the usually defined zero order tensor) will be very useful to us; it reflects the fact that V depends only on r and the angular displacement between the projectile and the nucleus.

We wish to evaluate $V^{I\pi}_{c_2 c_1}(r)$ where c_2 and c_1 denote

channels of particles of general spin s_c :

$$V^{I\pi}_{c_2 c_1}(r) = V(r)\delta_{c_2 c_1} + I \tag{22}$$

where

$$I = \langle \varphi^{M}_{c_2 \pi I} \Big| \sum_{\substack{L \\ k\geq 0}} V_{Lk}(r)\, Y_L \cdot \left(\frac{D^L_{,k} + D^L_{,-k}}{1+\delta_{k0}} \right) \Big| \varphi^{M}_{c_1 \pi I} \rangle \tag{23}$$

Now by recoupling equations (6) and (9) of Chapter V, we get

$$\varphi^{M}_{c\pi I} = (-)^{l_c + s_c - j_c} \left[\left[s_c, l_c \right]_{j_c}, J_c \right]^{M}_{I} \tag{24}$$

$$= (-)^{l_c+s_c-j_c} \sum_{\lambda} (\hat{\lambda}\cdot\hat{j}_c)^{1/2} (-)^{s_c+l_c+I+I} \left[s_c, \left[l_c, J_c \right]_\lambda \right]^{M}_{I} \times$$

$$\times \begin{Bmatrix} s_c & l_c & j_c \\ J_c & I & \lambda \end{Bmatrix} \tag{25}$$

$$\therefore I = (-)^{+j_{c_2} - j_{c_1} + J_{c_1} - J_{c_2}} \sum'_{\substack{\lambda\lambda' L \\ k\geq 0}} (\hat{\lambda}\hat{\lambda}'\hat{j}_{c_1}\hat{j}_{c_2})^{1/2} \begin{Bmatrix} s & l_{c_1} & j_{c_1} \\ J_{c_1} & I & \lambda \end{Bmatrix} \begin{Bmatrix} s & l_{c_2} & j_{c_2} \\ J_{c_2} & I & \lambda' \end{Bmatrix} \times$$

$$\times \sum_{\lambda} C^{s\,\lambda\, I}_{\mu\, M}\, C^{s\,\lambda' I}_{\mu\, M} \langle \alpha_{c_2} | V_{Lk} | \alpha_{c_1} \rangle \times$$

$$\times \langle \left[l_{c_2} J_{c_2} \right]^{\mu}_{\lambda'} \Big| Y_L \cdot \left(\frac{D^L_{,k} + D^L_{,-k}}{1+\delta_{k,0}} \right) \Big| \left[l_{c_1} J_{c_1} \right]^{\mu}_{\lambda} \rangle \tag{26}$$

Notes: 1. The scalar product, being invariant, is a constant in μ , and implies that $\lambda = \lambda'$
hence, the sum over μ , $\sum_{\mu} C^{s\,\lambda\, I}_{\mu\, M} C^{s\,\lambda\, I}_{\mu\, M} = 1$

2. If J_{c_1}, J_{c_2} correspond to the same intrinsic state, then

$$\langle \alpha_{c_2} | V_{LK} | \alpha_{c_1} \rangle = V_{LK}$$

However, if this is not the case (for instance may be a state of a gamma band) then V_{LK} contains not merely shape paramaters; the α_{LK} and δ_{LK} must be interpreted in terms of creation operators and $\langle \alpha_{c_2} | V_{LK} | \alpha_{c_1} \rangle$ is the intrinsic state transition matrix.

We rewrite eq(26) as

$$I = (-)^{j_{c_2}-j_{c_1}+J_{c_1}-J_{c_2}} \sum_{\substack{\lambda L \\ K\geq 0}} \hat{\lambda}\,(\hat{j}_{c_1}\hat{J}_{c_2})^{1/2} \begin{Bmatrix} s & \ell_{c_1} & j_{c_1} \\ J_{c_1} & I & \lambda \end{Bmatrix} \begin{Bmatrix} s & \ell_{c_2} & j_{c_2} \\ J_{c_2} & I & \lambda \end{Bmatrix} \times$$

$$\times \langle \alpha_{c_2} | V_{LK} | \alpha_{c_1} \rangle \langle [\ell_{c_2} J_{c_2}]^{\mu}_{\lambda} | Y_L \cdot \left(\frac{D^L_{,K} + D^L_{,-K}}{1+\delta_{K0}} \right) | [\ell_{c_1} J_{c_1}]^{\mu}_{\lambda} \rangle \qquad (27)$$

hence, using standard results

$$I = (-)^{j_{\ell_2}-j_{c_1}+J_{c_1}+\ell_{c_1}} \sum_{\substack{L\lambda \\ K\geq 0}}{}' (-)^{\lambda} \hat{\lambda}\,(\hat{j}_{c_1}\hat{j}_{c_2})^{1/2} \begin{Bmatrix} s & \ell_{c_1} & j_{c_1} \\ J_{c_1} & I & \lambda \end{Bmatrix} \begin{Bmatrix} s & \ell_{c_2} & j_{c_2} \\ J_{c_2} & I & \lambda \end{Bmatrix} \begin{Bmatrix} \lambda & J_{c_2} & \ell_{c_2} \\ L & \ell_{c_1} & J_{c_1} \end{Bmatrix}$$

$$\times \langle \ell_{c_2} \| Y_L \| \ell_{c_1} \rangle \langle \alpha_{c_2} | V_{LK} | \alpha_{c_1} \rangle \left\langle J_{c_2} K_{c_2} \middle\| \frac{D^L_{,K} + D^L_{,-K}}{1+\delta_{K0}} \middle\| J_{c_1} K_{c_1} \right\rangle \qquad (28)$$

$$= (-)^{j_{c_2}-j_{c_1}+J_{c_1}+\ell_{c_1}} \sum_{\substack{L\lambda \\ K\geq 0}}{}' (-)^{\lambda} \hat{\lambda}\,(\hat{j}_{c_1}\hat{j}_{c_2})^{1/2} (-)^{\ell_{c_1}} \left[\frac{\hat{\ell}_{c_1}\hat{L}\hat{\ell}_{c_2}}{4\pi} \right]^{1/2} \begin{pmatrix} \ell_{c_2} & L & \ell_{c_1} \\ 0 & 0 & 0 \end{pmatrix} \begin{Bmatrix} s & \ell_{c_1} & j_{c_1} \\ J_{c_1} & I & \lambda \end{Bmatrix}$$

$$\times \begin{Bmatrix} s & \ell_{c_2} & j_{c_2} \\ J_{c_2} & I & \lambda \end{Bmatrix} \begin{Bmatrix} L & \ell_{c_1} & \ell_{c_2} \\ \lambda & J_{c_2} & J_{c_1} \end{Bmatrix} V^{LK}_{c_2 c_1} \; B^{LK}_{c_2 c_1} \qquad (29)$$

where

$$B^{Lk}_{c_2c_1} = \langle J_{c_2} K_{c_2} \| \frac{D^L_{J,k} + D^L_{J,-k}}{1+\delta_{k0}} \| J_{c_1} K_{c_1} \rangle \qquad (30a)$$

$$V^{Lk}_{c_2c_1} = \langle \alpha_{c_2} | V_{Lk} | \alpha_{c_1} \rangle \qquad (30b)$$

The calculation of V^{Lk} will be given in Chapter VII. Now using equation (6.2.12) of Edmonds[9] (p.97), and rearranging, we get

$$V^{I\pi}_{c_2c_1}(r) = V(r)\delta_{c_2c_1} + (-)^{I+J_{c_2}+2j_{c_1}+s}\left(\frac{\hat{s}_{c_1}\hat{j}_{c_2}\hat{\ell}_{c_1}\hat{\ell}_{c_2}}{4\pi}\right)^{1/2} \times$$

$$\times \sum_{Lk\geq 0} (\hat{L})^{1/2}(-)^L \begin{pmatrix} \ell_{c_2} & L & \ell_{c_1} \\ 0 & 0 & 0 \end{pmatrix} B^{Lk}_{c_2c_1} V^{Lk}_{c_2c_1} \begin{Bmatrix} L & \ell_{c_1} & \ell_{c_2} \\ s & J_{c_2} & j_{c_1} \end{Bmatrix} \begin{Bmatrix} j_{c_1} & L & j_{c_2} \\ J_{c_2} & I & J_{c_1} \end{Bmatrix} \qquad (31)$$

For s=0, this agrees with eq(6.19) of Glendenning.[35] This result has been used to calculate the (d,d') scattering in the entrance channels and (p,p') scattering in the exit channels.

We note in passing that a striking simplification takes place for s=1/2. The l dependence appears in the factor

$$f(\ell_1,\ell_2) = (\hat{\ell}_1\hat{\ell}_2)^{1/2}\begin{pmatrix} \ell_1 & \ell_2 & J \\ 0 & 0 & 0 \end{pmatrix}\begin{Bmatrix} \ell_1 & \ell_2 & J \\ j_2 & j_1 & \frac{1}{2} \end{Bmatrix}.$$

It turns out for $j_1 = \ell_1 \pm \frac{1}{2}$ and $j_2 = \ell_2 \pm \frac{1}{2}$ (which, of course, is true in our case) that

$$f(\ell_1\ell_2) = -\begin{pmatrix} j_1 & j_2 & J \\ \frac{1}{2} & -\frac{1}{2} & 0 \end{pmatrix}$$

The proof is not trivial but hardly worth reproducing here.* This means that provided l_1 and l_2 are allowed and have correct parity $\left[\begin{pmatrix} l_1 & L & l_2 \\ 0 & 0 & 0 \end{pmatrix} \neq 0 \right]$, then eq(31) is independent of them despite appearances. No such simplification occurs in the deuteron case. For even nuclei in which J_1, K_1, J_2, K_2 are integral, the expressions for the reduced matrix elements B^{Lk} given by Glendenning[35] are appropriate (for $k \geq 0$, even):

$$B^{Lk}_{12} = \langle J_1 K_1 \| \frac{D^L_{,k} + D^L_{,-k}}{1+\delta_{k,0}} \| J_2 K_2 \rangle$$

$$= \begin{cases} (\hat{J}_1 \hat{J}_2)^{\frac{1}{2}} \begin{pmatrix} J_1 & L & J_2 \\ 0 & 0 & 0 \end{pmatrix} \delta_{k,0}, & \text{if } K_1 = K_2 = 0 \\ (2\hat{J}_1 \hat{J}_2)^{\frac{1}{2}} \begin{pmatrix} J_1 & L & J_2 \\ 0 & -K_2 & K_2 \end{pmatrix} \delta_{k K_2}, & \text{if } K_1 = 0,\ K_2 \neq 0 \\ \frac{(-)^{J_1} (\hat{J}_1 \hat{J}_2)^{\frac{1}{2}}}{1+\delta_{k0}} \left\{ \begin{pmatrix} J_1 & L & J_2 \\ -K_1 & K & K_2 \end{pmatrix} + \begin{pmatrix} J_1 & L & J_2 \\ -K_1 & -K & K_2 \end{pmatrix} + (-)^{J_2} \begin{pmatrix} J_1 & L & J_2 \\ -K_1 & K & -K_2 \end{pmatrix} \right\} & \text{if } K_1 \neq 0,\ K_2 \neq 0 \end{cases} \quad (32)$$

These are employed in the deuteron scattering in the entrance channels: in fact, except where we consider the gamma band in Erbium, we need only the first of these relations. We must examine the case of half integral-spin nuclei more closely. Let us consider only axially symmetric optical potentials for which k=0. As stated previously, we permit only intraband

---

*The author "discovered" this "well-known" fact by accident when debugging the program!

transitions for which $k_1 = k_2$. The matrix element

$\langle J_1 k_1 M_1 | V_{LO} D^L_{M0} | J_2 k_1 M_2 \rangle$ will be studied, and its collective model factorization $B^{LL}_{c_1 c_2} V^{LL}_{c_1 c_2}$ elucidated.

In general, V_{LO} may be an operator expression, but in any case will be expressed in terms of collective coordinates. Consider

$$\langle J_1 K_1 M_1 | V_{LO} D^L_{M0} | J_2 k_1 M_2 \rangle$$

$$= \frac{(\hat{J}_1 \hat{J}_2)^{1/2}}{16\pi^2} \int \left(D^{J_1 *}_{M_1 K_1} \chi^*_{k_1} + (-)^{J_1 + K_1} D^{J_1 *}_{M_1 - K_1} \chi^*_{-K_1} \right) V_{LO} D^L_{M0} \times$$

$$\times \left(D^{J_2}_{M_2 K_1} \chi_{K_1} + (-)^{J_2 + K_1} D^{J_2}_{M_2 - K_1} \chi_{-K_1} \right) d^3\Lambda \, d(\text{Internal coords.})$$

$$= \frac{(\hat{J}_1 \hat{J}_2)^{1/2}}{16\pi^2} \Big\{ \int D^{J_1 *}_{M_1 K_1} D^L_{M0} D^{J_2}_{M_2 K_1} d^3\Lambda \langle \chi_{K_1}, V_{LO} \chi_{K_1} \rangle$$

$$+ (-)^{J_1 - J_2} \int D^{J_1 *}_{M_1 - K_1} D^L_{M0} D^{J_2}_{M_2 - K_1} d^3\Lambda \langle \chi_{-K_1}, V_{LO} \chi_{K_1} \rangle$$

$$+ \text{Integral} \times \langle \chi_{K_1}, V_{LO} \chi_{-K_1} \rangle + \text{Integral} \times \langle \chi_{-K_1}, V_{LO} \chi_{K_1} \rangle$$

(34)

The last two terms are zero.

We have used $(-)^{J_1 + J_2 + 2K_1} = (-)^{J_2 - J_1} = (-)^{J_1 - J_2}$ to get the second term. We observe that confining ourselves to macroscopic excitation is tantamount to making the following identification from the microscopic picture:

$$\langle \chi_{K_1}, \sum_i V_L(r, r_i) Y_{LO}(\Omega_i) \chi_{K_1} \rangle = V_{LO}(r) \qquad (35)$$

which is just $\langle \chi_{K_1}, V_{LO}\, \chi_{K_1} \rangle$ as we have defined it where V_{LO} is a c-number function. However, it is <u>not</u> true that the microscopic model quantity

$$\langle \chi_{-K_1}, \sum_i V_L(r, r_i) Y_{LM}(\Omega_i)\, \chi_{K_1} \rangle = \tilde{V}_{LM}$$

vanishes in general. Thus, Y_2 component in the interaction can flip the intrinsic state of a k=1/2 band, and Y_4 component for a k=3/2 band, etc. These terms can only be calculated in a microscopic model: outside the province of the present work. Furthermore, they are of the order of one particle strength, whereas the collective term is of the order of A particle strengths. This rough statement is less useful in the A=25 region where Crawley and Garvey[56] report empirical interband transitions which are not so much weaker than (i.e. transition amplitudes about one quarter of) those within a band - this suggests that the A particle versus one particle strength argument is less than fully valid in this region. We shall simply state that the 3rd and 4th terms of eq(34) disappear, that $\langle \chi_{K_1}, V_{LO}\, \chi_{K_1} \rangle = \langle \chi_{-K_1}, V_{LO}\, \chi_{-K_1} \rangle \equiv V_{LO}$ where V_{LO} is obtained from a surface expansion of the optical potential and finally that particular care should be exercised in interpreting our findings in particularly unfavorable cases such as k=1/2 bands in ^{25}Mg. Hence

$$\langle J_1 K_1 M_1 | D^L_{M_0}\, V_{LO} | J_2 K_1 M_2 \rangle = V_{LO} \frac{(\hat{J}_1 \hat{J}_2)^{1/2}}{2} \left\{ (-)^{M_1 - K_1} \begin{pmatrix} J_1 & L & J_2 \\ -M_1 & M & M_2 \end{pmatrix} \begin{pmatrix} J_1 & L & J_2 \\ -K_1 & 0 & K_1 \end{pmatrix} \right.$$

$$\left. + (-)^{J_1 - J_2} (-)^{M_1 + K_1} \begin{pmatrix} J_1 & L & J_2 \\ -M_1 & M & M_2 \end{pmatrix} \begin{pmatrix} J_1 & L & J_2 \\ K_1 & 0 & -K_1 \end{pmatrix} \right\} \quad (36)$$

To derive this, we use

$$\frac{1}{8\pi^2}\int D^{J_1 *}_{M_1 K_1} D^{L}_{M 0} D^{J_2}_{M_2 K_1} d^3\Lambda = (-)^{M_1 - K_1} \begin{pmatrix} J_1 & L & J_2 \\ -M_1 & M & M_2 \end{pmatrix} \begin{pmatrix} J_1 & L & J_2 \\ -K_1 & 0 & K_1 \end{pmatrix}$$

(a formula which is true in the quite different conventions of Edmonds[9] and Preston,[57] for example). We have shown that the factorization at issue is good if we remain within the macroscopic picture. Using Racah's definition and factoring the V_{LO}, we get for B^{LO} as defined previously:

$$B^{LO} = \langle J_1 K_1 \| D^{L}_{0} \| J_2 K_2 \rangle = \frac{\langle J_1 K_1 M_1 | D^{L}_{M,0} | J_2 K_1 M_2 \rangle}{(-)^{J_1 - M_1} \begin{pmatrix} J_1 & L & J_2 \\ -M_1 & M & M_2 \end{pmatrix}}$$

$$= (\hat{J}_1 \hat{J}_2)^{1/2} (-)^{J_1 - K_1} \begin{pmatrix} J_1 & L & J_2 \\ -K_1 & 0 & K_2 \end{pmatrix} \quad (L \text{ even})$$

$$= 0 \quad (L \text{ odd}) \qquad (37)$$

Equation (37) is not an obvious generalization of eq(32).

VII. OPTICAL MODEL

A. Introduction

The use of the optical model for elastic scattering (see, for example, P.E. Hodgson[59]) from nuclei and for nuclear reactions is well known. However, this phenomenological model merits discussion here because the determination of the parameters is intimately connected with our overall procedure, and our calculations can be expected to depend quite strongly on how they are chosen. Although the optical potential must ultimately be regarded as empirically determined (see, however, Greenlees, Pyle, and Tang[60] for a recent essay towards making this statement less true), the formal derivation from the Feshbach theory which we have employed in Chapter III, makes it possible to exhibit certain general properties that a "physical" optical potential should have. The non-trivial problem of the optical potential for composite particles is then discussed, and in Appendix II we show how a special case of the Greenlees model can be applied to composite particles and deformed nuclei in a simple way.

All the optical potentials used in the stripping calculations are discussed in detail at the end of this chapter together with some inelastic scattering results.

In the first appendix to this chapter we have set out the definition of the optical potential parameterization for the

spherical case and then defined the parameters by which the deformation is described. Finally, we have given a generalization of the standard Taylor expansion of the surface leading to an explicit expression for a deformed optical potential. These results will be used throughout the chapter, and they may be referred to for a definition of surface thickness, etc.

B. Formal Considerations

1. The Effective Interaction and the Optical Potential

The following discussion employs the notation of Chapter III together with aspects of Feshbach's reaction theory introduced there. Consider an arbitrary partition L and a subspace defined within it corresponding to projection operator P_L with $P_L+Q_L=1$ (as before, we shall speak of subspace P_L, corresponding to projection operator P_L). Then that part of the exact solution Ψ, belonging to this subspace $P_L\Psi$ is a solution of the Schroedinger equation

$$(E - H_L - \mathcal{V}_L) P_L \Psi = 0 \qquad (1)$$

where $\mathcal{V}_L$ is the effective interaction, complex and non-local, defined by

$$\mathcal{V}_L = P_L \left(V_L + V_L Q_L \frac{1}{E^{(+)} - Q_L H Q_L} Q_L V_L\right) P_L \qquad (2)$$

The optical potential, $\tilde{V}$, is a complex, phenomenological, parametrized approximation to V_L, determined by the condition that $\tilde{\Psi}$, defined within P_L and calculated from $\tilde{V}$ by means of the equation

$$(E - H_L - \tilde{V})\tilde{\Psi} = 0 \qquad (3)$$

is a close approximation to $P_L\Psi$ in the asymptotic region, where $P_L\Psi$ can be regarded as known provided there exists sufficiently accurate experimental data. That is, $\tilde{V}$ reproduces certain scattering data. In this discussion, we assume that the energy is above that with large excitation fluctuations. We shall refer to $\tilde{\Psi}$ and $\tilde{V}$ referring to P_L projecting onto the elastic channel only as $\tilde{\Psi}_0$ and $\tilde{V}_0$.

The effective interaction, V_L, will depend on the states included in P_L. The contribution to V_L due to the majority of the large number of states in Q_L will normally vary slowly with A; however, particular strongly collective states are found to have an influence upon V_L which is not submerged in the vast number of more weakly excited states. The nature of the collective spectrum may vary widely in a small range of A, but provided the very strong collective states are included within P_L, a smoothly varying optical potential can be found. This has been strikingly demonstrated for alpha particle scattering in the samarium transition region by Glendenning, Hendrie and Jarvis.[61]

The optical potential appropriate to a rotation band

calculated using (3) (i.e., in a coupled-channel "cc" calculation) differs from that $\tilde{V}_o$, found when the ground state alone is included (i.e., a distorted wave "dw" calculation, elastic or inelastic) primarily in two respects: geometrically - the surface thickness is reduced; and in the absorption - this being reduced from that in the elastic case where it must account for the flux lost to the collective inelastic channels. Empirically, we have also found, in every case examined herein, that the product $V r_o^2$ is greater for cc than for dw calculations. The elastic channel wavefunction will clearly depend on the definition of P_L. The following consideration suggests how. As we have said, the true effective interaction, $\tilde{V}_L$, given by (2) is non-local. However, almost invariably $\tilde{V}$ is taken to be local and thus must be energy dependent. In fact, non-local optical potentials can be found which are very nearly energy independent. To the extent that certain (collective) states individually play a significant role in determining the elastic scattering, the inclusion of them in P_L will constitute an explicit representation of some part of the non-locality (equivalently, energy dependence) required of $\tilde{V}$. To this same extent, the wavefunction $\tilde{\Psi}$ will, in the elastic channel, depart from $\tilde{\Psi}_o$ calculated from a local elastic scattering optical potential in a somewhat similar fashion that a wavefunction determined by a non-local potential departs from the wavefunction determined by an equivalent (i.e., with wavefunctions

the same in the external region) local potential. The theorem discussed by Austern[15] states that for attractive potentials the former wavefunction will always be less than the latter within the interaction region. Hence, we expect that the deexcitation of collective states back into the elastic channel will correspond to amplitudes that add destructively with the elastic channel wavefunction, somewhat, within the nucleus, reducing the probability density of deuterons in the nuclear interior.

2. Optical Potential for Composite Particles

In the event that the "projectile" in partition 1 is composite, Q_L will contain the excited states of the projectile which may all be unbound. In order to sketch the formal implications of this in the specific case of the deuteron, let us write equation (11) of Chapter III in the following form, where we label the nuclear and particle states separately

$$\Psi = \sum_{i,\mu} \nu_i(A)\, \Pi_\mu(r_p - r_n)\, f_{i\mu}(R) \qquad (4)$$

where R is the deuteron centre of mass. Such an expansion can always be made: what is not immediately clear is how many terms μ are needed. If an adequate representation of Ψ can be obtained by including only the deuteron ground state ($\mu=0$) by means of absorbing the effect of the other states into an optical potential, then we have effectively uncoupled the deuteron centre of mass motion. The somewhat surprising

success of the deuteron optical potential (see Hodgson[62]) shows that the asymptotic wavefunctions can be described in these terms. It is still not obvious how good a simple product wavefunction is in the region of the nucleus. We shall indicate one formal approach to this problem. Consider the simplest case of the elastic scattering of deuterons for which $P_L = P_o^\pi P_o^\nu$. Then Mukherjee[63] shows that the single particle optical potential for the deuteron can be written, where E_o is the nucleus ground state energy, as:

$$V(R) = \langle \pi_o | V(r_n, r_p) | \pi_o \rangle + \langle \pi_o | V(r_n, r_p) Q_o^\pi \frac{1}{E^{(+)} - E_o - Q_o^\pi h Q_o^\pi} Q_o^\pi V(r_p, r_n) | \pi_o \rangle \quad (5)$$

where, in the notation of eq.'s 3,4,5 of Chapter III (in which equations we have identified L $\equiv d$), we have defined:

$$h = T_d + H_d^p + V(r_n, r_p)$$

and

$$V(r_n, r_p) = \langle \nu_o | P_o^\nu (v_n + v_p) P_o^\nu | \nu_o \rangle + \langle \nu_o | P_o^\nu (v_n + v_p) Q_o^\nu \frac{1}{E^{(\nu)} - Q_o^\nu H Q_o^\nu} Q_o^\nu (v_n + v_p) P_o^\nu | \nu_o \rangle \quad (6)$$

Mukherjee then shows that

$$V(r_n, r_p) = \bar{V}_{opt}^{(n)}(r_n) + \bar{V}_{opt}(r_p) + \text{higher order terms} \quad (7)$$

i.e., the sum of the proton and neutron optical potentials at the appropriate energy, together with higher order terms. Thus, the optical potential for a deuteron may be written

$$V(R) = \langle \pi_0 | V_{opt}(r_n) + V_{opt}(r_p) | \pi_0 \rangle + \text{higher order terms.} \quad (8)$$

This last form, eq(8) might have been written down immediately. However, various estimates can be made of the higher order terms in various approximations, and the important point is that such studies by Mukherjee and by Testoni and Gomes[64] and others suggest that the first term of (8) is by far the most important: this allows us to choose between widely differing alternative sets of deuteron optical parameters. It is noteworthy that Lee, Schiffer et al [16] found that the most "physical" (that nearest to the first term of (8)) optical potential was the only one of several alternative deuteron optical potentials that was satisfactory for stripping confirming earlier speculation.[65] We remark that Testoni and Gomes give in their work an interesting physical picture, albeit based on the somewhat dubious adiabatic approximation, of the polarization phenomena a deuteron undergoes as it approaches a nucleus. Their important results, following from the smallness of the higher order terms, are (a) that the skin thickness for the deuteron optical potential is greater than for a nucleon owing to the finite size of the deuteron; (b) the radius parameters should be somewhat smaller; (c) with surface absorption in the nucleon potentials, the imaginary depth is not

much increased - absorptive region is thickened. With volume absorption, the imaginary part is about equal to the sum of the imaginary parts of the nucleon potentials. (d) The spin-orbit term has the same geometrical parameters as the central term and about the same strength as the nucleon spin-orbit potential. These conclusions are to be regarded in the first place as a guide amongst the ambiguous potentials which will fit elastic scattering.

3. Spin-orbit Potential for Deformed Nuclei

The rigorous extension of the Thomas form (for the particularly simple spherical form, see eq(2) of the first appendix to this chapter) to the case of a deformed field is quite complex. There is no a priori reason to expect a Thomas form (especially in view of the fact that in the spherical case, the radius parameter is optimally not that of the central field), although Sherif and Blair,[66] and also Sherif and deSwiniarski[67] have found that improved polarization calculations are possible with it, as opposed to the simpler forms. These latter are (a) simply a spherical spin-orbit potential as given in eq(2) of Appendix I, or (b) the following hermitian form

$$V_{so} = 2\left(\frac{\hbar}{m_\pi c}\right)^2 \sum_{LM}{}' \tilde{N}_{LM}(r)\, \tfrac{1}{2}\left\{(\tilde{l}\cdot\tilde{s})Y_{LM} + Y_{LM}(\tilde{l}\cdot\tilde{s})\right\} \qquad (9)$$

where $\tilde{N}_{LK}$ is essentially the derivative of N_{LK} in equation (11) of the appendix which, for the case of expansion of r_0 only, becomes

$$\tilde{N}_{LK}(r) = \sum_{n=1}^{\infty} \frac{(-r_0)^n}{n!} \delta_{LK}^{(n)} \frac{1}{r} \frac{\partial^{n+1}}{\partial r^{n+1}} \left(V_{so} f(r, r_{so}, a_{so} + \right.$$
$$\left. + i W_{so} f(r, \bar{r}_{so}, \bar{a}_{so}) \right) \qquad (10)$$

Note that in this equation we have, for convenience, used r_0 as an operator taking values r_{so} and $\bar{r}_{so}$. In the calculations we have almost entirely confined ourselves to a spherical spin-orbit potential. We have performed some calculations using the form given by (9) and (10), but the effect of deforming the spin-orbit potentials has proven slight in the cases we have considered (q.v. Chapter VIII).

C. The Proton Optical Potentials-- Specific Cases

We will find that the determination of a suitable optical potential for any particular case involves its own characteristic problems which must be discussed separately. It will become apparent that the particular approaches we have used in certain cases constitute further reasons beyond those arising from the pictures we employ for the stripping process and for the nuclear structure, that our calculation must be regarded as having a distinct model calculation character. We always have in mind deuterons incident on an even nucleus.

In the first place, where inelastic scattering data on an odd nucleus is available, by necessity, it is only the scattering within the ground band that is useful to us. There may be scattering to other bands by means of single particle transitions, but this is not within the scope of our model to study. It is by no means clear that the deformation will be the same within each band; for ^{25}Mg it almost certainly varies considerably between bands. Furthermore, the number of states we may wish to include in the calculation will vary from band to band. The appropriateness of our macroscopic picture of intraband scattering will vary with the K of the band considered; ideally any inaccuracy in our picture might be absorbed within an appropriate optical potential together with appropriate deformation parameters, identifying, as usual,

the best wavefunction in the asymptotic region. Thus, a k=1/2 band may require quite a different optical potential than a k=1/2 band in the same nucleus for reasons discussed in the previous chapter, where we mention that the validity of the macroscopic model will be expected to depend on the k of the band being treated.

The problem is compounded by the fact that for light nuclei, there appears to be a large difference between the optimum elastic scattering optical potential and the optimum stripping optical potential (see Smith and Ivash,[25] also Cujec[68] for a discussion of this). This could in principle be the result of attempting to simulate stripping amplitudes which contain just the inelastic components that are under study by manipulating the parameters of the potentials. It would seem that this can be no more than part of what is involved. A real failure of a stripping theory in which the stripping amplitude arises from V_{np} acting in Born approximation seems to be the case; in any event, greatly reduced imaginary parts are often useful in fitting the stripping into the backward hemisphere. The required enhancement of the contribution of the nuclear interior is quite the reverse of the expected effect of renormalizing the elastic channel wavefunction in the nuclear interior by including inelastic effects -- the effect of the other channels is not so obvious. We recall from Chapter II that the usual procedures whereby the finite range of V_{np} is

accounted for reduce the effect of the interior.

Two other problems are correctable in principle. The proton scattering wavefunctions χ^- are calculated by the stripping program; no program was written specifically for (p,p')on odd nuclei, although scattering on an even-even nucleus in the absence of a spin-orbit interaction may be calculated using the available spin-zero program. In some cases (rare earths) where parameters are expected to be stable, it was thought reasonable to study a similar, nearby, even-even nucleus omitting V_{so} . This latter could be added with a reasonable strength for both the DW and CC optical potentials for comparison, if desired. We note in connection with V_{so} , the extreme paucity of polarization data available at suitable energies. Finally, we might justify this procedure in terms of the findings of Siemssen and Erskine[28] that average optical potentials give better stripping results in the rare earth region than those optimised for individual nuclei.

1. Magnesium

We desire an optical potential for the system p+^{25}Mg. At 10.1 MeV deuteron energy, we have adopted as the DW optical potential that found by Smith and Ivash[25] to be suitable in this nucleus for l=0 transitions. As we must use one potential for all states of a band in CC calculations, we have done the same for the corresponding DW calculations. This potential is labelled A in Table VII.1. The small value of W is noteworthy.

The CC optical potential was obtained from this by reducing the absorption and surface thickness according to rules which apply in similar cases (Tamura;[69] also Glasshauser,[70] for cases of 17.5 MeV protons on ^{24}Mg). The potential obtained is "B" of Table VII.1. The results of stripping calculations where these parameters were varied (e.g. larger W) to determine the effect on the proton angular distributions will be discussed in Chapter VIII.

For the case of protons corresponding to 12.3 MeV deuterons (16-17 MeV), we use an optical potential derived from that of Crawley and Garvey ("C" of Table VII.1) as follows. The spin-orbit potential is set equal to zero, and W_D, a_0 and $\bar{a}_0$ are reduced as shown to give potential D. This was then employed in a coupled channel calculation involving the 0+ and 2+ states of Mg^{24} and 16 MeV with $\beta_2 = .4$. The angular distribution leading to the ground state was then used as "experimental" input for the optical model search code Mercy.[71a] The resulting potential is "E." Finally, we arbitrarily add a spin-orbit component $V_{so} = 7.5$ to the DW and CC optical potentials to give "F" and "G" respectively which are suitable for model calculations of inelastic effects in Magnesium. If suitable data had been available, we would probably have wished to fit it using the coupled channel code - a very laborious process, as no coupled channel search program was available to us.

2. Deformed Rare Earths

Our stripping calculations on the deformed rare earths were mostly carried out for the case of 12.1 MeV deuterons. Thus the (p,p') scattering on the samarium isotopes of 15 MeV performed by Stoler et al[72] should provide a suitable optical potential over a reasonable range of A. The nucleus ^{154}Sm is sufficiently past the transition region to be as collective as those, such as ^{166}Er, in the middle of the deformed region; see Stelson and Grodzins.[73] Optical potentials for both DW and CC calculations were determined by Ascuitto and Brown.[74] Their calculations were such as to give the same ground state angular distributions of ^{154}Sm for coupled channel and DW and which fitted the 2+ and 4+ reasonably in the coupled channel case. The resulting potentials are "H" and "I" of Table VII.1. Note the characteristic thickening of the surface and deepening of the absorptive part of the DW as opposed to the CC potential. In order to obtain from these potentials others suitable for use with 16 and 20 MeV deuterons, we transform the real and imaginary depths of the CC potential, I, to obtain a new CC potential as follows:

$$-V = -V_0 + .3\,(E-E_0)$$
$$-W = -W_0 - .15\,(E-E_0)$$

We then fit the ground state cross section with a Mercy search to obtain DW optical potentials. These potentials are J,K,L and M of Table VII.1. The correspondence between the

CC and DW optical potentials is not so clear cut at these energies. The optical model code Mercy, however, found a set that give a very good fit. The geometrical parameters for the "J" do not appear physical, and the possibility that Mercy discovered a minimum within another family of potentials remains. Concerning I, K, M, the CC calculations were performed including 0+, 2+, and 4+ states -- the 4+ state had little effect on the ground state but an appreciable effect on the 2+. The deformation parameters were found to fit 15 MeV (p,p') data and are a little different from those employed when the potentials were used to calculate the odd nucleus exit channel scattering (β_2 =.25 , β_4 =.05). Finally, we mention that we performed these calculations at an energy $E_{prot} = E_{deut}$ +4 MeV corresponding to a stripping Q value compromise for Sm and Er. We believe that this will be sufficient for our purposes and note that an optical potential which fitted the Q of each state of the bands of the residual nucleus is, in any case, not possible with our programs. To give an indication of the extent to which the "experimental" elastic cross section was fitted by Mercy, we can take the example of 20 MeV protons. Arbitrarily giving the 35 "experimental" points 5% accuracy, we find χ^2 =.638. Other cases give a comparable or lower χ^2 .

D. <u>The Deuteron Optical Potentials -- Specific Cases</u>

Many of the general comments concerning the proton optical

potential apply to the case of deuterons. As has been discussed above, the separation of the deuteron centre of mass motion and the use of a one-body optical model must be justified by its utility in describing deuteron scattering. Equivalently, the perturbation series for the optical potential must converge rapidly. In fact, though elastic scattering from a given nucleus can usually be described by some optical potential, the ambiguities are more serious (for example, one can find a series of equally good optical potentials for the real potential depth in multiples of the smallest) than for the case of protons. It is also harder to find smoothly varying optical potentials for a large range of A and E than is the case for protons. The review article of Hodgson[62] contains a useful summary of the problems involved. Until quite recently polarization data for deuteron elastic scattering was rare. There are still few good deuteron polarization data for inelastic states. In every case discussed below where a spin-orbit interaction is used, we choose a "likely" value. The formal considerations above and the work of Lee, Schiffer et al[16] suggest that we seek a deuteron optical potential of $V \sim$ 80-90 and a somewhat thicker surface than for nucleon optical potentials. This immediately disqualifies a large number of published optical potentials . The energy dependence of the deuteron optical potentials is not double that of the nucleon optical potentials owing, no

doubt, to the energy dependence of the perturbation effects. According to Dickens and Perey[75] the most "physical", $V \approx 90$, optical potential appropriate to nickel and deuterons well above the coulomb barrier varies as $V_2 = V_1 - .22\ (E_2 - E_1)$.

1. Magnesium

For the calculations at 10.1 MeV, we used for a DW optical potential that employed by Buck and Hodgson.[76] It is listed as A in Table VII.2. Unfortunately, this optical potential which gives a reasonable fit to the elastic ^{24}Mg (d,d) scattering has a considerably thinner surface than would be expected for the most physical optical potential. This is especially true as they are representing a deformed nucleus by a spherical potential. The elastic and inelastic scattering of deuterons has been studied for a range of energies about 10 MeV by Mayer-Böricke and coworkers,[77, 78] Anomalies appear in the elastic channel, the Blair phase rule breaks down and the excitation function is not at all smooth; the inelastic scattering of deuterons from magnesium below about 15 MeV seems, therefore, not to be well described by the simplest models. Our procedure for the 10.1 MeV case was to use the elastic DW angular distribution calculated using potential A as the ground state data for a search with a coupled channel program. We attempted to fit the 9.97 MeV data of Mayer-Böricke et al for the 2+ state. We did not, as a rule, include the 4+ state in the calculations -- it is

rather close to the bandhead of the quasi-gamma band and has not been resolved in (d,d') reactions in this energy range. In the process of fitting this data (without the use of a search routine for coupled channel calculations), we had occasion to make a series of CC test runs in which each of the A (i.e., Buck and Hodgson) parameters was varied one by one. The result of varying the geometrical parameters is shown in fig. VII.1 and of varying the potential depth parameters in fig. VII.2. From these figures the problem of fitting the 2+ state at back angles is already apparent. This state cannot be fitted by this model. The structure which can be seen[78] varies rather smoothly with energy and may be due to scattering into the 2+ channels from, perhaps, stripping channels or other collective levels. In an attempt to fit this level we also tried a Y_2 expansion of the surface thickness, but with no conclusive improvements. We finally settled on parameter set X listed in Table VII.2, with a deformation of β_2 =.4. The angular distribution using "X" is shown in fig. VII.3. The elastic fit is not perfect -- in view of the fact that this reaction is imperfectly understood, it is not obvious that, if any parameters were found giving an exact fit, they would be the most physical. On this figure, we also show the effect of including a spin-orbit potential (a deformed spin-orbit potential gives almost indistinguishable results); of including the 4+ state (at large angles, the

result is somewhat like that of deepening the absorption slightly, i.e., reducing the oscillations) and increasing the deformation to .5. We have chosen $\beta_2 = .4$ as it seemed more important to fit the scattering at the peak than at the back angles. It could be argued that the deuteron flux corresponding to the back angle scattering can also contribute to the stripping source, and this must be borne in mind. We did perform a stripping calculation (See Chapter VIII.) with $\beta_2 = .5$. Although compound nucleus effects are certainly significant in weaker states than can be produced from $d + Mg^{24}$, the 2+ state of Mg^{24} is too strong for this to be likely here. It is quite possible that second order processes involving the stripping interaction are responsible, although their effect on the ground state cross section may be small. It is interesting that the CC potential X does not have a shallower absorptive part nor could a better fit be obtained with a smaller W. The thinner surface was expected and the deeper real part for coupled channel calculations seems to confirm a trend apparent in the proton results for samarium. The relatively large W seems to underline the important part played by the other low-lying collective states of ^{24}Mg; the 2+ state of the ground band no longer being the only state with a marked individual contribution to the elastic channel. Finally, we note that the fit to the 0+ obtained using the X parameters is at least as good as that obtained by Iano, Penny,

and Drisko[3] using their $\beta_2 = .3$ parameters, which, moreover, appear to have an unphysically large W. Thus we can now state that their model calculations for which the greatest deformation was $\beta_2 = .3$ must underestimate the role of inelastic processes in the entrance channels. Because we were concerned by the seemingly unphysical thinness of the optical potential surface, we carried out a Mercy search to fit the elastic data (that is, the result of a DW calculation using the parameters of Buck and Hodgson) using as a starting point the deuteron optical potential of Smith and Ivash[25] (used also by Cujec[68]). The hope was that the search would find a member of a new family with a larger surface thickness. The program returned a potential very nearly that of Buck and Hodgson. It is possible, of course, that if we had had the original data* used by B. and H. that this search would have discovered quite different parameters. We remark that the absorptive part of the Smith and Ivash optical potential was about half that required to fit elastic scattering and that this optical potential gives a very poor ground state angular distribution indeed. In order to get the DW and CC optical

*Mayer-Böricke and Siemssen[78] fit their 10 MeV (d,d) data with an optical potential with a much more diffuse surface: V=-80, W=-17.3, $r_0 = 1.05$, $\bar{r}_0 = 1.35$, a=.804, $\bar{a}$=.73. We now feel that this would have provided a more realistic starting point for our calculations.

potentials for 12.3 MeV, we apply the Dickens and Perey algorithm quoted above to determine a new CC optical potential. The 0+ cross section obtained was then matched by a Mercy search to obtain DW parameters. A spin-orbit potential was added to each of these to obtain the results shown in Table VII.2 as cases B and C.

2. Deformed Rare Earths

With one exception, our calculations in this region are carried out with 12.1 MeV deuterons. Inelastic scattering measurements with deuterons of this energy have been carried out for various rare earth nuclei including Er by Tjøm and Elbek[79] and Sm by Veje, Elbek et al.[80] In these experiments, the multipolarity of the transitions leading to low-lying states is determined from the partial differential cross section at, typically, two or three angles. Unfortunately, this implies ambiguities in the optical potential obtained by fitting their data. The optical potential given by Tjøm and Elbek[51] but with surface rather than volume absorption was found not quite to fit the ground state of ^{154}Sm and ^{166}Er satisfactorily in DW. However, it is of the correct depth to give physical stripping results and it was merely necessary to increase the real surface thickness to .91 (from .87) to obtain potential D of Table VII.2, fitting the elastic scattering of 12.1 MeV deuterons from ^{154}Sm and ^{166}Er. In order to get a reasonable fit when used in a coupled channel code,

it was merely necessary to reduce A to .87. Because inelastic cross sections are not large (12.1 MeV deuterons are not far above the coulomb barrier) and have a small effect back on the elastic scattering, this small change in the optical potential is sufficient to account for the data that we have. In the case of ^{154}Sm(see fig. VII.4) it was necessary to increase the various deformation parameters beyond those found in (α,α') scattering, in spite of the greater spatial extension of the deuteron. This was particularly true of the Y_4 deformation. The fit shown in fig. VII.4 still badly undershoots the 4+ 90^{o} datum. A possible interpretation is that, as the deuteron is near the coulomb barrier, it sees a deformation characteristic of the far surface of the nucleus. A long series of attempts to fit this level more closely by including, for example, a deformation in the surface thickness or a Y_4 deformation of the coulomb field resulted in no satisfactory conclusion. We emphasize that although the Elbek group may have been able to identify level spins with data at two or three angles, it is not sufficient to study the nature of these states in detail. In fig. VII.4 we give the CC angular distribution of the 0+, 2+, 4+ of ^{154}Sm using parameters "E." In fig. VII.5 we have the DW and CC angular distributions for the 0+ and 2+ states of the ground band of ^{166}Er using parameters "D" and "F" respectively (but the DW calculation used the "F" deformation parameters). Although

the CC (A =.87) and DW (with A =.91) theoretical curves both fit the small number of elastic data points reasonably well, the curves are rather different. It might well be argued that we should have obtained better DW parameters by fitting the CC elastic data with a Mercy search. This was done (see below) at 16 MeV. At 12 MeV, the small effect of the 2+ state on the elastic scattering makes it, perhaps, plausible that the requisite change in optical potential will have a small effect on stripping. We shall see, too, that for the geometric parameters of the imaginary part, the DW and CC deuteron optical potentials differ considerably more at 20 MeV than at 16 MeV. Strictly speaking, it would have been more consistent to have chosen optical potentials with the same elastic scattering rather than with equally good fits to the (meager) elastic scattering data. It is noteworthy that the Tjøm/Elbek optical potential, slightly modified, works reasonably well over this range of atomic mass. That we have not had the data to obtain a detailed fit to the elastic data may be more detrimental in the present case where we include the states with the greatest effect on the g.s. in our calculation. Siemssen and Erskine[28] find that an average optical potential may be much better than particular potentials that fit the elastic cross sections exactly for each nuclide for which stripping is to be calculated by using DWBA. Presumably, this is largely due to precisely the variability

from nucleus to nucleus of the inelastic processes which we are explicitly including. Thus our inability to determine unambiguously all the parameters needed to describe inelastic processes implies that we are not fulfilling the possible full potential of our procedure. We expect that the effect back onto the g.s. of states other than the 2+ and 4+ of the ground band to be quite small (Glendenning and Mackintosh[54]). For the gadolinium optical potential, we argue that, as the samarium DW and CC optical potentials work satisfactorily for erbium, we believe a fortiori, they must be suitable for gadolinium (^{156}Gd has nearly the same β_2 as ^{154}Sm.)

Suitable CC and DW optical potentials were determined for 16 and 20 MeV deuterons by extrapolating the CC optical potential by means of the above mentioned energy dependence and then obtaining the DW parameters by means of a Mercy search on the elastic scattering. The calculations were performed using ^{156}Gd mass parameters. We find that the product $V r_o^2$ for 16 and 20 MeV is about 8% greater for CC than for DW, confirming a trend that we found for 10.1 and 12.3 MeV deuterons (in the 10.1 MeV case where r_o was fixed, V had to be deepened for CC).

There remains the question of the gamma band in erbium. We commented (Mackintosh[29]) that the custom of speaking of an l=2 excitation as if it meant the same for a k=0 or k=2 state was to be called in question, at least for the case of

50 MeV alpha particles. We were informed* that in some cases, at least, Y_{20} and Y_{22} excitation lead to very similar results. We have attempted to fit the gamma bandhead of ^{166}Er using a ("correct") Y_{22} deformation (a_{22}=.035; it was important to have the same coulomb a_{22}) and, alternatively, an ad hoc a_{20}=.043 together with the DW optical parameters "D." The curves resulting were rather different and the fit corresponding to the Y_{20} deformation was inferior. These are shown in fig. VII.6 where we also show how the inclusion of a (somewhat too weak) ground band 2+ state spoils the fit to the gamma 2+. We conclude that for the purposes of calculating stripping to the gamma band in ^{167}Er, a CC calculation, including the g.s. and the γ 2+ state and using the DW optical potential together with an appropriate Y_{22} deformation, should provide a deuteron wavefunction suitable for a model calculation.

---

*D.L. Hendrie, private communication.

Appendix I

Definition of Optical Potential and Specification of Deformation

1. Spherical Optical Potential

The deformed optical potential is defined in terms of the following form for the central potential

$$V f(r, r_0, a) + i\left(W f(r, \bar{r}_0, \bar{a}) - 4\bar{a} W_D \frac{d}{dr} f(r, \bar{r}_0, \bar{a})\right) \qquad (I\cdot1)$$

and for the spin-orbit potential:

$$\tilde{\sigma}\cdot\tilde{\ell}\left(\frac{\hbar}{M_\pi c}\right)^2 \frac{V_{so}}{r}\frac{d}{dr} f(r, r_{os}, a_{so})$$

$$= 2(\tilde{\ell}\cdot\tilde{s})\ 1.99798\ \frac{V_{so}}{r}\frac{d}{dr} f(r, r_{so}, a_{so}) \qquad (I\cdot2)$$

For the coulomb potential:

$$\begin{cases} Z z' e^2/r & r > R_c \\ \dfrac{Z z' e^2}{2R_c}\left(3 - \dfrac{r^2}{R_c^2}\right) & r \le R_c \end{cases} \qquad (I\cdot3)$$

This is the convention we have used: unfortunately with it V, W and W_D are negative, V_{so} is positive.

The formfactor $f(r, r_0, a)$ is of Saxon-Woods form with radius parameter r_0 and surface thickness a:

$$f(r, r_0, a) = \left\{1 + \exp\left[(r - (r_0 A^{1/3} + r_{con}))/a\right]\right\}^{-1} \qquad (I\cdot4)$$

where r_{con} is a constant, associated with the projectile size, introduced so that r_0 should be constant over a range of A.

In fact, we have taken $r_{on}=0$ unless otherwise stated. We note that our program has provision for a complex spin-orbit potential.

2. Deformed Optical Potential

In general, both the radius and the thickness of the surface may vary around the nucleus. We may parameterize this as follows - expand r_o and a in spherical harmonics:

$$r_o' = r_o \left(1 + \sum_{\lambda\mu}' \beta_{\lambda\mu} Y_{\lambda\mu}(\theta',\varphi')\right) \qquad (I\cdot5)$$

$$a' = a \left(1 + \sum_{\lambda\mu}' \alpha_{\lambda\mu} Y_{\lambda\mu}(\theta',\varphi')\right) \qquad (I\cdot6)$$

where θ' and φ' are the intrinsic frame angular coordinates. Then, for the real part of (1), we can make the following expansion in terms of derivatives of f :

$$V(r) = V f(r, r_o, a) +$$

$$+V \sum_{\Lambda\bar{k}}' \sum_{\nu=1}^{\infty} \sum_{\mu=1}^{\infty} \frac{(-r_o)^\nu a^\mu}{\nu!\,\mu!} \Delta_{\Lambda\bar{k}}^{(\nu,\mu)} \frac{\partial^{\nu+\mu}}{\partial^\nu r\, \partial^\mu a} f\, Y_{\Lambda\bar{k}} \qquad (I\cdot7)$$

where

$$\Delta_{\Lambda\bar{k}}^{(\nu,\mu)} = \sum A\begin{pmatrix} Lk \\ L'k' \\ \Lambda\bar{k} \end{pmatrix} \delta_{Lk}^{(\nu)} \tilde{\delta}_{L'k'}^{(\mu)} \qquad (I\cdot8)$$

$$\left(\sum \beta_{\lambda\mu} Y_{\lambda\mu}\right)^n = \sum_{Lk} \delta_{Lk}^{(n)} Y_{Lk} \qquad (I\cdot9a)$$

$$\left(\sum \alpha_{\lambda\mu} Y_{\lambda\mu}\right)^n = \sum_{Lk}' \tilde{\delta}_{Lk}^{(n)} Y_{Lk} \qquad (I\cdot9b)$$

and

$$A\begin{pmatrix} L & k \\ \Lambda & M \end{pmatrix} = \left[\frac{\hat{L}\,\hat{L}'\,\hat{\Lambda}}{4\pi}\right]^{1/2} \begin{pmatrix} L & L' & \Lambda \\ 0 & 0 & 0 \end{pmatrix} \begin{pmatrix} L & L' & \Lambda \\ k & k'-M \end{pmatrix} \qquad (I\cdot 10)$$

Equation (9a) and (9b) are to be regarded as defining $\delta^{(n)}$. These definitions are a generalization of those given by Glendenning[35] to include the surface thickness expansion. The imaginary part is entirely analogous. The formulation of the coulomb deformed potential is exactly as given by Glendenning. Including the complex parts, we can write (7) as

$$V(r) = Vf + \sum_{\Lambda \bar{k}}{}' N_{\Lambda \bar{k}}(r)\, Y_{\Lambda k}(\theta', \varphi') \qquad (I\cdot 11)$$

Transforming to the space fixed frame, using the same convention of rotation matrix elements that is customarily used in the collective model, we get

$$V(r,\theta,\varphi) = Vf(r) + \sum_{\Lambda M} Y_{\Lambda M}(\theta,\varphi) \sum_{\bar{k}\geq 0}{}' V_{\Lambda \bar{k}}(r)\, \frac{D^{*\Lambda}_{M,\bar{k}} + (-)^{\bar{k}} D^{*\Lambda}_{M,-\bar{k}}}{1+\delta_{\bar{k}0}} \qquad (I\cdot 12)$$

where $V_{\Lambda\bar{k}} = N_{\Lambda\bar{k}} + C_{\Lambda\bar{k}}$ where $C_{\Lambda\bar{k}}$ is coefficient for deformed coulomb potential. This is the form we use in Chapter VI.

Appendix II

Composite Particles and Deformed Nuclei

There is no comprehensive, self consistent theory which links the various different measurements of nuclear deformation in a perfect way. Different projectiles often give different deformations, and so they should, for they never measure quite the same thing. For example, one should not expect the deuteron to be sensitive to Y_6 components on the surface, because of the large physical extension of the deuteron. The problem is partly one of "folding in" the size of the projectile into a single particle field. We expect greater accuracy for the real part when we do this than for the imaginary part, as the higher order terms are proportionally greater for the latter.

Let us start with the result employed by Greenlees, Pyle and Tang[60] to calculate the first order real part of nucleon optical potential. The basic input is the nuclear density distribution $\rho(r)$. We shall generalize the Greenlees model to include a deformed density parameterized as follows (axially symmetric):

$$\rho(r) = \sum_{\lambda=0}^{\lambda_{max}} f_\lambda(r) Y_{\lambda 0} \qquad (II\cdot 1)$$

The f_λ may be obtained from a Taylor expansion, exactly as are the coefficients for a deformed optical potential. Then Greenlees et al evaluate

$$V(r_1) = \int \rho(r) V(r - r_1)\, d^3r \qquad (II\cdot 2)$$

where $V(r-r_1)$ is the interaction between a nucleon at r_1, and one at r. Their results for the spin-orbit term are more complex and we shall not attempt to generalize them here. Considerable simplification ensues if we choose a gaussian for V (the full extent of this will become apparent when we generalize a deuteron)

$$V(|r_1 - r|) = V \exp\left(-\frac{(r_1 - r)^2}{b^2}\right) \qquad (II\cdot3)$$

$$\therefore \quad V(\vec{r}_1) = V \int \sum_{\lambda} f_\lambda(r)\, Y_{\lambda 0}(\theta,\varphi)\, \exp\left(-\frac{|r_1 - r|^2}{b^2}\right)$$

$$= V \exp\left(-\frac{r_1^2}{b^2}\right) \int \exp\left(\frac{-r^2}{b^2}\right) \sum_{\lambda} f_\lambda(r)\, Y_{\lambda 0}(\theta,\varphi) \times$$

$$\times \exp(2 r_1 r \cos\omega / b^2)\, d^3 r \qquad (II\cdot4)$$

where ω is the angle between vectors $\vec{r}_1$ and $\vec{r}$.

Now

$$\exp(i \vec{k}\cdot\vec{r}) = 4\pi \sum_{l=0}^{\infty} \sum_{m=-l}^{l} i^l j_l(kr)\, Y^*_{lm}(\theta,\varphi)\, Y_{lm}(\Theta,\Phi)$$

(θ,φ) being the angular coordinates of $\vec{r}$ and (Θ,Φ) of $\vec{r}_1$. Using this expansion with a real argument, we get

$$\exp(2 r_1 r \cos\omega / b^2) = 4\pi \sum_{\lambda,\mu} i^\lambda j_\lambda\left(\frac{2 i r_1 r}{b^2}\right) Y^*_{\lambda\mu}(\theta,\varphi)\, Y_{\lambda\mu}(\Theta,\Phi)$$

Inserting this in (II.4) we readily find that we can expand:

$$V(r_1) = \sum_{l=0}^{l_{max}} W_l(r_1)\, Y_{l,0}(\Theta,\Phi) \qquad (II\cdot5)$$

where

$$W_l(r_1) = 2\pi^{3/2} V \left(\frac{b}{r_1}\right)^{1/2} \exp\left(-\frac{r_1^2}{b^2}\right) J_l(r_1) \qquad (II\cdot6)$$

and where

$$J_\ell(r_1) = \int_0^\infty \exp\left(\frac{-r^2}{b^2}\right)\left[\frac{b}{r}\right]^{1/2} f_\ell(r)\, I_{\ell+\frac{1}{2}}\left[\frac{2r_1 r}{b^2}\right] r^2 dr \qquad (II.7)$$

The functions I are "modified Bessel functions of first kind" defined by $I_\nu(z) \equiv i^{-\nu} J_\nu(iz)$ and are real. Thus we can get from expansion (II.1) to expansion (II.5) with a simple transformation. Note that expansion (II.1) can be made by applying a surface expansion, to, for example, a Saxon Woods formfactor, as is usually done for the optical potential. (See Appendix I.)

To calculate the first order term a deformed optical potential for a deuteron from the nuclear density distribution (II.1), we must insert $V(r_1)$ given by (II.5) into $V(R) = \langle o | V_p + V_n | o \rangle$. This expression, we note, has been calculated for the much easier case of spherical nuclei by S. Watarabe[81] and J.R. Rook.[82] In the simple treatment below we treat V_n and V_p as the same and real. There is no problem involved in generalizing this. We must evaluate

$$V(\hat{R}) = \sum_\lambda \left\langle \chi_o(r_p - r_n) \right| W_\lambda(r_p) Y_{\lambda o}(\theta_p, \varphi_p) + W_\lambda(r_n) Y_{\lambda o}(\theta_n, \varphi_n) \left| \chi_o(r_p - r_n) \right\rangle \qquad (II.8)$$

The difficulty arises in the non-central terms. Let us write $V(\tilde{R})$ in the simple form

$$V(\tilde{R}) = \int d^3\rho\, \chi^*(\rho) \left(V_n\left(\hat{R} + \frac{\hat{\rho}}{2}\right) + V_p\left(\tilde{R} - \frac{\tilde{\rho}}{2}\right)\right) \chi_o(\rho) \qquad (II.9)$$

Consider a s-wave deuteron, then

$$V(\tilde{R}) = 2\int d^3\rho \, |\chi_o(\rho)|^2 V_n(R+\rho/2)$$

$$= 2\int d^3\rho \, |\chi_o(\rho)|^2 V_n(r_n)$$

Now we note (see Watanabe) that $d^3\rho = 2\, d^3 r_n$, hence

$$V(\tilde{R}) = 4\int d^3 r_n \, |\chi_o(2|r_n - R|)|^2 V(r_n) \qquad (II\cdot 10)$$

Now, take a <u>gaussian</u> wavefunction for the deuteron. We assume that as we are essentially studying an effect due to the extension of the deuteron, that a reasonable representation of this effect can be achieved with a gaussian that reproduces the deuteron size. Hence we take

$$\chi_o = A\exp(-\mu\rho^2) = A\exp[-4\mu(r_1 - R)^2]$$

$$= A\exp[-4\mu(R^2 + r_1^2)]\exp(8\mu\tilde{R}\cdot\tilde{r}_1)$$

which we may now insert in (10).

Following through the procedure exactly as before, we get

$$V(R) = \sum_{\lambda=0} V_\lambda(R)\, Y_{\lambda 0}(\theta_R, \phi_R) \qquad (II\cdot 11)$$

where

$$V_\lambda = 16\pi A^2 \exp(-8\mu R^2)\left[\frac{\pi}{32\mu R}\right]^{1/2} J_\lambda \qquad (II\cdot 12)$$

where J_λ is now a transform of W_λ :

$$J_\lambda = \int r_n^{3/2} dr_n \exp(-8\mu r_n^2) W_\lambda(r_n) I_{\lambda+\frac{1}{2}}[16\mu R r_n] \qquad (II\cdot 13)$$

Thus, for the case of a gaussian deuteron, exactly the same mathematical process is involved in folding the deuteron size into a deformed single particle potential as is involved in folding a gaussian nucleon-nucleon potential into an arbitrary nuclear density distribution. Similar procedures could be used to obtain first order optical potentials for other composite particles. It would be a necessary first step in a comprehensive theory connecting nuclear shape to composite particle optical potentials. We note that composite particles such as alphas are commonly used for shape determination because, being strongly absorbed, their interaction with the nucleus takes place largely in the surface. The usefulness of a projectile is a combined function of the shortness of its wavelength, the strength of its absorption, and the smallness of its spatial extension, and the extent to which it will maintain its structural integrity in a nuclear field. The second and the last requirements are not necessarily contradictory if it is unlikely that a particle, once absorbed, will be reemitted leaving the nucleus in a state belonging to P_L.

Table VII.1 (part one). The proton optical potentials discussed in Chapter VII and used in the stripping calculations of Chapter VIII. In the cases listed here, the geometrical parameters for the spin-orbit potential were the same as for the real part of the central potential. The parameters are defined in the Appendix to Chapter VII.

* $\beta_2 = .23$ $\beta_4 = .055$ $\beta_6 = -.015$ $\beta_2(\text{coul.}) = .315$

Label	Nucleus	Deformation	E_{deut}	V	W	W_D	V_{so}
A	Mg	-----	10.1	-50.	-4.	0	0
B	Mg	$\beta_2 = .3$	10.1	-50.	-3.	0	0
C	Mg	-----	12.3	-46.1	0	-9.3	7.5
D	Mg	$\beta_2 = .4$	12.3	-46.1	0	-8.5	0
E	Mg	-----	12.3	-46.161	0	-8.843	0
F	Mg	-----	12.3	-46.161	0	-8.843	7.5
G	Mg	$\beta_2 = .4$	12.3	-46.1	0	-8.5	7.5
H	Sm	-----	12.1	-49.201	0	-14.91	0
I	Sm	*	12.1	-51.438	0	-13.4	0
J	Sm	-----	16.0	-46.3	0	-14.6	0
K	Sm	see I	16.0	-49.983	0	-14.15	0
L	Sm	-----	20.0	-47.98	0	-14.862	0
M	Sm	see I	20.0	-48.738	0	-14.75	0

Table VII.1 (part two).

Label	Nucleus	Deformation	DW/CC	r_0	$\bar{r}_0$	a_0	$\bar{a}_0$	r_c
A	Mg	-----	DW	1.25	1.25	.5	.5	1.25
B	Mg	=.3	CC	1.25	1.25	.47	.47	1.25
C	Mg	-----	DW	1.25	1.25	.65	.47	1.25
D	Mg	=.4	CC	1.25	1.25	.6	.45	1.25
E	Mg	-----	DW	1.228	1.176	.632	.586	1.25
F	Mg	-----	DW	1.228	1.176	.632	.586	1.25
G	Mg	=.4	CC	1.25	1.25	.6	.45	1.25
H	Sm	-----	DW	1.25	1.278	.821	.73	1.2
I	Sm	*	CC	1.25	1.293	.765	.61	1.2
J	Sm	-----	DW	1.297	1.241	.723	.732	1.2
K	Sm	see I	CC	1.25	1.293	.765	.61	1.2
L	Sm	-----	DW	1.262	1.243	.756	.715	1.2
M	Sm	see I	CC	1.25	1.293	.765	.61	1.2

* $\beta_2 = .23$ $\beta_4 = .055$ $\beta_6 = -.015$ $\beta_2(\text{coul.}) = .315$

Table VII.2 (part one). The deuteron optical potentials discussed in Chapter VII and used in the stripping calculations of Chapter VIII. See Table VII.1 for further description.

Label	Nucleus		Energy	V	W	W_D	V_{so}
A	Mg	-----	10.1	-83	-27.8	0	0
X	Mg	.4	10.1	-95	-27.8	0	0
XVLS	Mg	.4	10.1	-95	-27.8	0	5
B	Mg	.4	12.3	-94.0	-28.0	0	5*
C	Mg	-----	12.3	-92.247	-27.975	0	5*
D	Sm,Er	-----	12.1	-86	0	-12	0
E	Sm	.23**	12.1	-86	0	-12	0
F	Er	.26***	12.1	-86	0	-12	0
G	Gd	.23**	16.0	-84	0	-12.8	0
H	Gd	-----	16.0	-86.068	0	-12.669	0
I	Gd	.23**	20.0	-82.0	0	-13.6	0
J	Gd	-----	20.0	-87.987	0	-14.136	0

*r_{so}=1.4 a_{so}=.6

** β_4 =.055 β_6 =-.015 β_2(coul) =.315

*** β_2(coul.) =.307 β_4 =0.

Table VII.2 (part two).

Label	Nucleus		DW/CC	r_0	$\bar{r}_0$	a_0	$\bar{a}_0$	r_c
A	Mg	-----	DW	1.5	1.5	.55	.55	1.5
X	Mg	.4	CC	1.5	1.5	.52	.52	1.5
XVLS	Mg	.4	CC	1.5	1.5	.52	.52	1.5
B	Mg	.4	CC	1.5	1.5	.52	.52	1.5
C	Mg	-----	DW	1.327	1.424	.614	.760	1.5
D	Sm,Er	-----	DW	1.15	1.37	.91	.7	1.20
E	Sm	.23**	CC	1.15	1.37	.87	.7	1.20
F	Er	.26***	CC	1.15	1.37	.87	.7	1.20
G	Gd	.23**	CC	1.15	1.37	.87	.7	1.2
H	Gd	-----	DW	1.098	1.279	.905	.866	1.2
I	Gd	.23**	CC	1.15	1.37	.87	.7	1.2
J	Gd	-----	DW	1.065	1.302	.953	.853	1.2

*r_{so}=1.4 a_{so}=.6

** β_4 =.055 β_6 =-.015 $\beta_{2(coul.)}$ =.315

*** $\beta_{2(coul.)}$ .307 β_4 =0.

Figure Captions for Chapter VII

Fig. VII.1 The inelastic scattering of 10.1 MeV deuterons from ^{24}Mg. The data for the 0^+ state is the result of a DWBA calculation using the parameters of Buck and Hodgson.[76] That for the 2^+ state is taken from the 10 MeV curve of ref.[77] In this coupled-channel calculation, the effects of successively changing various of the geometrical parameters was studied.

Fig. VII.2 As for Fig. VII.1, but here well depth parameters are varied.

Fig. VII.3 The same reaction showing the fit obtained with the use of the X-parameters. Also illustrated is the effect of increasing the deformation to $\beta_2 = .5$ (with a concomitant decrease in surface thickness), the result of including the 4^+ state in the calculation (no data), and the result of including a spherical spin-orbit potential.

Fig. VII.4 Inelastic scattering of 12.1 MeV deuterons from ^{154}Sm. For parameters used, see text.

Fig. VII.5 Inelastic scattering of 12.1 MeV deuterons from ^{166}Er. For parameters used, see text. Comparison of cc and DWBA calculations. The real surface thickness parameter was reduced somewhat for the coupled-channel case.

Fig. VII.6 Coupled-channel study of inelastic scattering leading to the gamma band head of ^{166}Er. For the stripping calculation leading to the gamma band of ^{167}Er, we required a calculation of the entrance channel problem involving the ground state and the γ_{2+} only. We did not alter the surface thickness in this case. It is clear that γ_{20} and γ_{22} deformations give different angular distributions and that γ_{22} is distinctly preferable. We also see that coulomb excitation plays an extremely important role in the excitation of this energy and that the inclusion of the 2^+ of the ground band upsets the calculation. In our model we assumed that if the angular distribution was fitted, the wavefunction in the interaction region was suitable for a stripping calculation. This is not obvious, and probably not accurately true.

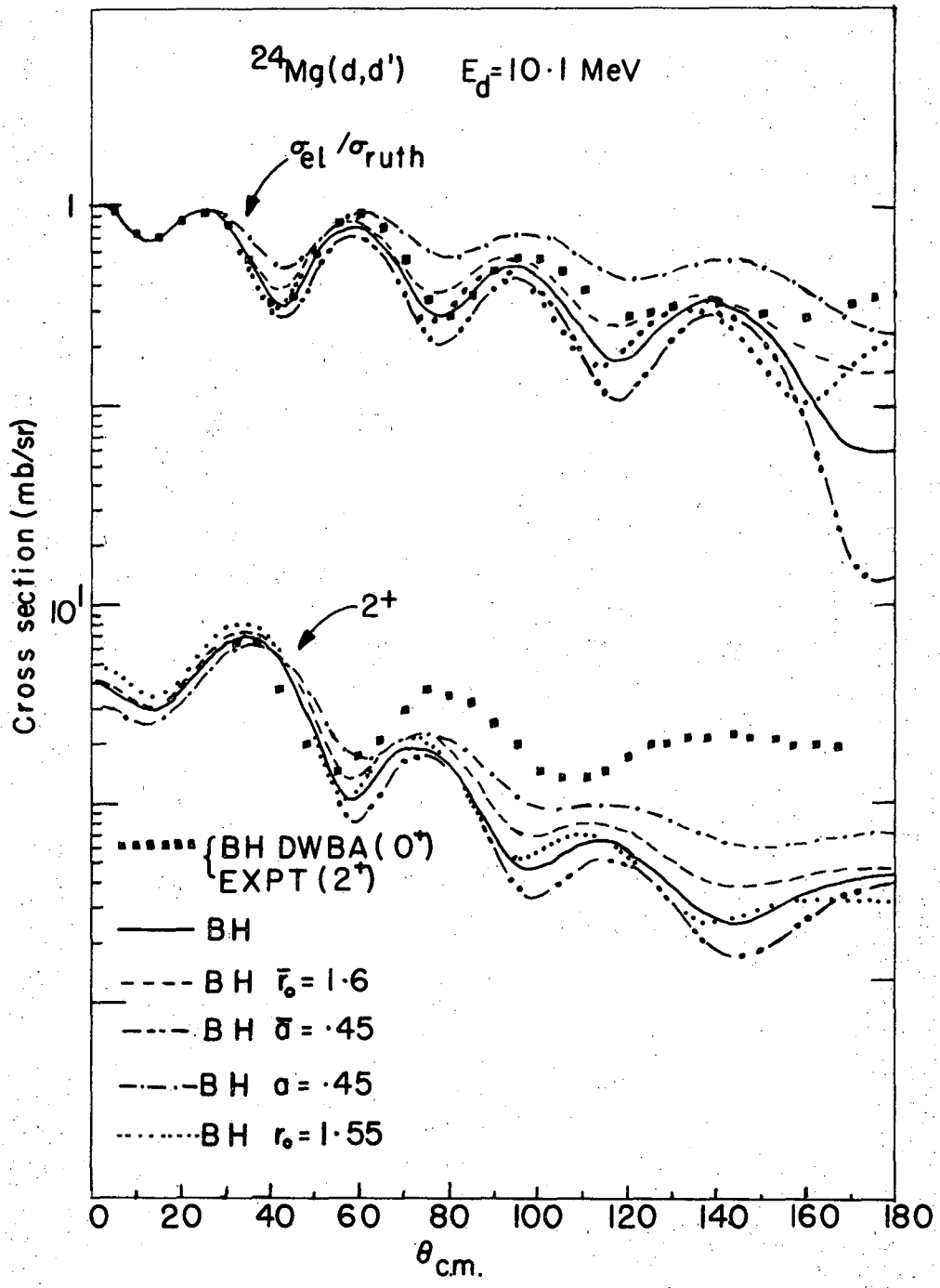
^{24}Mg(d,d') E_d=10·1 MeV
$\sigma_{el}/\sigma_{ruth}$
1
10^{-1}
2+
Cross section (mb/sr)
{BH DWBA (0+)
EXPT (2+)
BH
BH $\bar{r}_o$=1·6
BH $\bar{a}$=·45
BH a=·45
BH r_o=1·55
0 20 40 60 80 100 120 140 160 180
$\theta_{cm.}$
XBL 701-214

Fig. VII.1

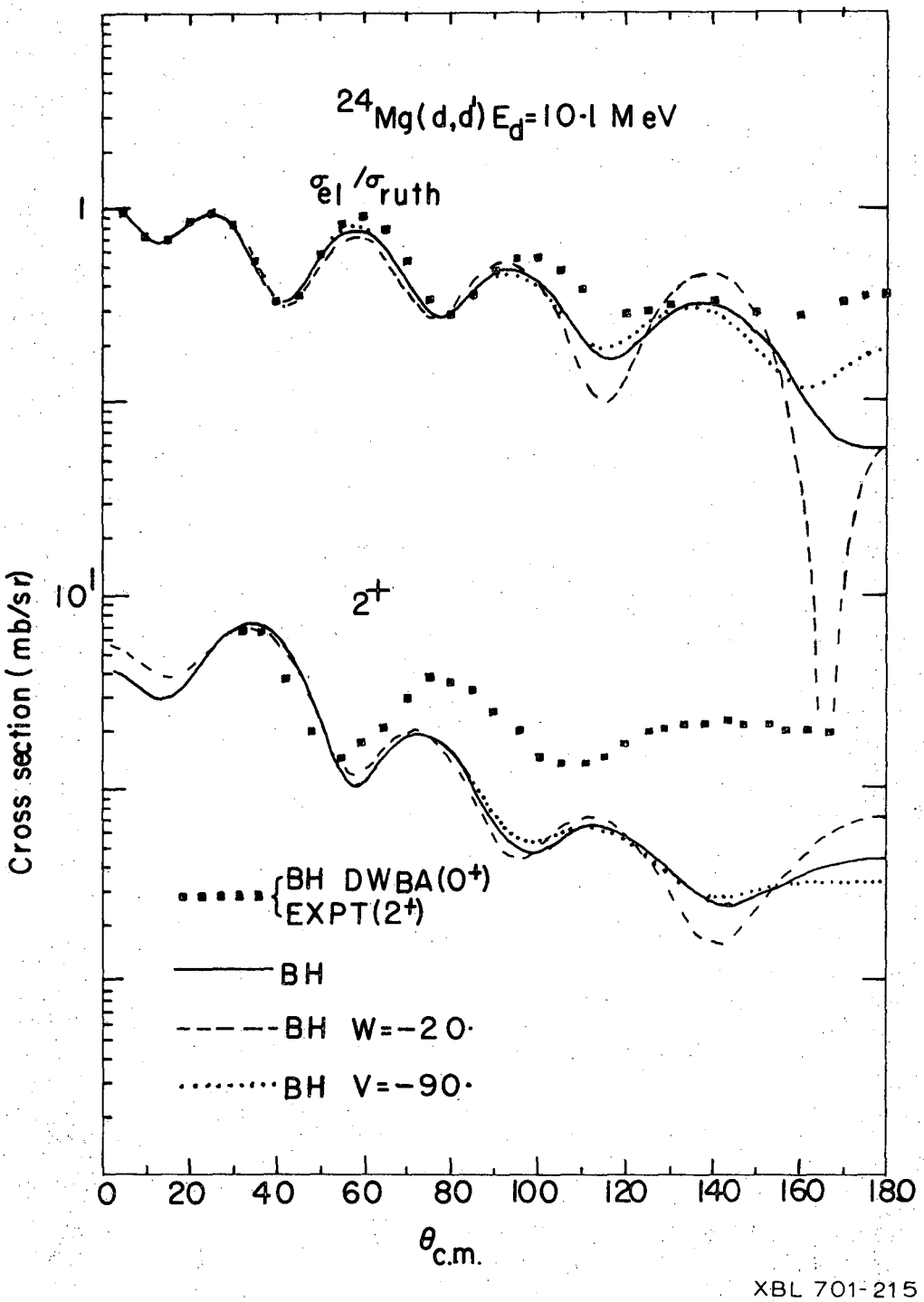
^{24}Mg(d,d') E_d=10.1 MeV
$\sigma_{el}/\sigma_{ruth}$
1
10^{-1}
2^+
Cross section (mb/sr)
BH DWBA(0^+)
EXPT(2^+)
BH
BH W=-20·
BH V=-90·
0
20
40
60
80
100
120
140
160
180
$\theta_{c.m.}$
XBL 701-215

Fig. VII.2

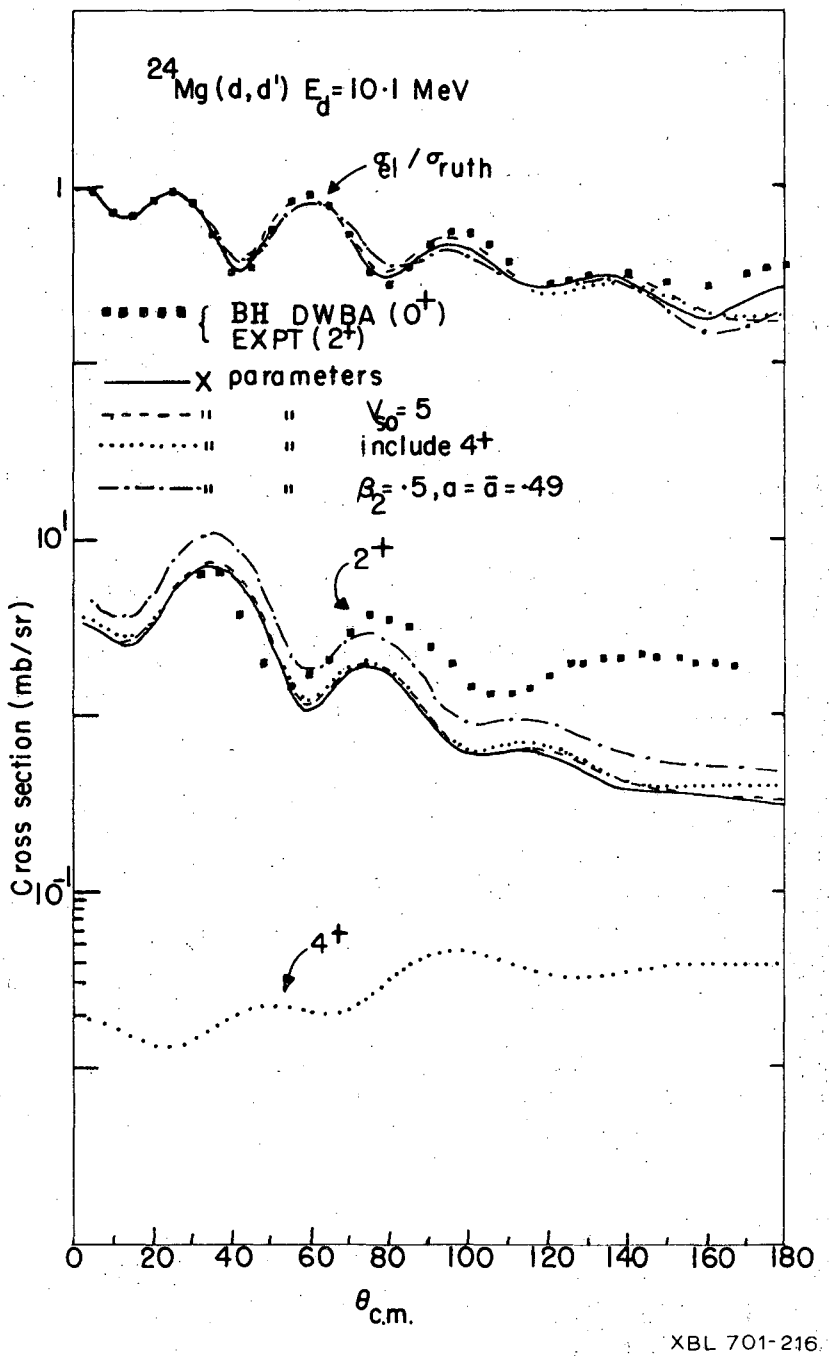
^{24}Mg(d,d') E_d=10·1 MeV
$\sigma_{el}/\sigma_{ruth}$
BH DWBA (0$^+$)
EXPT (2$^+$)
X parameters
" " V_{so}=5
" " include 4$^+$
" " β_2=·5, a = ā = ·49
2$^+$
4$^+$
Cross section (mb/sr)
$\theta_{c.m.}$
XBL 701-216

Fig. VII.3

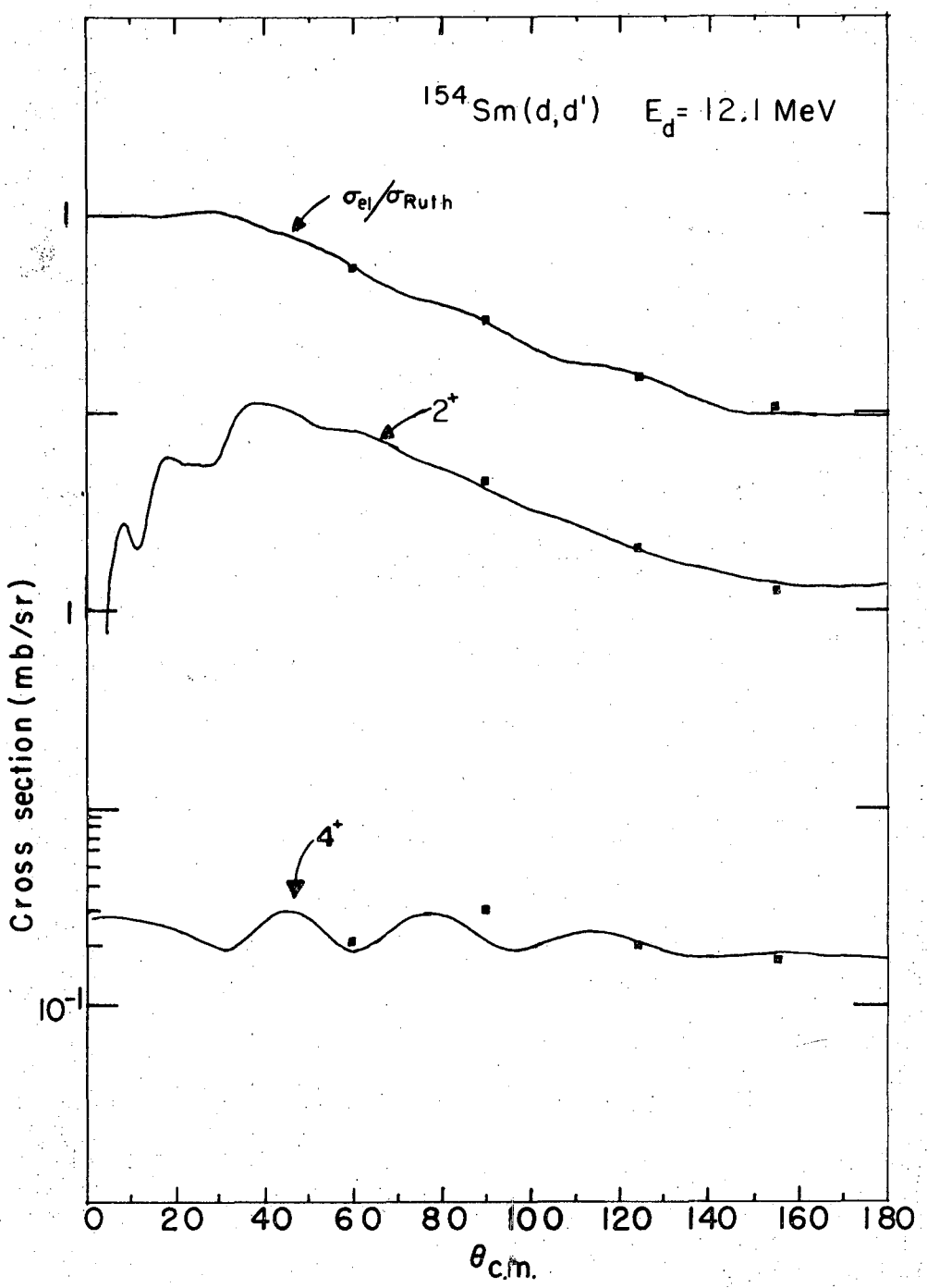
^{154}Sm(d,d') E_d= 12.1 MeV
$\sigma_{el}/\sigma_{Ruth}$
2$^+$
4$^+$
Cross section (mb/sr)
1
1
10^{-1}
0 20 40 60 80 100 120 140 160 180
$\theta_{c.m.}$
XBL 701-217

Fig. VII.4

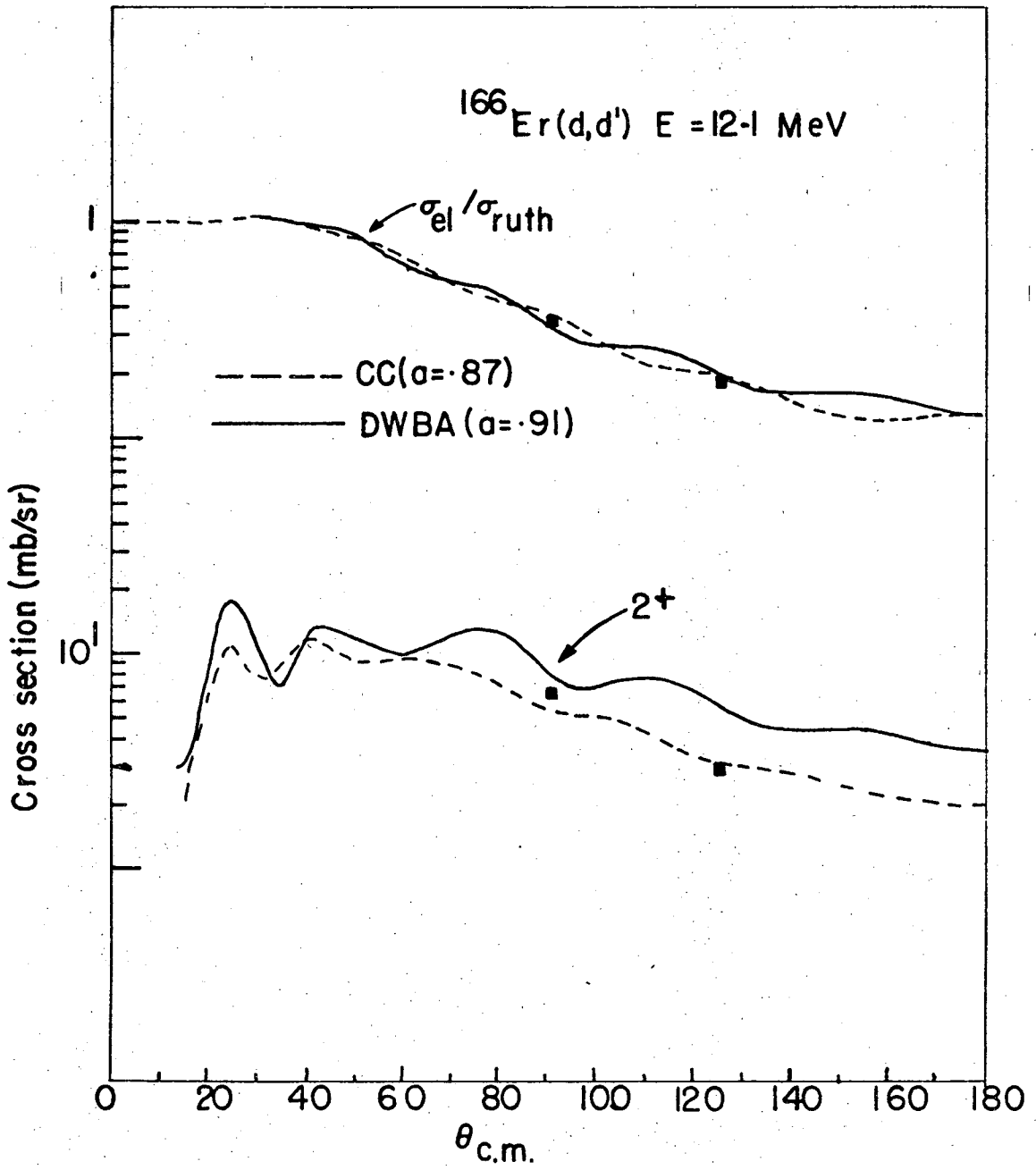
166Er(d,d') E =12-1 MeV
σel /σruth
CC(a=·87)
DWBA (a=·91)
2+
Cross section (mb/sr)
1
10
0
20
40
60
80
100
120
140
160
180
θc.m.
XBL 701 218

Fig. VII.5

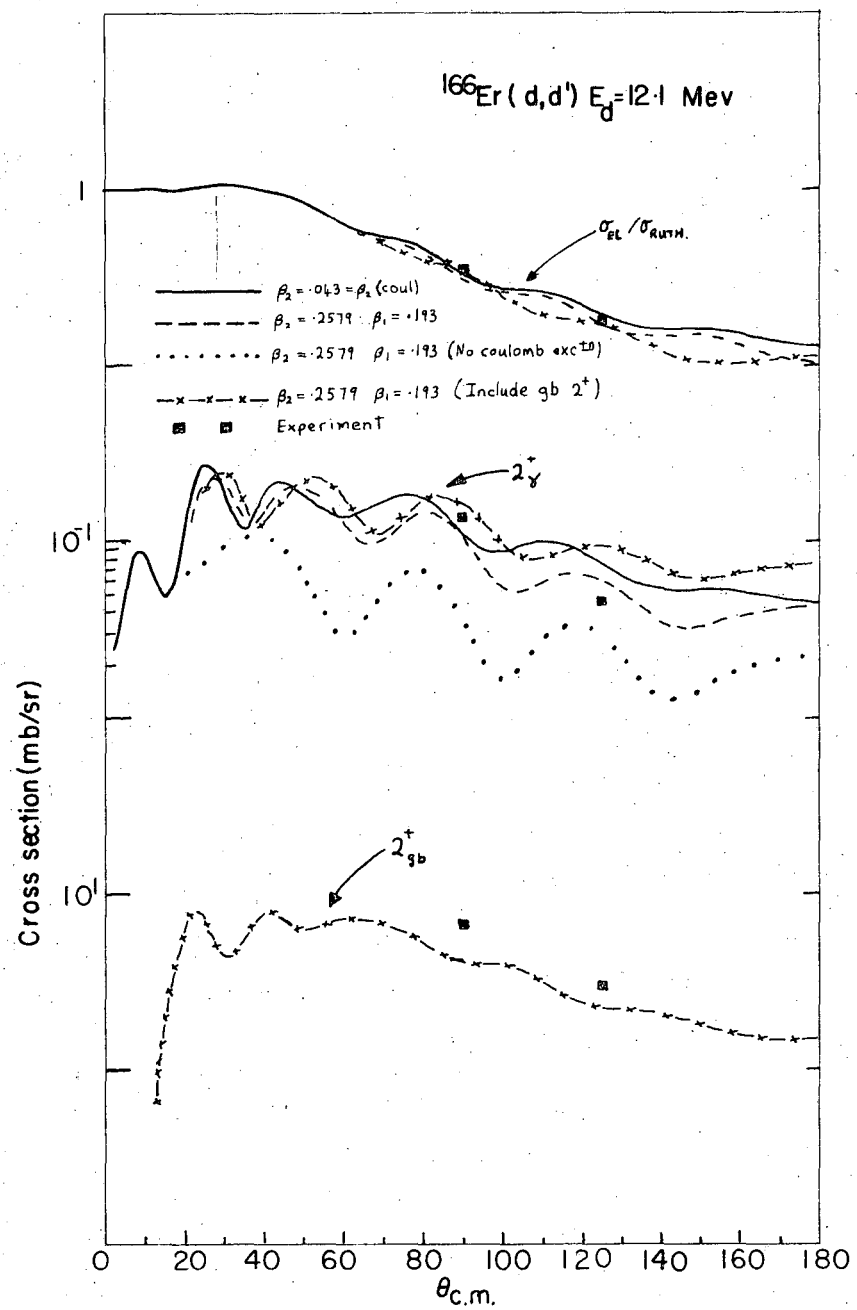
166Er (d,d') Ed=12·1 Mev
1
σEL /σRUTH.
β2 = ·043 = β1 (coul)
β2 = ·2579 β1 = ·193
β2 = ·2579 β1 = ·193 (No coulomb exc to gb)
β2 = ·2579 β1 = ·193 (Include gb 2+)
Experiment
2+γ
10-1
2+gb
10-2
Cross section (mb/sr)
0 20 40 60 80 100 120 140 160 180
θc.m.
XBL 701-219

Fig. VII.6

VIII. THE STRIPPING CALCULATIONS

In this chapter we describe the calculations that were actually carried out on a series of rotational bands in magnesium and in three rare earth nuclei. The calculational procedure and the programs on which the calculations were carried out evolved somewhat during the course of the work with the consequence that the degree to which any calculation is a model calculation or one in which meaningful spectroscopic information was obtained varied from case to case. We do not treat the cases in exactly the order in which the calculations were carried out. Section B also expands the general discussion in the Introduction of stripping on deformed rare earth nuclei.

A. Magnesium

The reaction $^{24}Mg\ (d,p)^{25}Mg$ was studied in a series of model calculations intended to explore in detail the effect of inelastic processes. The advantage of working with light nuclei is that, owing to the smaller radius of integration and smaller number of partial waves required, the computing time needed for a complete study is much less. The fortuitous circumstance that the bands are probably rather free of first order coriolis mixing (the two $k = 1/2$ bands can mix; but they are 2 MeV apart in energy (See A(c).)) is offset by a congeries of drawbacks: first, as we have discussed in Chapter

II, the customary stripping formalism seems not always to work satisfactorily for light nuclei; then, the ^{24}Mg core is not at all stable under the influence of the 25^{th} particle; and finally, the adiabatic wavefunction has been described (Ripka[38]) as a much less valid approximation in this region than it is for the rare earth deformed nuclei. Another problem that may effect our fit to the weaker levels is that compound nucleus processes seem to be present (but see Pearson and Wilcott[22]). Possibly related to this is the impossibility of fitting Mg^{24} (d,d') as discussed in Chapter VII.

Of the rotational bands in ^{25}Mg shown in fig. IV.1, our study has been confined to those based on the [202] 5/2+ and [211] 1/2+ intrinsic states. In particular, we shall attempt to fit the "forbidden" 7/2+ levels at 1.611 and 2.736 MeV. Magnesium region calculations differ from those in the rare earth region in the relatively larger range of outgoing proton energies involved.

The reaction was studied at 10.1 and 12.3 MeV, energies at which this reaction has been studied by Middleton and Hinds[83] and by Hosono[26] respectively. We shall not expect to calculate perfect angular distributions for the case of magnesium for reasons discussed in Chapter II.

(a) The Reaction ^{24}Mg (d,p) ^{25}Mg at 10.1 MeV.

The wavefunctions employed for most of the following

calculations are those listed in Table IV.2 and Table IV.3, calculated using the Faessler-Sheline program. We remark that in spite of the fact that the binding energies were about right, the deformation used is probably too small resulting, in this case, in wavefunction components with excessively long tails. See, however, section A(d) below where, in particular, we give a reference to a very recent use of the "constant deformation" assumption. Unless explicitly mentioned, all calculations employ proton parameters "A" or "B" of Table VII.1, according as the protons are treated in DW or CC approximations. Similarly, we always use "A" or "X" of Table VII.2 for the deuterons. The results of a model calculation of stripping leading to the ground band of ^{25}Mg are illustrated in figs. VIII.1 to VIII.5.

Note: These ground band calculations were performed with six radial components in the wavefunction. The DWBA calculations without spin-orbit interactions that appear in figures VIII.1, VIII.2, VIII.4 were calculated with seven components. The comparison in these figures should be made with a DWBA calculation with six components. This latter is very close to the seven components calculation except that the stripping peak is reduced about ten percent. Thus, the apparent effect shown in fig. VIII.4 where spin-orbit interactions have reduced

the 5/2+ cross section ten percent, is spurious. The seventh radial component makes a smaller difference to the cross section than the sixth. See Appendix I of Chapter IV.

From fig. VIII.1 we conclude that inelastic process in the exit and entrance channels contribute comparable amplitudes to the "forbidden" 7/2+ state, but that the strong 5/2+ state is affected only in the details of its angular distribution by its coupling to the weak 7/2+ state. The 2+ state in the entrance channels, excited in this instance according to a DW calculation, has had a clear effect (50% increase at the stripping peak) on the ground state. In this case, of course, the various amplitudes all involve the same 5/2+ component. Figure VIII.2 illustrates the effect of varying the deformation in the outgoing channels and also compares the effect on the stripping reaction of the DW and CC excitation of the target 2+ state. The smaller effect when the latter state is CC excited corresponds to the smaller inelastic cross section when compared with DW excitations using the same deformation. The different angular distribution, however, reflects the qualitatively different deuteron wavefunction in the stripping region. In fig. VIII.3 we illustrate the effect of including a spin-orbit interaction in the entrance or exit channels. The "forbidden" 7/2+ state is depressed about 20% by a deuteron spin-orbit interaction

V_{so} =5 (as we shall see, the effect is exactly the reverse for the 7/2+ state of the k= 1/2 band). Deforming the deuteron spin-orbit optical potential was found to have a very small effect. The spin-orbit potential in the proton channels had some effect on improving the angular distribution in a CC calculation, but a lesser one in a DWBA calculation as can be seen in fig. VIII.4 where we match the data[83] with the angular distributions of DWBA and complete CCBA calculations including spin-orbit interactions. The 7/2+ state is underestimated by a factor from two to three over most of the angular distribution. The excess measured protons could come from a number of sources. For reasons mentioned in Chapter VII, compound nucleus effects are likely to play a role in levels this weak. (A comparison with the case of calcium where compound nucleus effects play a role in levels this strong discussed by Lee, Schiffer et al[16] suggests that, a fortiori, they should play a role in the lighter magnesium nucleus.) We find that increasing the entrance channel deformation to .5 increases the 7/2+ cross section by 20% rather uniformly. (It also increased the 5/2+ level 10% at the stripping peak.) Including transitions through the 4+ state of ^{24}Mg hardly affected the 5/2+ state but increased the 7/2+ by 20% at 90^{o} with no effect at 0^{o} and 180^{o}. We estimate from the experiments of Crawley and Garvey[56] and the gamma decay experiments of McCallum and Sowerby[84] that the

amplitudes of the single particle interband transitions from the 3/2+ and 5/2+ states of the [21$\bar{1}$] 1/2+ might be about .25 of the intraband transition amplitude from the ground state. There is also the 3/2+ state of the [200] 1/2+ band that is strongly excited in stripping. It is quite conceivable, then, that the coherent sum of amplitudes from these inelastic processes could double the cross section to the 7/2+ state. Finally, although it is probably true that this band of ^{25}Mg has a smaller deformation than ^{24}Mg, the low calculated 7/2+ cross section could be taken as an indication that we have underestimated this (and perhaps the ^{24}Mg) deformation. (See fig. VIII.2.)

In fig. VIII.5 we compare the polarization from the complete DWBA and CCBA calculations with $\beta_2(\text{deut.}) = .4$, $\beta_2(\text{prot}) = .3$. We shall comment about the somewhat surprisingly low overall experimental cross section of this band below (section A(d)).

A series of model calculations of stripping to the [21$\bar{1}$] 1/2+ bands were carried out using the F-S wavefunctions listed in Table IV.2; for reasons mentioned above and in Chapter IV, these are probably not good wavefunctions: although the c_{j1} are probably about right, the tail on the $j = 3/2$ component is relatively too long, and we have seen in Appendix I to Chapter IV that this could drastically overemphasize the cross section of the 3/2+ state.

In fig. VIII.6, the effect of proton coupling between the states of the residual nucleus is shown. The overall cross sections of the three strong levels are not changed much; they are of comparable strength to each other and we shall find a tendency for weaker levels to be boosted by exit channel inelastic effects. Thus, in this case, the weaker 5/2+ state (weaker, that is, where, as in this case, there are no transitions through the target 2+ state) is not reduced by these processes, whereas the 1/2+ and 3/2+ states are depressed by about 20% and the 7/2+ state, which, with this wavefunction, would otherwise be forbidden, is now weakly excited. It is noteworthy that the angular distributions to the 3/2+ and 5/2+ levels are respectively depressed and augmented just beyond the stripping peak. This is in qualitative agreement with the data [83] shown with the more realistic case in fig. VIII.8 discussed below. Figure VIII.6 also shows the effect on a DWBA calculation of increasing the number of radial quanta included in the neutron wavefunction from seven to eight. By comparing with Table IV.2, it is clear that there is an immediate correspondence between the effect seen in any level and the amplitude of the corresponding eighth radial quantum. The result of including stripping amplitudes arising from the first order (DWBA) excitation of the target 2+ state was studied and the results are shown in fig. VIII.7. The effect on the bandhead state is rather

small but the 3/2+ and 5/2+ states are respectively depressed by 50% and doubled at their stripping peaks. This figure also shows the effect of exit channel coupling. The changes evident in the previous figure in the two l=2 levels persist. The larger effect of proton coupling on the 1/2+ state (c.f. fig. VIII.6)must be due to the fact that the 5/2+ state is now stronger. Again it seems that entrance and exit channel inelastic processes are of comparable importance for the 7/2+ state. The amplitudes arising from the 2+ state are smaller when a coupled channel deuteron calculation is employed to calculate the deuteron wavefunctions; these wavefunctions also result in a less drastic attenuation of the 3/2+ cross section in the backward hemisphere. This can be seen in fig. VIII.8 where we compare complete (i.e., including spin-orbit interactions) DWBA and CCBA calculations of this band and compare the results with the data.[83] The levels are of incorrect strengths: the data, of arbitrary normalization, must be multiplied by .2882, .5714, and .40 for the three states in order to obtain the fit shown. These factors should be equal. Probably, the main source of error lies in the j=3/2 component having too long a tail. When the calculation, identical but for the 3/2+ formfactor being scaled by .74 ($.74^2$=.55) was carried out, the cross section of the 3/2+ state was scaled by .51 at the stripping peak, but was attenuated much less at back angles giving an overall improvement

to the angular distribution. As is clear from the figure, these normalizations factors would have varied over a much greater range in a DWBA calculation. The 7/2+ state was considerably weakened by this change in $c_{3/2}$, due possibly to either entrance or exit channel effects. The 5/2+ state was not changed much but the last diffraction minimum of the 1/2+ state was somewhat displaced. The significant conclusion, however, is that even with inelastic processes present, the cross sections still retain a semblance of proportionality to c_j^2 over a fairly wide range. The .51 factor (in particular, the fact that it is lower than the .55 reduction factor for c^2) is easily understandable in terms of the reduction of the largest of several destructively coherent amplitudes for this state. Because the degree to which this approximate proportionality to c_j^2 might vary from state to state, we should probably make use of it only over a small range of c_j^2 where a few percent change might improve the overall fit. In the present case, however, making use of this approximate linearity, the orthonormality ($c_{1/2}^2 + c_{3/2}^2 + c_{5/2}^2 = 1$, in this case) and the data normalization numbers cited above, we find $c_{1/2}^2 = .3962$, $c_{3/2}^2 = .3933$, $c_{5/2}^2 = .2104$. We give these for reference; apart from their approximate method of derivation, the corresponding c_j's are amplitudes of incorrect radial wave-functions. We give "better" values later in this section.

The influence of spin-orbit interactions in the proton and deuteron channels is illustrated in fig. VIII.9. In this case, a deuteron spin-orbit interaction enhances the 7/2+ state, contrary to what was discovered for the ground band.

There is one inconsistency in the above calculations: the deuteron optical potential was found by fitting scattering; the proton optical potential was determined as suitable for stripping and has a very small absorptive part. In fig. VIII. 10, we illustrate the effect of deepening $W_{(prot)}$ from -3 to -6. This figure also demonstrates that the l=4 components of the wavefunction used had a smaller effect on all but the 7/2+ angular distribution. Unfortunately, the SAXOND wavefunction employed in this calculation corresponds to $\beta_2 = .2$ and the l=4 components have about half the amplitude of those in Table IV.6 so that this figure represents a lower limit of the effect of the l=4 components.

A stripping calculation was performed using the "best" wavefunction (Table IV.6a) and the fit to the experimental data is shown in fig. VIII.11. We have normalized the results as follows: the experimental points for each state are scaled so that the best (subjective) fit near the stripping peak is obtained. The scaling factors for the three states are, respectively, starting with the bandhead, 1.055, 1.333, 1.222, 1.285. (These numbers are relative; they should not be compared with others that might be quoted.) The fourth of

these factors was a compromise value not obtained by fitting the 7/2+ state for which the theory is clearly too low. We note that this fit corresponds to the theoretical values of $c_{1/2}^2 = .283$, $c_{3/2}^2 = .501$ and $c_{5/2}^2 = .197$. If we assume that cross sections are still roughly proportional to c^2, we can extract "theoretical" c^2 values by scaling c^2 so that the factors by which the experimental data for each state would have to be multiplied for a match with the theory are all equal. In this manner we determine normalized values $c_{1/2}^2 = .333$, $c_{3/2}^2 = .467$, $c_{5/2}^2 = .200$. We emphasize that these are probabilities for the particular radial wavefunctions implicit in Table IV.6a, and that small changes in radial form can potentially entail c^2 values that are considerably different. A problem that is evident from fig. VIII.11 is the difficulty, engendered by the imperfect fit to the l=0 state, of determining the best angle for normalizing theory to experiment for this state. The fit of the strengths of these states is quite good, differing greatly from what would be the case for these wavefunctions in a DWBA calculation. We conclude that our adiabatic nuclear model based on a prolate, axial intrinsic state of $\beta_2 = .4$ is substantially correct - for further comment see section A(d) below and ref.[86] Moreover, the qualitiative difference between the shapes of the two l=2 levels is reproduced in a way that is not possible with any spin-orbit potentials alone. However, real discre-

pancies remain - the stripping peaks and minima for the three strong states are not perfectly reproduced in shape. This may in part be a result of incorrect geometric factors in the optical potentials - perhaps the too thin surface of the deuteron potential. The angular distribution to the 3/2+ state is not well explained at back angles. Very possibly there is coupling in the proton channels from the quite strong 3/2+ state of the [200] 1/2+ band. It is just possible that compound nucleus components are present in the 7/2+ cross section; however, our theory does not explain the large cross section at 150°. The difference is probably the sum of effects due to (a) inadequacy of treatment of proton channel scattering for k = 1/2 bands (b) interband coupling (c) the l=4 components might very well be much larger than used in our calculation. An increase of the deformation of the optical potential and the introduction of a Y_4 intrinsic deformation could both have a significant effect on this state; (d) coriolis mixing with the [200] 1/2+ band (see discussion in section A(c) below).

The sensitivity of our results to the Y_2 deformation employed in the scattering part of the calculation will be shown for the case of 12.3 MeV deuterons in the following section.

It is to be noted that the calculations illustrated in figures VIII.4 and VIII.8 required rather different normalization

factors in order to fit the data.* This may be interpreted in terms of a core overlap $\langle \tilde{\sigma} | \sigma \rangle$ for the ground band of ^{25}Mg of about 0.8. Owing to uncertainties in the wavefunction, this must be regarded as a tentative figure. For further discussion, see the account of the 12.3 MeV reaction below.

(b) The Reaction ^{24}Mg (d,p) ^{25}Mg at 12.3 MeV

We have attempted to fit the 12.3 MeV data of Hosono.[26] For our study, we used proton optical potentials "F" and "G" of Table VII.1 and deuteron potentials B and C of Table VII.2. With one exception, we used the wavefunctions of Tables IV.4 and IV.5. The deuteron optical potential was (see Chapter VII) obtained by extrapolation. Such procedures are somewhat doubtful for light nuclei. Energy dependent effects are, we believe, most realistically studied where the deuteron and proton scattering can be fitted to each energy. For this reason, we employed the more "realistic" proton optical parameters and neutron wavefunctions noted above, hoping to achieve good agreement with the 12.3 MeV angular distributions rather than attempt to study the energy dependence of the inelastic processes. To be realistic, such a study requires, if not detailed elastic and inelastic scattering data at each

*The fact that those for the calculations illustrated in fig. VII.10 were quite different is a result of different overall normalization employed in these later calculations.

energy, then at least a well established energy dependence of the optical parameters, and we do not believe this exists for deuterons in magnesium. Unfortunately, it turns out that our angular distributions are not close enough to those measured[26] (which look somewhat unphysical in places) to allow us to unambiguously give normalizations. Qualitatively, the phenomena observed are similar to those at 10.1 MeV.

Ground Band

In fig. VIII.12 we give our results for the ground band. The DWBA cross section to the 7/2+ state is non-vanishing because of the small direct component. Including the 9/2+ state in the calculation had very little effect other than a 30% decrease in the extreme back angle 7/2+ cross section. We see from this figure that the 7/2+ state is underestimated by a factor of 25.19/1.749 = 14.4.

The k=1/2 Band

It was here that there were normalization ambiguities. The results were qualitatively similar to those illustrated for 10.1 MeV. The approximate normalization factors by which the theory must be multiplied to fit the data for the three lowest states (there is no 7/2+ data) are approximately given by:

1. DWBA 6.097 (j=1/2), 2.452 (j=3/2), 9.673 (j=5/2).
2. CC in, direct out 7.794, 4.525, 6.223.
3. CCBA 7.236(-), 5.050(-), 5.952.

two points emerge: (i) these factors are much more uniform for CCBA than for DWBA, (ii) we see that they are greater by a factor of about 3.5 than the ground state factors given in fig. VIII.12. This large ratio (for 10.1 MeV, using F-S wavefunctions, it was about 1.5) reflects the much longer tail of the 5/2+ component of the wavefunction in Table IV.5 than of that in Table IV.4. The possibility that $\langle\tilde{\sigma}|0\rangle$ may depart substantially from unity was examined. Using SAXOND wavefunctions and assuming the core for the ground band had a Y_2 deformation of .3 and that that for k=1/2 band was .4, then $\langle\tilde{\sigma}|0\rangle \approx .95$. It seems quite plausible from the different moments of inertia for these bands[85] (see Chapter IV section F.1) that the deformations could differ this much. Therefore, unless the core is a completely different self consistent solution for a [202] 5/2+ or a [211] 1/2+ orbital, the above mentioned ratio must result from an excessively long tail of the neutron wavefunction. There is no way that $c_{5/2+}$ for the ground band can be substantially less than .98. If the asymptotic radial wavefunctions are about right, then the 10.1 and 12.3 MeV data imply that $\langle\tilde{\sigma}|0\rangle \approx .6 - .8$

(c) Note on Coriolis Mixing

We have not studied the [200] 1/2+ band in ^{25}Mg, although the 5/2+ state, for which $c_{5/2+}$ is very small and which has a greater than "expected" stripping cross section, would be

an interesting level to study. However, this level is also very sensitive to the coriolis mixing of the two bands.[90] We comment that of the levels in the [211] 1/2+ band, the 3/2+ will probably be most affected by the coriolis admixing.[90] The fact that the coriolis admixed components contribute coherently to the cross section could mean that the relative strengths of the 1/2+, 3/2+ and 5/2+ states could have been affected. Litherland et al[90] give admixing amplitudes as follows (for the [211] 1/2+ band), written symbollically:

$$|1/2+\rangle = .99[211] - .13[200]$$
$$|3/2+\rangle = .97[211] - .24[200]$$
$$|5/2+\rangle = .95[211] - .31[200]$$
$$|7/2+\rangle = .92[211] - .39[200]$$

The [200] 1/2+ intrinsic state has the largest probability amplitude for the 3/2+ component and almost zero for the 5/2+ component which is the reason for our statement above that the 3/2+ state is the most affected by band mixing. We add the proviso that with the above admixing and inelastic processes, the cross section of the 7/2+ state of the [211] 1/2+ band could in principle be as much as doubled.

(d) Conclusions for A~25

1. The relative strengths of levels within a band may be drastically changed when inelastic effects are included.

2. Certain features of the angular distribution that might be described as "j-dependence," appear for the two l=2 levels within the [211] 1/2+ band in Mg.

3. The present generalization of zero range DWBA without cutoff is unable to account for the detailed shape of angular distributions for stripping in light nuclei.

4. The finding of Parikh,[86] who uses the results[68] of stripping at 15 MeV to determine that magnesium is prolate and axially symmetric is substantiated. Our best c^2 values for the k=1/2 band; $c_{1/2}{}^2 = .333$, $c_{3/2}{}^2 = .467$, $c_{5/2}{}^2 = .200$ are close to those of Cujec,[68] because in her work, the result of an incorrect radial wavefunction and the neglect of inelastic processes seem to cancel within the k=1/2 band.

5. We do not regard the parameters employed in the calculation of the ground band neutron intrinsic wavefunction to have been sufficiently well chosen (as compared with those for our "best" k=1/2 band calculation) to permit us to finally settle the question of the value of $\langle \hat{\sigma} | 0 \rangle$ for the ground band. We can say that our wavefunctions calculated according to the (probably erroneous) assumption that the deformation was the same in each band (see Chapter IV) lead to stripping results which suggest $\langle \hat{\sigma} | 0 \rangle \approx .8$. We note, however, that this assumption of equal deformations (again, probably erroneous) has recently been invoked,[87] together with axial asymmetry in a rather unsuccessful attempt at the explication of the ^{25}Mg spectrum. We regard this last work to be, if anything, evidence that this nucleus is axially symmetric and that the k=1/2 and k=5/2 band have quite different deforma-

tions. In fact, this should already have been clear from fig. 10 of the 1959 paper of Mottelson and Nilsson.[85]

B. Stripping Reactions on Deformed Rare Earth Nuclei

Since the (d,p) experiments of Vergnes and Sheline,[46] a wealth of nuclear level data have been amassed by this method for the deformed rare earth nuclei. These experiments have confirmed that the adiabatic model, together with the Nilsson scheme, contain a large degree of physical truth for strongly deformed nuclei. With an even-even target, we can see from the results of Chapter II together with eq(18) of Chapter VI, that the DWBA stripping cross section is of the form $C_{j\ell}^2 \sigma_\ell(\theta)$ where $\sigma_\ell(\theta)$ can be tabulated as a function of Q. Each band, then, has a characteristic "fingerprint" depending on the c_{j1}'s of the underlying single-particle state when the cross section for its members are plotted on a logarithmic bar graph. In this way, the band based on a particular Nilsson orbital can be traced through all the nuclides in whose spectra it appears. Most of the available data for this region are either for one angle or a small number of angles. Various authors claim that this is sufficient to determine the orbital angular momentum transferred with the neutron. (This procedure is probably not unconnected with the large number of levels found. Detailed angular distributions for a few levels along the lines of the work of Siemssen and Erskine[28] would be welcome in some lighter

rare earth nuclei chosen so that coriolis ambiguities will not cloud the inelastic processes issue.) This claim deserves examination as does any claim that c_{jl} can be measured without taking account of inelastic processes. It is probably true that, by and large, the identification of bands using "fingerprint" techniques and the c_{jl} tabulation of Vergnes and Sheline (really, Nilsson translated into c_{jl}-ese) is sound - especially when it is known what bands should be present. A possible exception will be discussed below. Our calculation will also involve a better treatment of the state where a particular component of an intrinsic state may have the characteristic long tail of a nearly unbound state - with a profound effect on the angular distribution.

A very recent review article on the DWBA approach to nucleon transfer on strongly deformed nuclei has been presented by Elbek and Tjøm.[1] All of the calculations discussed below were carried out before the analysis[88] of coriolis coupling in various odd deformed rare earth nuclei were published.

1. The reaction ^{166}Er (d,p) at 12.1 MeV

The low lying levels of ^{167}Er which are shown in fig. IV.3 are particularly appropriate for study because, in the first place, the level structure suggests that the ground bands at least have little first order coriolis mixing (allowing for a less ambiguous interpretation of our findings)

and then, there are certain levels, the ground state, for example, which should have very small direct amplitudes and should therefore be very sensitive to inelastic effects. The reaction ^{166}Er (d,p) was studied by Harlan and Sheline[40] at 12.026 MeV, and the relative cross section at one angle, 45°, was listed for many levels. We have studied the [633]7/2+ and the [512]5/2- bands as well as the "gamma band" at 532 KeV.

The [633]7/2+ Band

As can be seen from the wavefunction for the [633]7/2+ intrinsic state which is given in Table IV.7, by far the largest component is that with j=13/2+. As l=6 levels are much lower in cross section than l=4 levels of the same strength (by a factor of 20 at 45° with 12 MeV deuterons[1]), the 13/2+ level (c^2=.85) is actually weaker than the 9/2+ level (c^2=.14). As our program was unable to handle more proton channels than those corresponding to the 7/2+, 9/2+ and 11/2+ states, the 13/2+ state was omitted from the calculation. We note, however, that the strong 13/2+ components were retained in the neutron wavefunction. In view of the moderate strength of the 13/2+ level, we might have expected a modification of the (weakish) 11/2+ cross section had it been included. The effect on the 7/2+ state would have been smaller as it is not coupled to the 13/2+ by the l=2 (first order) components of the deformed optical potential. The calculations were performed at 12.1 MeV, the energy of the standard CC and DW optical

potentials, "H" and "I" of Table VII.1 and "D" and "F" of Table VII.2. In order to study the consequences of scattering in the entrance and exit channels separately, we calculate the angular distribution first in pure DWBA, and then repeat first with scattering in the outgoing channels, scattering in the ingoing channels and finally the complete problem. Whenever there is a coupled channel or distorted wave calculation, we use the corresponding optical potential. In this case, we included only the 2+ state of ^{166}Er in the deuteron wavefunction. The deformations were: ^{166}Er $\beta_2 = .26$, $\beta_4 = 0.0$, $\beta_2(\text{coul}) = .307$; ^{167}Er $\beta_2 = .25$, $\beta_4 = .05$, $\beta_2(\text{coul}) = .3$. The existence of Y_4 deformation in Er is doubtful, but will make very little difference in this case where there are no states to be coupled by it in first order that cannot be coupled by Y_2 in first order. The DWBA calculations of the two l=4 states are of interest in themselves; while $c_{9/2}{}^2/c_{7/2}{}^2 = 140$, the corresponding ratio of the DWBA cross sections is about 40. That must necessarily be a result primarily of the different radial formfactors; the Q dependence could have only a slight effect (see fig. 10 of the review article[1] of Elbek and Tjøm). As we found in Chapter IV, the details of the wavefunctions depend sensitively on the separation energy. As explained there, it was not always possible to establish the best value for this perfectly and this might explain the large direct (DWBA) 7/2+ cross section. We believe it <u>is</u> high,

for when the inelastic scattering is switched on, the cross section at 45^{o} exceeds the experimental value in this case. The angular distributions for the three states of this band for the four cases are shown in fig. VIII.13. The numerical results at one angle are summarized in Table VIII.1.

The following points emerge:

(a) The 7/2+ and 11/2+ levels are increased by factors of four and five respectively when the full calculation is carried out.

(b) The relatively strong 9/2+ level is little changed, being reduced markedly (40%) only near 60^{o}.

(c) For the 7/2+ level, inelastic effects are about equally important in the exit and entrance channels. The exit channel scattering has less effect, except at forward angles on the 11/2+ level. Possibly the inclusion of the 13/2+ level would have altered this last conclusion.

(d) In this particular case, the exit channel scattering appears to have induced a diffraction pattern on the angular distribution of the protons. We shall see that this does not happen in every case, however.

As mentioned, our overshooting of the 7/2+ level is probably due to an incorrect intrinsic wavefunction; this is not in conflict with the fact that inelastic effects have increased the cross section by a factor of four as can be seen by considering the fact that the various amplitudes add

coherently. These calculations did not include the 4+ target state which makes a significant contribution in some cases as we see below.

The [512] 5/2- Band in ^{167}Er

The wavefunction for the [512] 5/2- neutron intrinsic state of A = 167 is given in Table IV.8. In this case, the stripping strength should be predominantly in the l=3 and l=5 states. Harlan and Sheline[40] give the cross section for the 5/2-, 7/2-, 9/2- levels at one angle, 45°, and these three states have been coupled together in our calculations for this band, except in one case where we included the 7/2-, 9/2- and 11/2- states. In figure VIII.14 (see also Table VIII.2) we give the angular distribution to the first three states of the band (a) direct, (b) pure CC, including the 2+ state in the incoming channel, and (c) pure CC including also the 4+ state of the target. The data of Harlan and Sheline at 45° are given in Table VIII.2, normalized to the case (c) 7/2- state. The difference between cases (a) and (b) for the weaker 5/2- and 9/2- states is dramatic, but not unexpected. What is not expected is the magnitude of the effect that the 4+ target state has on the 5/2- level, and the fact that for cases (b) and (c) the forward angle cross section of this level is so strongly boosted by the inelastic processes. The 5/2- angular distribution appears now more like an l=1 transition than an l=3 transition. Although the 4+ cross section

is much lower than the 2+ cross section in inelastic deuteron scattering on ^{166}Er, it turns out that the scattering matrix elements leading to the 4+ state become comparable to those leading to the 2+ state for the higher partial waves. Hence, one might suppose the deuteron wavefunctions corresponding to the 4+ target state to have a relatively large amplitude at a large radius, so that they lead to neutron stripping at a large radius which, according to the usual semi-classical arguments associating l-transfer with a particular angular distribution, should result in a more forward peaked angular distribution. We remark in this connection, that the forward angle cross section is sensitive to quite small high partial wave s-matrix elements whose coherent effect may be larger than would be guessed from their magnitude. We determined the required number of partial waves empirically by demanding convergence of the forward angle differential cross section. We might conclude that at energies near the coulomb barrier, elastic and also inelastic scattering takes place outside the range of the nuclear forces. Those deuterons reaching the nuclear surface have a large probability of being associated with excited nuclear states. They are also, of course, moving very slowly having been nearly stopped by the coulomb field. It would seem, then, that the importance of inelastic processes in transfer reactions is greatest precisely where the adiabatic model is least appropriate. The adiabatic picture of scattering

was used in a previous study of inelastic processes in stripping by Iano and Austern.[3]

As can be seen from Table IV.8, there are small amplitude l=7 components in the bound state wavefunction. These do not correspond to direct amplitudes to any states considered. In order to determine their role in stripping, we performed a calculation in which they were omitted. The results are displayed in fig. VIII.15 and Table VIII.2. The only real effect these components have is to depress the 9/2- level. We illustrate in the same figure the effect of the proton channel inelastic processes. It is clear that in this case, at least, the exit channel scattering contributes to the distinct forward angle peaking of one level (the 5/2- level). The agreement with experiment, though greatly improved, is not perfect for the 5/2- level and is poor for the 9/2- level. The 11/2- level presumed by Harlan and Sheline to be at 668 KeV, and certainly weaker than the 9/2- level when directly excited, is not seen, apparently masked by levels at 654 KeV and 674 KeV. The level at 654 KeV is unassigned and is about four times the DWBA strength expected of the 11/2- level. Harlan and Sheline support their claim that the 11/2- level should be at 668 KeV with the datum that the 9/2- level fits the I(I+1) scheme quite well. However, if we examine the energies of the levels in the same band in ^{169}Er, we find that I(I+1) places the 11/2- level in that nucleus at 439 KeV, whereas

it is seen at 420 KeV. Granting then, the somewhat different inertial parameters in ^{169}Er, it is plausible that the 11/2- in ^{167}Er might be 14 KeV too low (the breakdown of adiabaticity always leads to higher levels of a band being somewhat low). A calculation was performed including the 7/2-, 9/2- and 11/2- levels together and the results are included on fig. VIII.14. Although the fit to the cross section of the 654 KeV level is not good, yet it is better than that for the 9/2- level. The DWBA cross section of the 11/2- level was not calculated, yet it is plain that inelastic effects have enhanced it by a greater factor than for the 9/2- level. We feel that, by including inelastic processes in this calculation, we can establish that the 654 KeV level is the 11/2- level with comparable plausibility to the hypothesis that the band is based on the [512] 5/2- intrinsic state (in view of the inability to fit the 9/2- level). We note that Tjøm and Elbek[51] note the "breakdown of the single particle description of the [512] 5/2- orbital" in Gd.

This last calculation also shows that omitting the 11/2- level from the previous calculations did not greatly affect the 9/2- level; the exit channel inelastic processes are dominated by the very strong 5/2- level.

After this work was completed, the coriolis coupling analysis of Kanestrøm and Tjøm[88] was published. This suggests that the 7/2- level is weakened and the 9/2- level

doubled by coriolis mixing; this would greatly improve our agreement with experiment. (Recall our scheme of normalizing the calculation to the 7/2- level. See Table VIII.2.)

It can be seen from ref.[88] that this band cannot be fully accounted for with coriolis admixing and DWBA and that the inelastic effects we describe are of comparable importance to this mixing in an overall picture of stripping on deformed nuclei.

Although the strong 7/2- level has been only slightly enhanced by inelastic processes, this has some importance when different bands are compared, when measurements of the BCS U^2 factors is attempted, or when absolute cross section calculations are essayed. We compare, for example, the slight reduction in the intensity of the strong (9/2+) level in the ground band (which would be drastic if the measurements were at 60° alone).

An Erbium Gamma Band at 12.1 MeV

The k=3/2+ band at 532 KeV in ^{167}Er is identified by Harlan and Sheline as being a gamma band on the [633] 7/2+ intrinsic state, together with various single quasi-particle admixtures. Probably these latter are dominant as far as stripping is concerned, for the 5/2+ level at 573 KeV in this band is excited in (d,p) nearly as strongly as the corresponding 9/2+ level of the ground band, whereas the amplitude for the γ 2+ state being excited by deuterons is about one tenth

(cross section one hundredth) of the amplitude for the rotational 2+ excitation. This would imply that levels of a pure odd-nucleus gamma band corresponding to those in the non-vibrational band on which it is based, which are excited largely through the rotational 2+ of the target, will have cross sections reduced by two orders of magnitude. Other levels of the gamma band are expected to have cross sections attenuated even more compared to non-vibrational levels with the same intrinsic state.

The empirically moderate excitation of the 5/2+ state of the gamma band is not inconsistent with this band indeed being largely of gamma band character as small non-vibrational admixtures with large stripping amplitudes could dominate the cross section. In spite of the large measured cross section a (model) calculation was carried out in which this band was considered as a pure gamma band excited entirely through the 2+ gamma bandhead of the target nucleus. The optical potential for the deuterons and the deuteron inelastic scattering are discussed in Chapter VII. We neglect in this case the effect of the possible excitation of the core phonon by protons which are associated with stripping to the ground band; our program was not set up to calculate interband scattering. Actually, in the one calculation performed there was not even intraband coupling in the exit channels. The angular distributions are shown in fig. VIII.16 where we compare them with a pure DW

calculation of the ground band, the latter being reduced in the figure by a factor of 100. The most conspicuous feature is the peaking at more forward angles, corresponding perhaps to the deuteron wavefunction in the gamma band channel having largest amplitudes at the nuclear surface.

We remark that the structure factor for the gamma band involves the product for state J of the gamma band:

$$C^{2\ j\ J}_{-2\ 1/2\ 3/2}\, C_{jl}$$

Thus for J=3/2, there is j=7/2 only as $j \geq 7/2$; for J=5/2, possible j values are j=9/2 or 7/2. As $c_{7/2} \ll c_{9/2}$ for the ground band, we may speak loosely of "corresponding levels" between these bands (in the context of stripping reactions) for the two lowest levels of the respective bands. This gives point to the comparison made in fig. VIII.16.

2. <u>The Reaction ^{154}Sm (d,p) at 12.1 MeV</u>

Deuteron stripping reactions on the even isotopes of samarium have been studied by Kenefick and Sheline[49] at deuteron energies around 12 MeV. The isotopes involved straddle the transition region from spherical to strongly deformed. The nuclide ^{154}Sm is apparently very well described by the adiabatic model and is probably relatively stable in deformation under the addition of one neutron (i.e., $\langle \tilde{\sigma} 10 \rangle \approx 1$); this is not so obviously true for ^{152}Sm.

Kenefick and Sheline measure the relative stripping

intensity of about one hundred levels in ^{155}Sm at a single angle, 65°, at 10.472 MeV. Our calculations were at 12.1 MeV, the energy of the optical potential (and the energy quoted in the abstract of ref.[49]). The low lying levels of ^{155}Sm as interpreted in ref.[49] have been discussed in Chapter IV and were illustrated in fig. IV.4. The present calculations are confined to the [521] 3/2- (ground) band, using the wavefunction of Table IV.10 or, in one case, that of Table IV.11. Because of the shortcomings in these wavefunctions, discussed in Chapter IV, and the energy discrepancy (10.4-12.1 MeV is in the region of the coulomb barrier where changes could be rapid) our serious attempt at spectroscopy will be made in the very similar nucleus ^{157}Gd as described below. However, our model calculations of the first four levels of the ground band have yielded useful information about inelastic processes. Most of the results discussed below in terms of figures are also given in a tabulated comparison with the 65° experimental results in Table VII.3.

The ground band will be somewhat mixed with the [523] 5/2- band. As the latter band is weakly excited in stripping, only the weak 5/2- level of the ground band should be much affected. In the [523] 3/2- band, however, the 426 KeV level (see fig. IV.4) is five times as strong as the 338 KeV level, whereas, from the Vergnes and Sheline c_j's, they should have much the same stripping strength (the 426 KeV level would mix

with the very strong 128 KeV level).

In fig. VIII.17, we compare the angular distributions for a pure DWBA calculation, a calculation including transitions through the 2+ and 4+ target states but with no coupling in the exit channels and the complete CCBA calculation. The strong levels are not markedly changed. The influence of the exit channel inelastic transitions is quite comparable to that of the entrance channel scattering; as for ^{167}Er it has imposed a relatively strong diffraction pattern on the bandhead angular distribution. A calculation was performed with the wavefunction of Table IV.11, and the angular distributions are compared with those using the previous wavefunction. The nonlinear effects discussed in Chapter II are evident; at 65^{o} the ratio of the cross sections using the Table IV.11 wavefunction to those using the wavefunction of Table IV.10 are respectively : 1.2557, 0.7418, 1.077 and 0.8826 for the four states. The ratios of the c_{jl}^{2} for the same two wavefunctions are 1.2826, 0.3091, 1.091 and 0.7647. For the weak states in particular, the departure from unity of these ratios has been clearly damped by the inelastic processes. We note that the shape of the angular distributions remains rather constant for this small change, except for the 5/2- level for which the new cross section is about 20% less depressed at the most forward angles following from the fact that the subcomponents of the 5/2- component of the wavefunction with

high n do not decrease commensurately with the principal component. This is also true for the 9/2- component.

The effect of adding a spin-orbit term to the proton optical potential is found to be very small, being a slight depression of the cross section at the most backward angles (3/2-, 5/2- states) or most forward angles (9/2- state). The strongest state, 7/2-, is virtually unaffected. This is not illustrated.

In view of the rather surprising contribution of amplitudes involving the target 4+ state for the 5/2- band in erbium, the calculation was repeated with the 4+ state omitted from the entrance channels. The results are shown in fig. VIII.18. Evidently the coherency between the various amplitudes feeding a particular state allows what must be a fairly small amplitude to have a significant effect on the angular distribution. Note the displacement of the diffraction minima for the 3/2- state. The addition of target states can depress a cross section, as is the case for the 5/2- level. If we compare the 9/2- angular distributions in fig. VIII.17 and fig. VIII.18, it becomes apparent that the 2+ target state and the 4+ target state result in respectively destructive and constructive coherent amplitudes. The provides a possible explanation of the over-estimation of the ^{167}Er g.s. cross section for which we did not include the target 4+ state.

3. The Reaction ^{156}Gd (d,p) at 12.1 and 16.0 MeV

The spectrum, fig. IV.5, of ^{157}Gd parallels that of ^{155}Sm quite closely. These nuclei have very similar deformations, as this depends mostly on the neutron number in this region. We have continued our study of the [521] 3/2- band in this nucleus for which these are differential cross section measurements at several angles, at 12.1 MeV, the energy of our standard optical potential. These are due to Tjøm and Elbek.[51] The neutron single particle wavefunction given in Table IV.12 is probably, as discussed in Chapter IV, better than that used for Sm. The larger separation between the 3/2- and 5/2- bands, as compared with ^{155}Sm, suggests that coriolis mixing is less for the [521] 3/2- band in this nucleus, though the weakly populated 5/2- level is no doubt affected. The predicted 5/2- direct amplitude is so small that in ref. [51] the measured intensity is attributed to band mixing. However, we shall show that indirect processes seemingly account for the cross section. (This weak level is not tabulated in Table 5 of ref.[51], but can be seen in their Fig. 11.) We have calculated the DWBA and CCBA cross sections for the 3/2-, 5/2-, 7/2-, 9/2- levels and compare them in fig. VIII.19 and Table VIII.4. The cross section of the 5/2- level is increased twentyfold at 60° and the strong 7/2- level is attenuated by about 20% rather uniformly. The ground state diffraction pattern is distinctly altered geometrically,

but not in overall strength: at 60°, one of the angles of measurement, a maximum takes the place of a minimum. This reveals not only a possible pitfall in the procedure of identifying angular momentum transfer by measuring three or four points, but the overall strength may not be well judged. The strongest level, in the cases we have seen, retains its shape; but the 5/2- level in this case is not that weak. Note that in this case, the DWBA 5/2- also has a distinct diffraction pattern. The predicted cross sections at 125° are all too low, a phenomenon familiar to us from Mg, but less expected here. A deuteron optical potential of excessive absorption seems a possible explanation or perhaps an inadequate representation of the proton coupling. To investigate the latter possibility, we repeated the calculation with $\beta_2 = .3$ in the exit channels, as is also shown in fig. VIII.19 — the 125° experimental points remain unaccounted for. The 7/2- level is too strong relative to the 3/2- and 9/2- levels. We have been able to get a reasonable fit to the data by multiplying $c_{7/2-}$ by .85. (The 7/2- level is scaled by almost exactly $.85^2$, the 5/2- by a factor somewhat less than $.85^2$, suggesting that the contribution from the 3/2- single particle component adds destructively.) It is to the 7/2- 60° result of this final calculation to which we normalize the data for each state in fig. VIII.19, in which the effect of the change in $c_{7/2-}$ on the 3/2- and 9/2- angular distributions is also

visible. By scaling $c_{7/2}$ in such a way as to fit the data, we may say we have determined (such is our agreement at 60^{o} and 90^{o}) normalized c_j's for the [521] 3/2- neutron, A=157: $c_{3/2}$= -.366, $c_{7/2}$= .651, $c_{9/2}$= -.515 (etc.) compared with the values of Vergnes and Sheline for these three components of -.32, +.73, and -.5 respectively (our convention).

Comment on the Structure of Gadolinium

The case of coriolis coupling in ^{157}Gd is not treated by ref.[88] However, the authors do study the [521] 3/2- band in ^{159}Gd. Band mixing should be greater in this case(the strongly admixed bands are much closer in energy), and we may infer from these calculations that coriolis admixing will have little effect on this band in ^{157}Gd. The 3/2- level will be barely affected, but probably the 9/2- level will be enhanced. This would be in the right direction, but the question remains: why is the $c_{7/2-}$ calculated in our Saxon-Woods model (discussed in Chapter IV) too high (apparently for this band in ^{159}Gd also[88])? Certainly, the value obtained by Vergnes and Sheline is too high to fit the stripping data. Neither coriolis admixing nor inelastic processes, though both help, can satisfactorily account for the discrepancy. In view of what we have learned concerning the crucial importance of the tail of the wavefunction, a suitable combination of changes in the potential parameters could possibly be sufficient and we may even have a means of determining these parameters. It is

unlikely that our choice of β_2=.3 for the bound state wavefunction is too high; a reduction in β_2 would result in $c_{7/2-}$ being increased.[46]

Nowhere have we considered (nor seen considered) any possible perturbation of the single particle radial wavefunction arising from the rotation-vibration interaction. A quite small effect in the surface region would be sufficient to affect stripping calculations.

16.0 MeV Deuterons

The DWBA and CCBA angular distributions were calculated at 16 MeV using the appropriate potentials discussed in Chapter VII. The results are shown in fig. VIII.20 and listed in Table VIII.5. There is no data.

The change in the 3/2- and 7/2- levels at 16 MeV is almost entirely a matter of altering the diffraction pattern without changing the overall strengths. In this respect, the effect is less than at 12.1 MeV where there was a distinct overall attenuation of the 7/2- level. The effect on the 5/2- and 9/2- levels is about the same as for 12.1 MeV, except at the most backward angles where it was greater.

We can give some answer to the question of energy dependence of inelastic processes. It appears that, once above the energy where the elastic scattering becomes significantly different from Rutherford (a more empirical criterion than "above the coulomb barrier"), then inelastic processes become

potentially significant. The coulomb barrier transition region is difficult to study, as optical parameters vary in a complex manner here, and scattering experiments would ideally be performed at each energy. Above the coulomb barrier (and 12.1 MeV is above in the sense defined above, for A ~160) the energy dependence of the importance of inelastic processes is rather small. The fact that at 12.1 MeV, the influence of the target 2+ state back on the ground state is small, seems not to imply necessarily that inelastic processes are without influence in stripping reactions. At 12.1 MeV, the elastic differential cross section of deuterons on Sm is about 0.1 x Rutherford at 180^{o} and greater everywhere else. As the Rutherford cross section is very small at back angles, this might be thought to correspond to a very small absorption for the elastic channels. However, the large forward angle coulomb cross section corresponds to an impact parameter beyond the range of stripping. Compare the comments we made above in connection with the 5/2- band in erbium.

4. A Note on Alternative DWBA Calculations

Our procedure used above to determine the deuteron "DW" optical parameters is not exactly that described in our general discussion. We required that the DW optical parameters fit the same (meagre) experimental data in a DW calculation as those fitted by the CC parameters in a CC (d,d') calculation . Subsequent to the above investigation,

we carried out trial DWBA calculations in order to compare the results obtained using the optical potentials discussed in Chapter VII with potentials obtained by requiring that the deuteron optical potentials give the same elastic scattering (in a DWBA calculation) as that found for the CC calculation when the 2+ state was included (we treat the case of ^{166}Er). We used the optical model search code Mercy for this as we did for 16 MeV and 20 MeV deuterons. The use of optical potential thus brings our investigation for the rare earths more strictly in line with the general procedure discussed above and in Chapter II. However, we note that although the new DWBA calculations now bear the correct relationship to the CCBA calculations discussed above (as far as our scheme of model calculations is concerned), optical model ambiguities still exist. The original (DW) optical potential fitted the small amount of elastic data for ^{166}Er; however, it has been used [79,80] satisfactorily in other deuteron scattering reactions. We might more realistically, therefore, have searched for CC parameters that fitted the DW elastic deuteron scattering (i.e., instead of vice versa). No automatic search program was available that could handle coupled channel calculations, and the parameters found in a manual search that fitted the same elastic data were discussed in Chapter VII and were the ones employed. Using program Mercy, we found the following parameters gave a good fit to

the CC calculated deuteron elastic cross section on ^{166}Er:

$$V=-86.6 \quad W_D=-8.9 \quad r_o=1.084 \quad \bar{r}_o=1.277 \quad r_c=1.2$$
$$a_o=.886 \quad \bar{a}_o=.939$$

These are to be compared with set D of Table VIII.2. The most notable feature is the reduction in overall strength of the absorptive potential which is apparently (as we shall see) more than countered by the greatly increased surface thickness of the absorptive region.

We then studied the 5/2-, 7/2- and 9/2- states in ^{167}Er using both the new set of deuteron optical potentials above, and the set of standard DWBA parameters.

The changes in the 5/2- and 7/2- levels were very similar to each other. Above about 90^o, the cross section using the Mercy parameters above was 10-20% reduced. The stripping peak was reduced 10% and moved from 52^o to 58^o and the slight peaking below 15^o was removed and becomes a dip so that the 0^o cross section was reduced 35%. Experimental results are not usually given for rare earths in this region. It is evident that the increase in $\bar{a}_0$ has resulted in a decrease of the wavefunction in the nuclear surface. The total cross section is reduced 10%. For the 9/2- level, for which the wavefunction has greatest amplitudes for the n=0 component, the cross section is reduced only by 2% at 180^o, 10% at 90^o, 5% at the stripping peak (which is moved from 70^o to 78^o, but the angular

variation of the cross section is small.) At forward angles the change* is more pronounced: 10% at 40°, 33% at 30°, 60% at 20°, 70% at 10°. The total cross section is reduced 6%. Thus, the changes in the optical potential appear to have reduced the deuteron wavefunction in the nuclear surface, but not changed it much in the nuclear interior. To interpret our previous results in terms of a model calculation in which the DW optical potential precisely fits the calculated CC elastic scattering, we should regard the DWBA curves, fig. VIII.14. For $l \geqslant 5$, there will be no appreciable change above 90°. At forward angles, the DWBA cross section will be lower to an extent which is greater for lower l transfers. The tendency for inelastic processes to increase stripping cross sections is thus somewhat enhanced in this model calculation.

---

*The percentages indicate the extent to which the cross section is reduced by using the Mercy parameters quoted on the previous page.

Table VIII.1. Stripping of 12.1 MeV deuterons leading to the [633]7/2+ band in ^{167}Er. The c.m. angle is 45°. Coupling in the entrance channels includes the target 2+ state only. In all these cases, the parameters are as specified in the text.

State.	Expt.[40]	N**	N	Y	Y
		N***	Y	N	Y
7/2+	$.9968\times10^{-3}$	$.484\times10^{-3}$	$.928\times10^{-3}$	1.11×10^{-3}	1.78×10^{-3}
9/2+	1.78×10^{-2}	1.83×10^{-2}	1.9×10^{-2}	1.55×10^{-2}	$*1.78\times10^{-2}$
11/2+	1.495×10^{-3}	$.502\times10^{-3}$	1.12×10^{-3}	2.39×10^{-3}	2.58×10^{-3}

* The experimental points were normalized to this.

** N here means no coupling in incoming channels, Y means coupling.

*** N here means no coupling in outgoing channels, etc.

Table VIII.2. Stripping of 12.1 MeV deuterons leading to the [512]5/2- band in ^{167}Er. The experimental cross section exists only for 45°.
$^{+}$N signifies no coupling in entrance channels, Y signifies coupling.
$^{++}$N signifies no coupling in exit channels, Y signifies coupling.

State	Angle	Expt.[40]	N^{+} / N^{++}	Y / N	Y / Y	Y^{**} / Y	$Y^{**,***}$ / Y^{***}
	45°	.054	.00769	.0159	.0187	.0345	.0339
5/2-	60°		.00802	.0157	.0215	.0385	.0386
	90°		.00582	.0090	.00746	.0118	.0116
	45°	.567	.549	.456	.475	.567*	.571
7/2-	60°		.555	.558	.641	.661	.675
	90°		.405	.381	.414	.459	.456
	45°	.0587	.00382	.00581	.0112	.0120	.0132
9/2-	60°		.00525	.00761	.0112	.0133	.0142
	90°		.00281	.00638	.0105	.0101	.0113

*We normalize the data to this number.
**Includes the 4+ state of the target nucleus. The other calculations include 2+ only.
***Calculation excludes the l=7 components of the single particle wavefunction.

Table VIII.3. Partial differential cross section at 65° for the stripping of 12.1 MeV deuterons leading to the [521] 3/2- band in ^{155}Sm. The data[49] was taken at 10.472 MeV. In this table, we have normalized both the data and the theory to 1.0 for the 7/2- state (lower of each pair). The upper of each pair is unnormalized; note the nearly constant strength of the 7/2+ state. Note that 65° at 10.472 MeV does not correspond to exactly the same point in the angular distribution at 12.1 MeV. The best improvement is in the 3/2- state where the experimental .633 is to be compared with DWBA (.4) and CCBA (.585 or .657) and in the weak 5/2- state.

State	Expt.	N^{+} / N^{++}	Y / N	Y / Y	Y^{*} / Y
3/2-	1.0	.026	.03	.038	.046
	.633	.4	.461	.585	.657
5/2-	.06	.0012	.0025	.0052	.0037
	.038	.0185	.038	.08	.053
7/2-	1.58	.065	.065	.065	.07
	1.0	1.0	1.0	1.0	1.0
9/2-	.12	.0056	.0056	.0083	.007
	.076	.086	.086	.127	.1

*For these, we employ the wavefunction of Table IV.11. In all other cases that of Table IV.10 was used.

+In first line, N and Y signify absence or presence of inelastic coupling in entrance channels.

++In the second line, N and Y refer to coupling in exit channels.

Table VIII.4 (part one). Stripping of 12.1 MeV deuterons leading to the [521]3/2- band in ^{157}Gd. The upper numbers of each pair are the theoretical numbers as calculated; the lower are the values of (Experimental/Theory) for that angle. These numbers should ideally all be equal; the great reduction in the range of values when inelastic processes are included is evident -- especially if the 125° results are ignored.

State		Expt.[51]	N^+ / N^{++}	Y / Y
3/2-	60	146	.0309 4725	.0416 3510
	90	55	.0152 3618	.0141 3901
	125	23	.00639 3333	.00422 5450
5/2-	60	0	.000189	.00442
	90	0	.000129	.00152
	125	0	.000063	.000529
7/2-	60	236	.1213 1946	.0981 2343
	90	132	.0660 1999	.0539 2449
	125	69	.0229 3013	.0199 3469
9/2-	60	23	.003263 6345	.0055 4182
	90	9	.0199 4520	.0034 2639
	125	11	.0134 8209	.0024 4490

For explanation of * and +, see Fig. VIII.4 (part two).

Fig. VIII.4 (part two). [+]In top row, N or Y signifies absence or presence of coupling in entrance channels. [++] Same for exit.

State		Y	N	Y**
		Y*	N	Y
3/2-	60	.0406 3596	***, **	.0415 3518
	90	.0139 3957		.0145 3846
	125	.0042 5470		.00456 5044
5/2-	60	.00492		.00333
	90	.00157		.00126
	125	.000515		.000447
7/2-	60	.0981 2405	.08764 2639	.0725 3255
	90	.0505 2614	.0447 2766	.0393 3358
	125	.0182 3791	.0166 4170	.0145 4759
9/2-	60	.00587 3918		.00507 4536
	90	.00355 2535		.00312 2885
	125	.0026 4255		.00222 4955

*In this case β_2=.3 in proton channels.

**In these cases, $c_{7/2-}$ is multiplied by .85.

*** Where not given, as for the other N, N column.

Table VIII.5. Stripping of 16 MeV deuterons leading to the [521] 3/2- band in ^{157}Gd. The effect on the geometry of the 3/2- diffraction pattern is dramatized by the way that the 45° cross section is halved, while at 30° and 60° it is nearly doubled.

State	θ°_{cm}	DWBA	CCBA
	30	.0676	.105
3/2-	45	.0470	.0242
	60	.0260	.0404
	30	.00052	.010
5/2-	45	.00031	.0054
	60	.00019	.0048
	30	.246	.202
7/2-	45	.117	.131
	60	.104	.0837
	30	.00484	.00974
9/2-	45	.00775	.0103
	60	.00388	.00738

Figure Captions for Chapter VIII

Fig. VIII.1 The influence on stripping of the presence or absence of transitions going through the 2+ of ^{24}Mg, and of no coupling or complete coupling among the two final states in ^{25}Mg (g.b.) are illustrated. The inelastic transition to the 2+ state is calculated in first order (DW) in this figure. The deformations assumed are $\beta_2 = .4$ in the deuteron channels and $\beta_2 = .3$ in the proton channels.

Fig. VIII.2 The same reaction as shown in Fig. VIII.1. Curves labelled $\beta_2 = .4$, $\beta_2 = .3$ have this deformation in cc calculation of outgoing inelastic scattering together with a cc calculation with $\beta_2 = .4$ of the deuteron scattering which includes the 2+ target state. Also shown is the effect on this calculation of projecting the 2+ state out of the entrance channel. For comparison we show the result (see Fig. VIII.1) of treating the incident channels in with the 2+ state excited in first order (dw), and the pure DWBA calculation.

Fig. VIII.3 The effect of varied spin-orbit interaction on CCBA calculation ($\beta_2 = .4$ in incident, $\beta_2 = .3$ in exit channel scattering). Curves labelled VLSP=6 have this spherical spin-orbit interaction in the proton channel, those labelled VLSD=5 have this spherical spin-orbit interaction in deuteron channels.

Fig. VIII.4 Comparison of complete DWBA and CCBA calculations with spin-orbit interaction ($V_{so} = 5$ for deuterons, $V_{so} = 6$ for protons) included. The data has been normalized at the stripping peak of the 5/2+ state. To facilitate comparison with other levels of the nucleus, we state that the experimental results have been multiplied by .625. For note on relative strength of the DWBA calculation without spin-orbit potentials, see text.

Fig. VIII.5 The reaction ^{24}Mg(d,p)^{25}Mg(g.b.) with 10.1 MeV deuterons. Comparison of polarization for CCBA and DWBA calculations leading to the ground state.

Fig. VIII.6 The influence of coupling in the exit channels upon the stripping of 10.1 MeV deuterons leading to the [211]1/2+ band of ^{25}Mg. The number of radial components in the Faessler-Sheline bound state neutron wavefunction is seven, except that the DWBA calculation is also shown where eight components are included. The calculation was performed with exit channel deformation $\beta_2 = 0.2, 0.3$; in each

case we used optical potential B of Table VII.1. The 1/2+, 3/2+, 5/2+ states are normalized to the DWBA cross section at 20^{o}, by multiplying by .785, .812, .99 respectively, for both values of β_2 . The 7/2+ level has been scaled by 1.225 for β_2=.2 and by .570 for β_2 =.3. We compare $(.3/.2)^2$=2.25 with 1.225/.570=2.15.

Fig. VIII.7 The stripping of 10.1 MeV deuterons on ^{24}Mg leading to the [211] 1/2+ band. The effect on a direct transition of successively adding transitions through the target 2+ state (excited in DWBA) and coupling among the exit channels (β_2 =.3) is illustrated. There are no spin-orbit potentials used in these calculations.

Fig. VIII.8 The effect of inelastic scattering processes in the reaction ^{24}Mg(d,p) at 10.1 MeV is illustrated by comparing the complete calculation CCBA with the usual DWBA which omits these processes. This calculation includes the four lowest states of the [211] 1/2+ band. Also shown is a CCBA calculation in which the nuclear deformation in the ^{25}Mg channels is increased from 0.3 to 0.4. Spin-orbit interactions, V_{so}(prot)=6 and V_{so}(deut)=5 were used.

Fig. VIII.9 The influence of spin-orbit terms in deuteron and proton optical potential is illustrated in a CCBA calculation of the [211] 1/2+ band in ^{25}Mg. We used V_{so}(prot)=6, V_{so}(deut)=5.

Fig. VIII.10 For the same reaction as Fig. VIII.9, we illustrate the effect of increasing the absorption of the proton optical potential by changing W from-3 to -6. Also shown is the effect of omitting the l=4 component of the bound neutron wavefunction. This wavefunction (see text) was different from that used for obtaining figures 6 through 9.

Fig. VIII.11 Illustrated is a complete calculation for the [211] 1/2+ band, comparing with the data[83] using the "best" wavefunctions (see text). The factor by which the data has been multiplied in order to fit the stripping peak for each state is shown.

Fig. VIII.12 Comparison of complete DWBA and CCBA calculations of the stripping of 12.3 MeV deuterons leading to the ground band of ^{25}Mg. Also shown on the figure is a hybrid calculation (in which the deuterons but not the protons undergo inelastic scattering) and a CCBA calculation in which the scattering in entrance and exit channels is calculated with nuclear deformation β_2=.5. The factors N(5/2) and N(7/2)

are the factors by which the theoretical numbers have been multiplied in order to get the normalization shown.

Fig. VIII.13 The influence of inelastic processes on the stripping of 12.1 MeV deuterons leading to states of the [633] 7/2+ band of ^{167}Er is illustrated. Inelastic processes involving the entrance channels (target 2+ only) and exit channels are included separately and together in calculations that are compared with the DWBA calculation.

Fig. VIII.14 The effect of inelastic processes on the stripping of 12.1 MeV deuterons leading to the [512] 5/2- band in ^{166}Er. We compare calculations in which transitions through the target 4+ state are included with those with the 2+ state alone. We also give the result of a calculation in which the 7/2-, 9/2- and 11/2- levels of this band are coupled together instead of the 5/2-, 7/2-, 9/2-.

Fig. VIII.15 Further study of the reaction of Fig. VIII.14. Here we illustrate the effect of omitting exit channel coupling and of omitting the l=7 components from the wavefunction of the bound neutron.

Fig. VIII.16 We compare the excitation of the 532 KeV gamma band of ^{167}Er with the DWBA excitation of the ground band. The states of the gamma band are fed directly through the 2+ state of ^{166}Er alone, with no exit channel coupling. The justification for this comparison is given in the text (end of Chapter VIII, section B.1).

Fig. VIII.17 A study of inelastic processes in the stripping of 12.1 MeV deuterons leading to the g.b. of ^{155}Sm. Apart from the DWBA case, we include transitions through the target 4+ state.

Fig. VIII.18 In this figure we illustrate the importance of the target 4+ state in the same reaction of Fig. VIII.17.

Fig. VIII.19 A study of stripping to the same band in the neighboring nucleus ^{157}Gd. We compare a DWBA calculation with a full CCBA calculations, and CCBA calculations in which we increase the exit channel optical deformation to 0.3 or scale $c_{7/2^-}$ by a factor of 0.85. The data is normalized to the 7/2- level, calculated using CCBA with $c_{7/2^-}$ scaled by 0.85. For the 7/2- level, we also give the DWBA scaled by $(.85)^2$.

Fig. VIII.20 The effect of inelastic processes at 16 MeV for the same reaction as that in Fig. VIII.19 is illustrated by comparing complete CCBA and DWBA calculations.

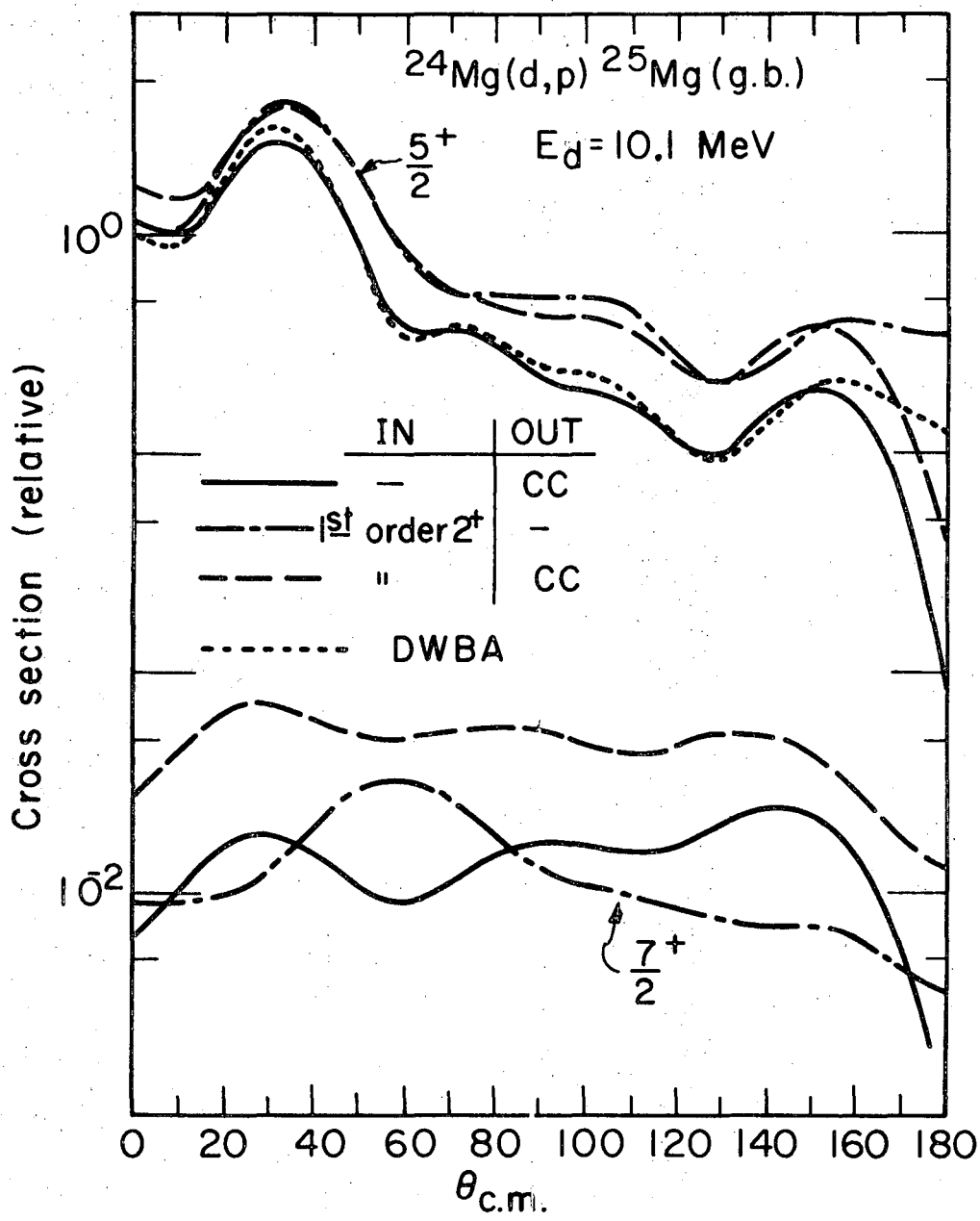
$^{24}Mg(d,p)\,^{25}Mg$ (g.b.)
E_d = 10.1 MeV
$\frac{5}{2}^+$
10^0
IN
OUT
—
CC
1st order 2^+
—
"
CC
DWBA
Cross section (relative)
10^{-2}
$\frac{7}{2}^+$
0 20 40 60 80 100 120 140 160 180
$\theta_{c.m.}$
XBL701-2233

Fig. VIII.1

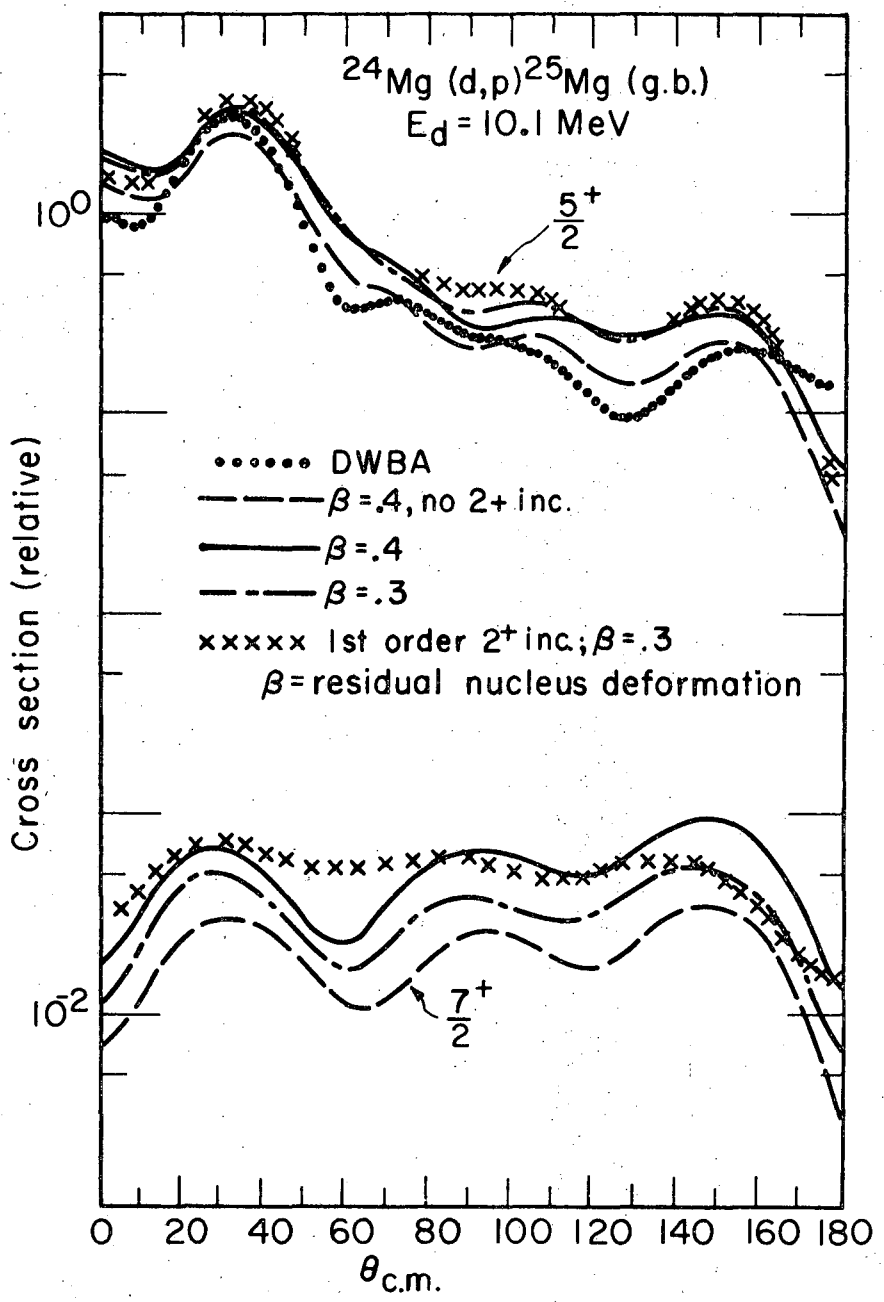
^{24}Mg (d,p)^{25}Mg (g.b.)
E_d = 10.1 MeV
$5^+/2$
DWBA
β = .4, no 2+ inc.
β = .4
β = .3
xxxxx 1st order 2$^+$ inc.; β = .3
β = residual nucleus deformation
$7^+/2$
Cross section (relative)
10^0
10^{-2}
0 20 40 60 80 100 120 140 160 180
$\theta_{c.m.}$
XBL701-2235

Fig.VIII.2

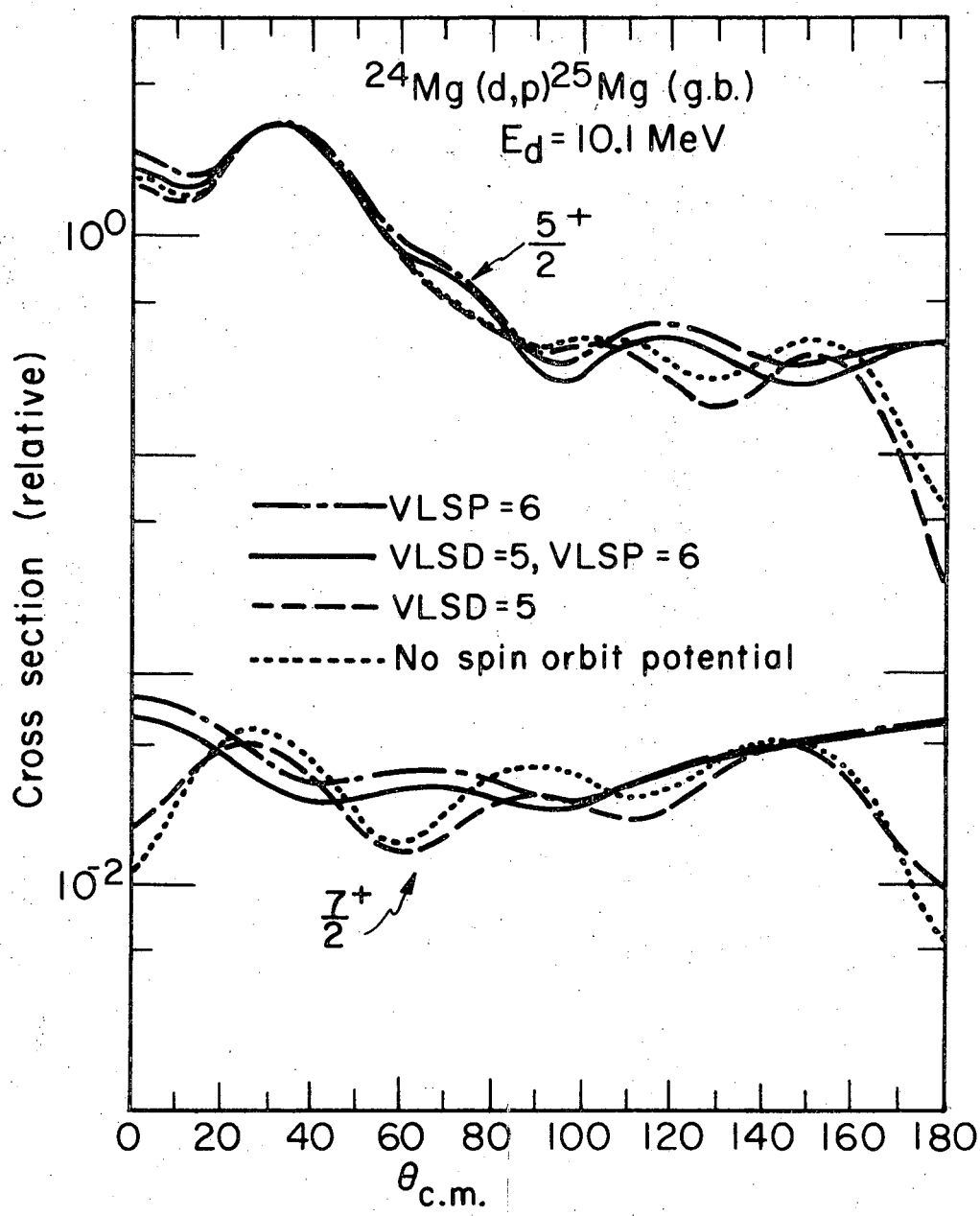

XBL701-2234

Fig. VIII.3

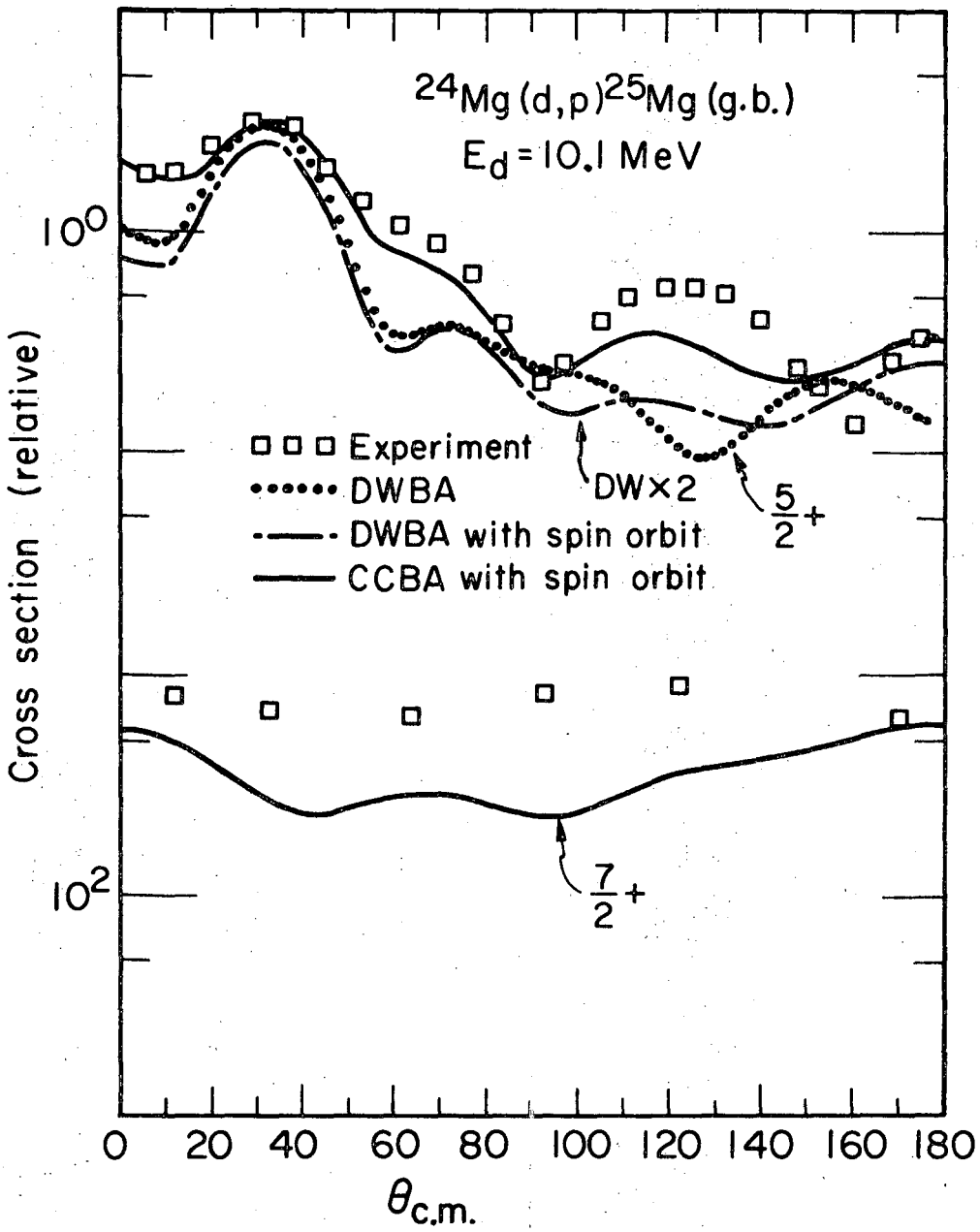

XBL701-2088

Fig. VIII.4

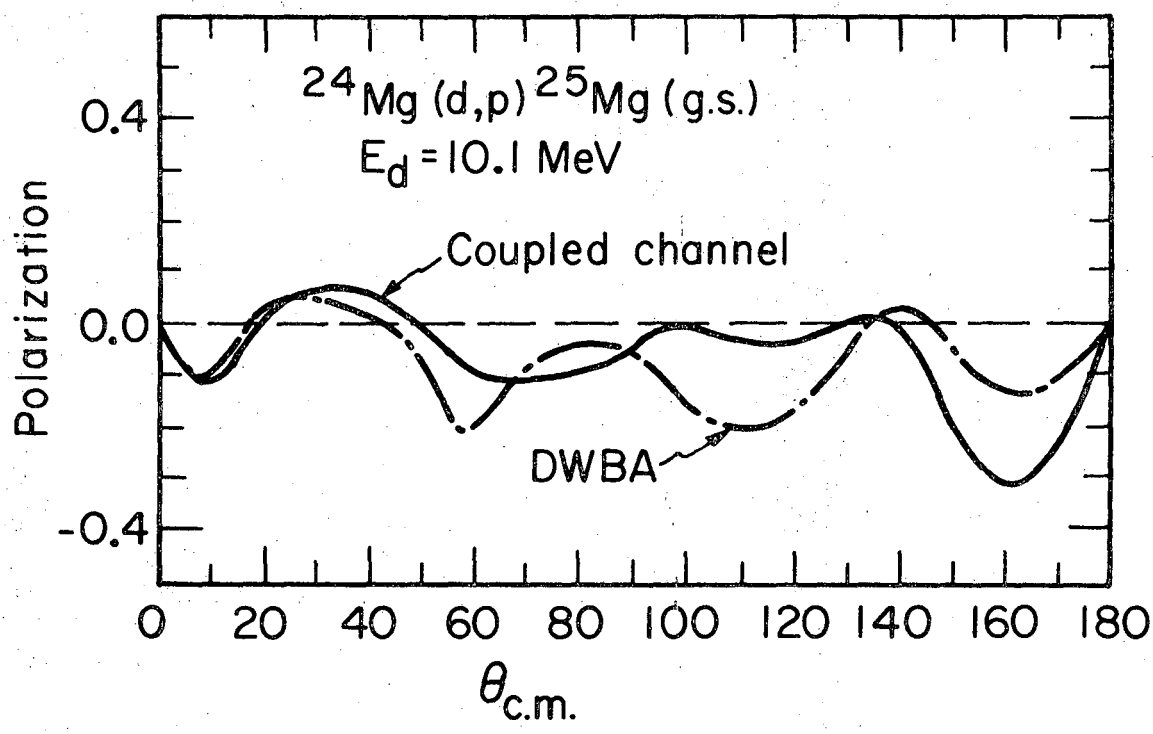

XBL701-2087

Fig. VIII.5

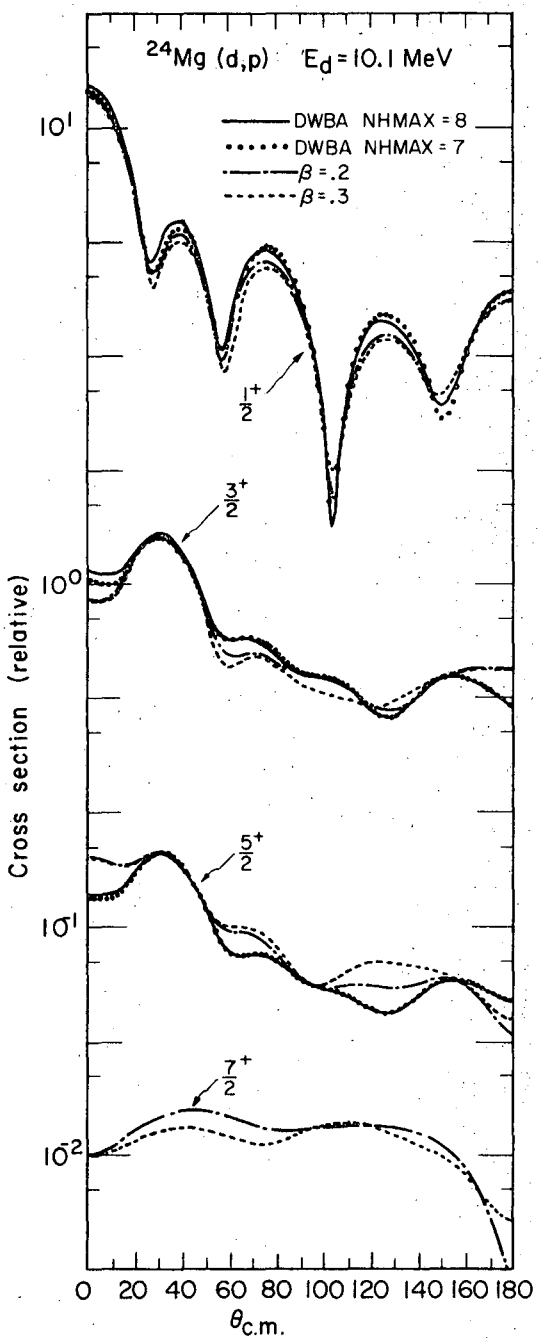
^{24}Mg (d,p) E_d = 10.1 MeV
DWBA NHMAX = 8
DWBA NHMAX = 7
β = .2
β = .3
$\frac{1}{2}^+$
$\frac{3}{2}^+$
$\frac{5}{2}^+$
$\frac{7}{2}^+$
Cross section (relative)
10^1
10^0
10^{-1}
10^{-2}
0 20 40 60 80 100 120 140 160 180
$\theta_{c.m.}$
XBL701-2240

Fig. VIII.6

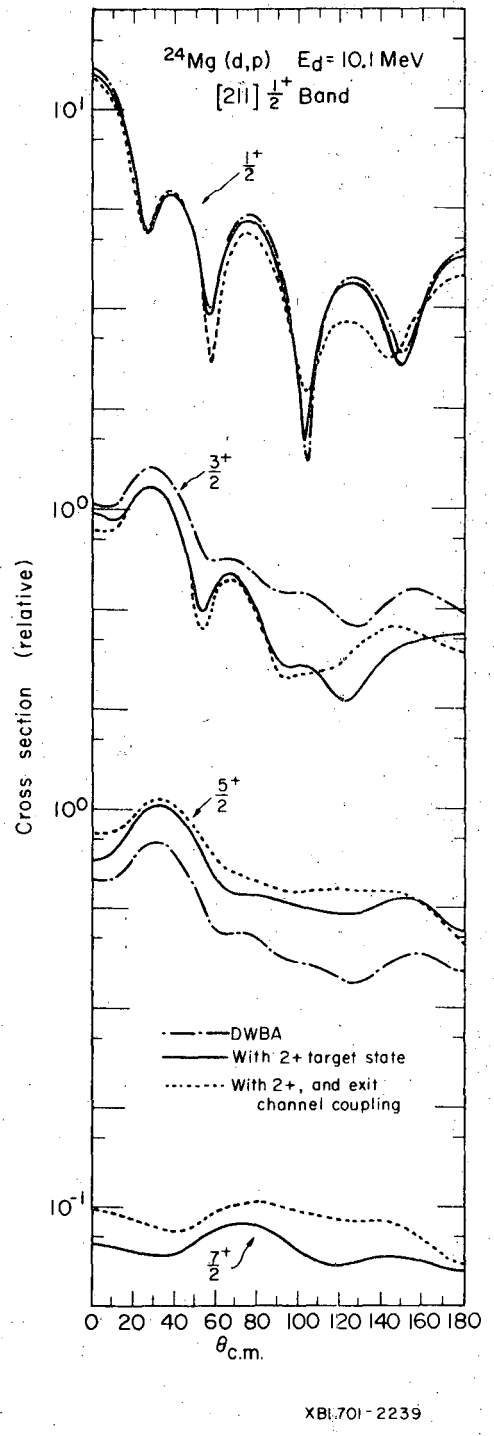
^{24}Mg (d,p) E_d= 10.1 MeV
[211] $\frac{1}{2}^+$ Band
$\frac{1}{2}^+$
$\frac{3}{2}^+$
$\frac{5}{2}^+$
$\frac{7}{2}^+$
DWBA
With 2+ target state
With 2+, and exit channel coupling
Cross section (relative)
10^1
10^0
10^0
10^{-1}
0 20 40 60 80 100 120 140 160 180
$\theta_{c.m.}$
XBL701-2239

Fig. VIII.7

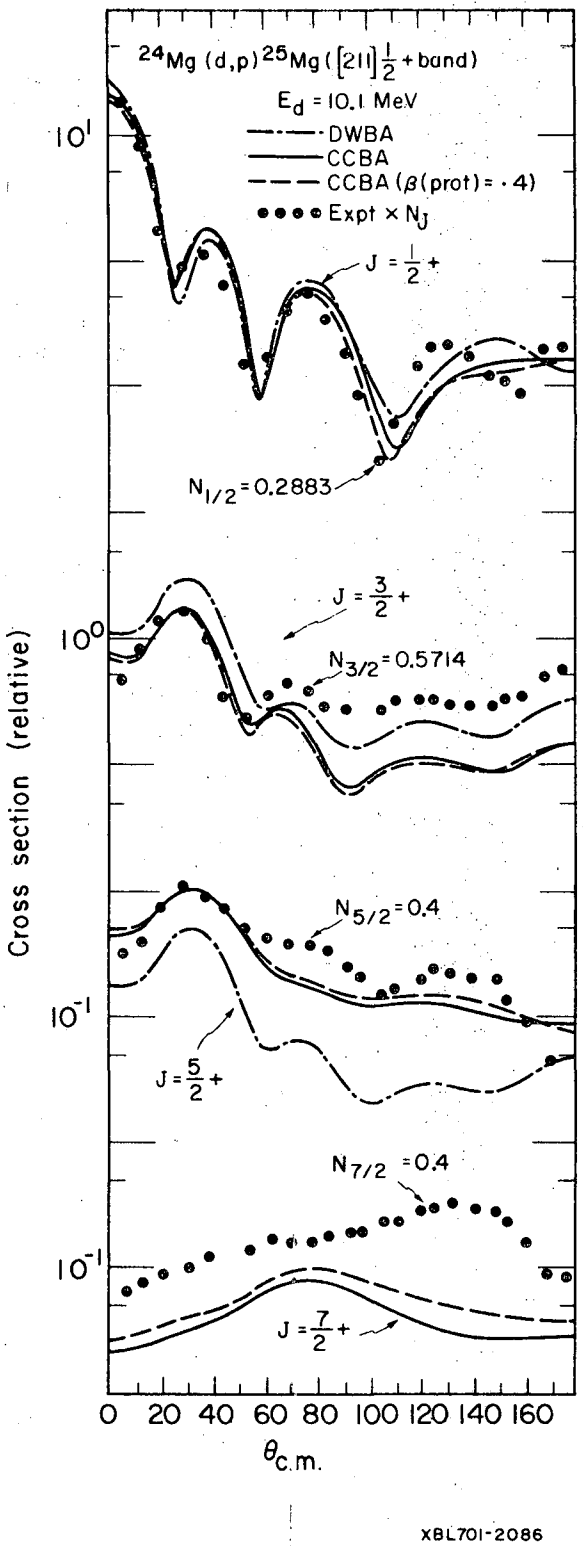
^{24}Mg (d,p)^{25}Mg ([211]1/2+ band)
E_d = 10.1 MeV
DWBA
CCBA
CCBA (β(prot) = .4)
Expt × N_J
J = 1/2+
$N_{1/2}$ = 0.2883
J = 3/2+
$N_{3/2}$ = 0.5714
$N_{5/2}$ = 0.4
J = 5/2+
$N_{7/2}$ = 0.4
J = 7/2+
Cross section (relative)
10^1
10^0
10^{-1}
10^{-1}
0 20 40 60 80 100 120 140 160
$\theta_{c.m.}$
XBL701-2086

Fig. VIII.8

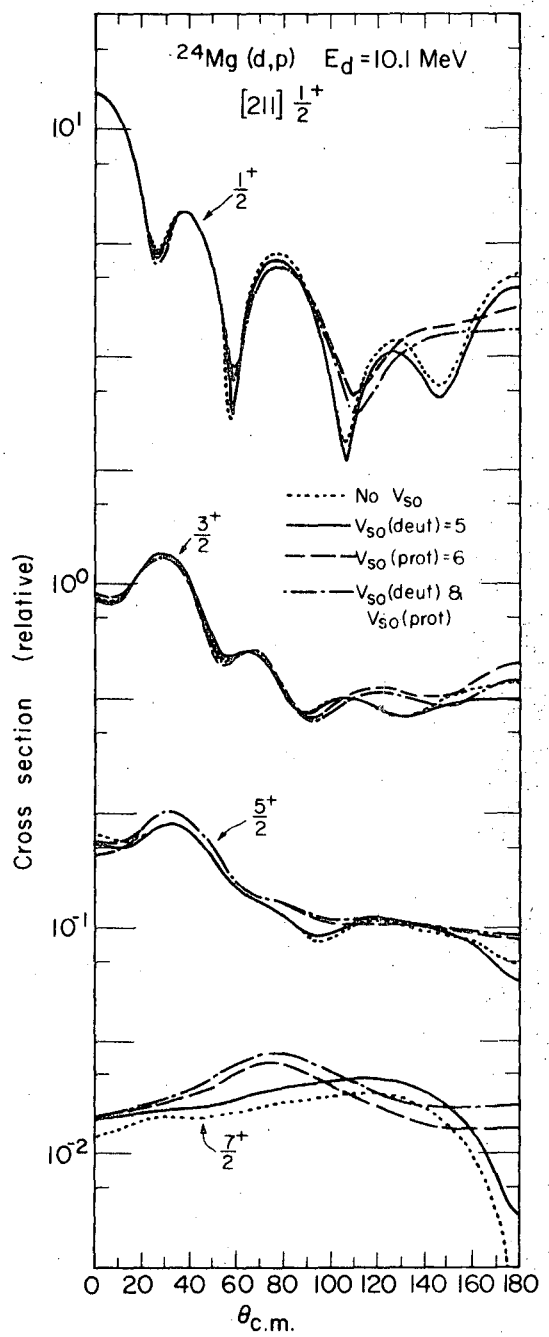
^{24}Mg (d,p) E_d = 10.1 MeV
[211] $\frac{1}{2}^+$
10^1
$\frac{1}{2}^+$
No V_{so}
V_{so}(deut) = 5
V_{so} (prot) = 6
V_{so}(deut) & V_{so}(prot)
$\frac{3}{2}^+$
10^0
$\frac{5}{2}^+$
10^{-1}
10^{-2}
$\frac{7}{2}^+$
Cross section (relative)
0 20 40 60 80 100 120 140 160 180
$\theta_{c.m.}$
XBL701-2238

Fig. VIII.9

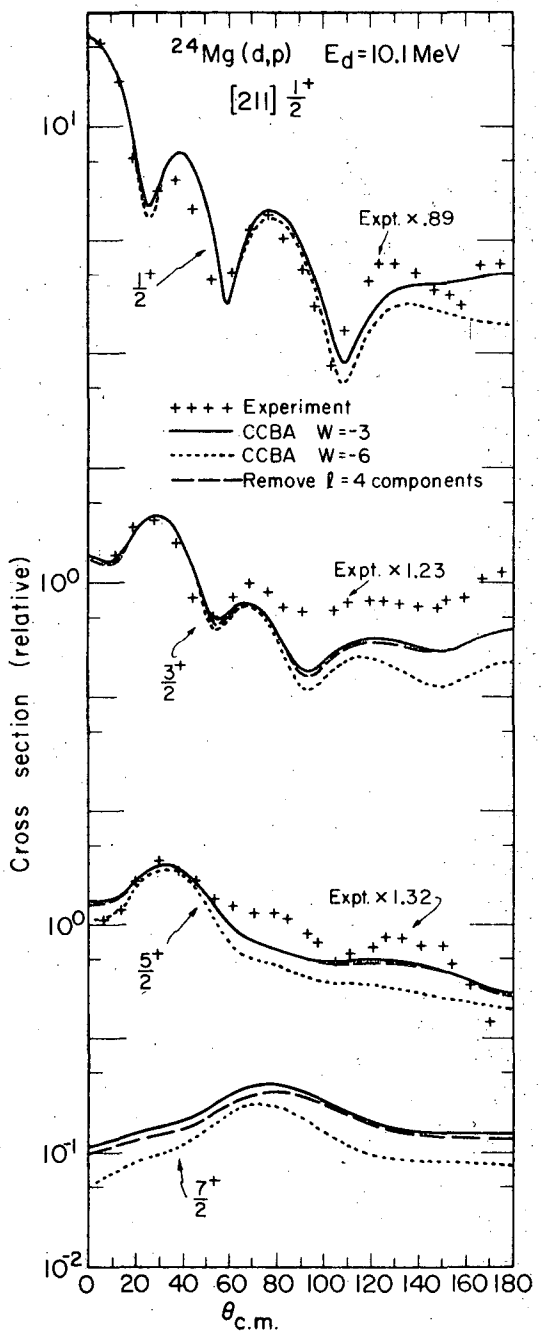

XBL701-2237

Fig. VIII.10

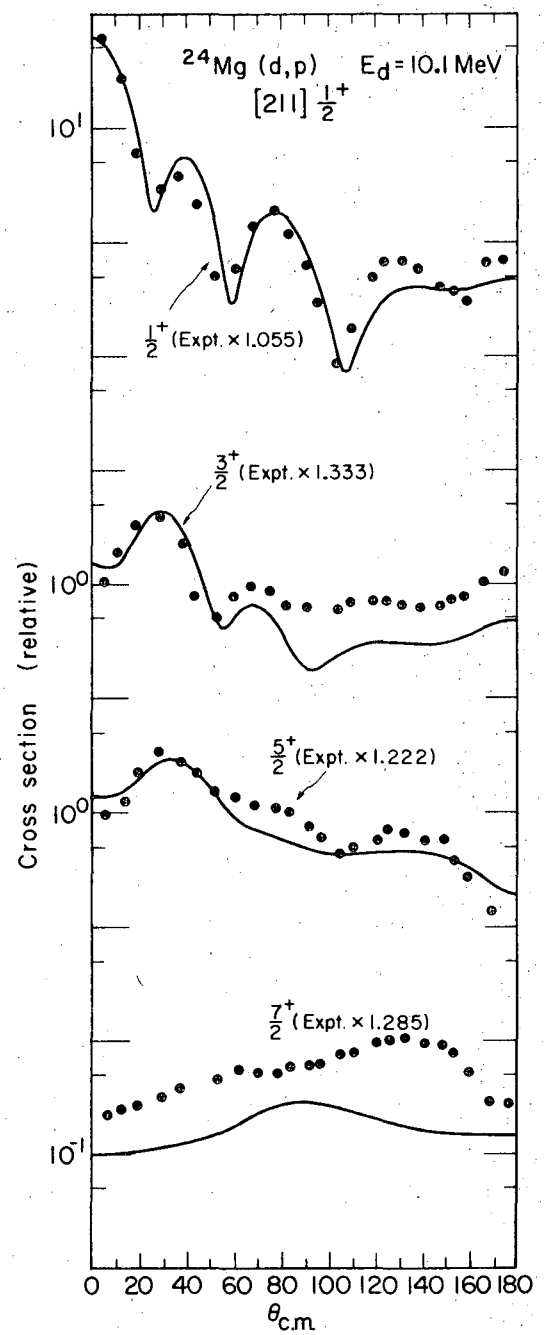

XBL701-2236

Fig. VIII.11

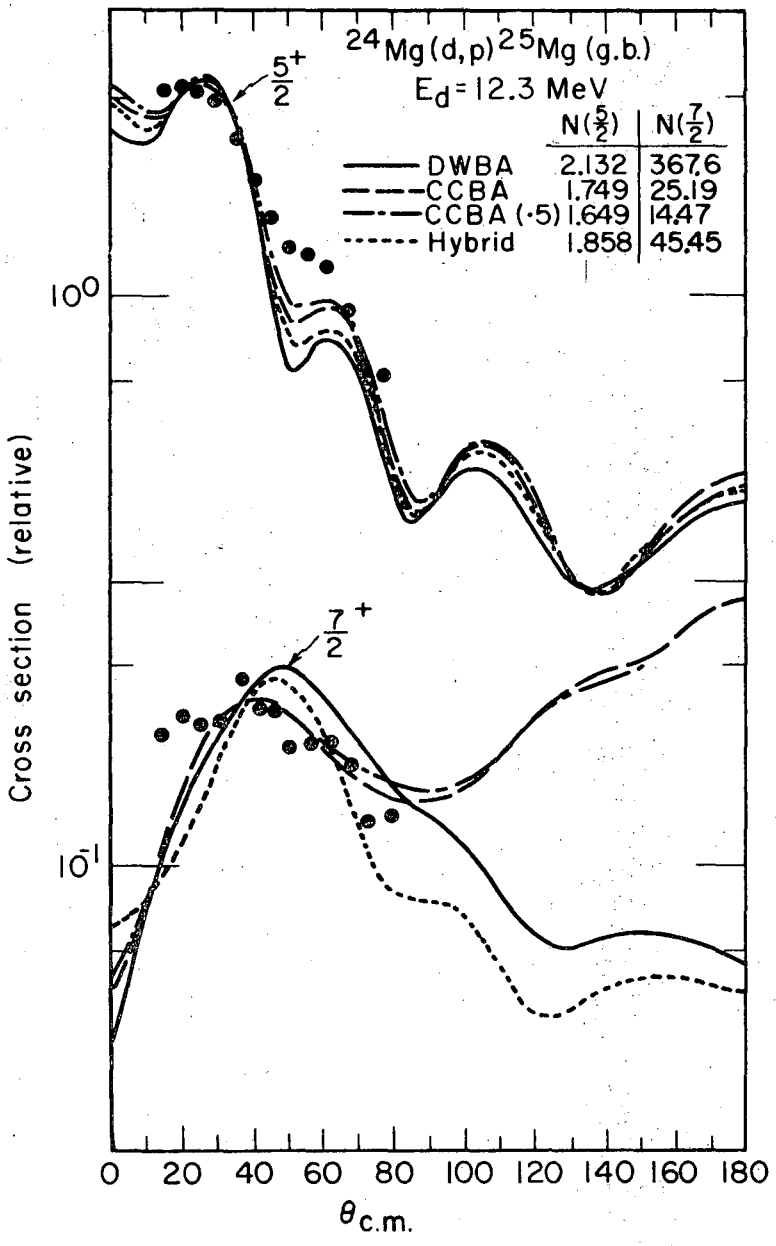
^{24}Mg(d,p)^{25}Mg (g.b.)
E_d = 12.3 MeV
$\frac{5}{2}^+$
$\frac{7}{2}^+$
N($\frac{5}{2}$) | N($\frac{7}{2}$)
DWBA 2.132 | 367.6
CCBA 1.749 | 25.19
CCBA (·5) 1.649 | 14.47
Hybrid 1.858 | 45.45
10^0
10^{-1}
Cross section (relative)
0 20 40 60 80 100 120 140 160 180
$\theta_{c.m.}$
XBL701-2225

Fig. VIII.12

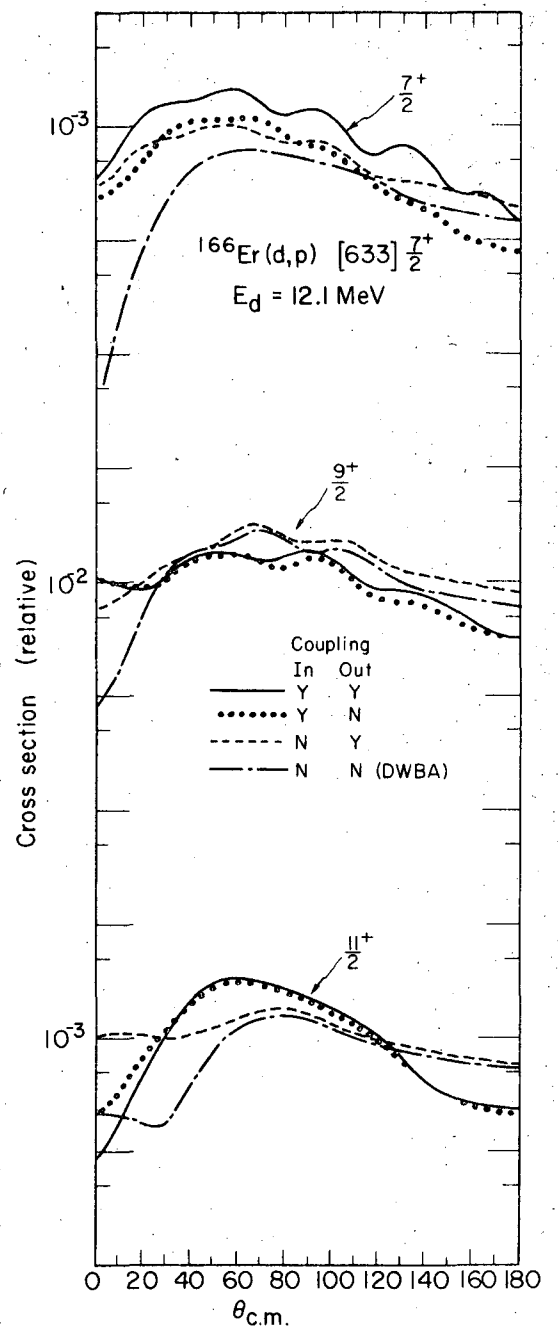
$\frac{7^+}{2}$
10^{-3}
^{166}Er(d,p) [633] $\frac{7^+}{2}$
E_d = 12.1 MeV
$\frac{9^+}{2}$
10^{-2}
Coupling
In Out
Y Y
Y N
N Y
N N (DWBA)
$\frac{11^+}{2}$
10^{-3}
Cross section (relative)
0 20 40 60 80 100 120 140 160 180
$\theta_{c.m.}$
XBL701-2226

Fig. VIII.13

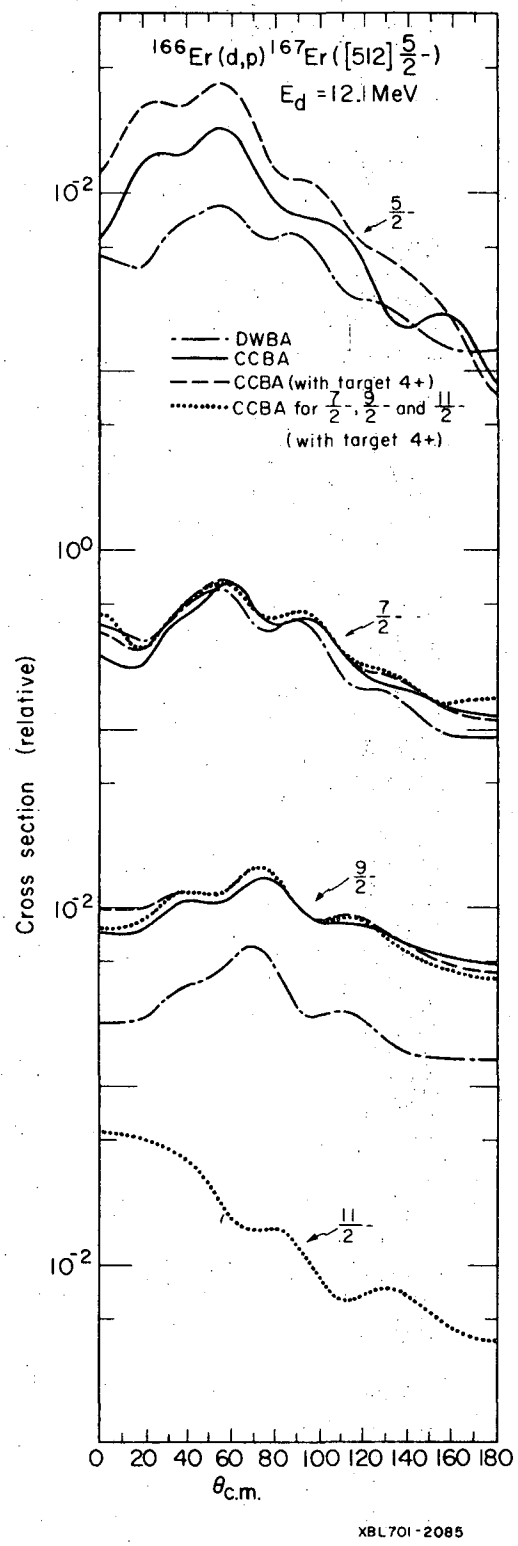
^{166}Er(d,p)^{167}Er([512]$\frac{5}{2}$-)
E_d = 12.1 MeV
10^{-2}
$\frac{5}{2}^-$
DWBA
CCBA
CCBA (with target 4+)
CCBA for $\frac{7}{2}^-$, $\frac{9}{2}^-$ and $\frac{11}{2}^-$ (with target 4+)
10^{0}
$\frac{7}{2}^-$
Cross section (relative)
10^{-2}
$\frac{9}{2}^-$
$\frac{11}{2}^-$
10^{-2}
0 20 40 60 80 100 120 140 160 180
$\theta_{c.m.}$
XBL701-2085

Fig. VIII.14

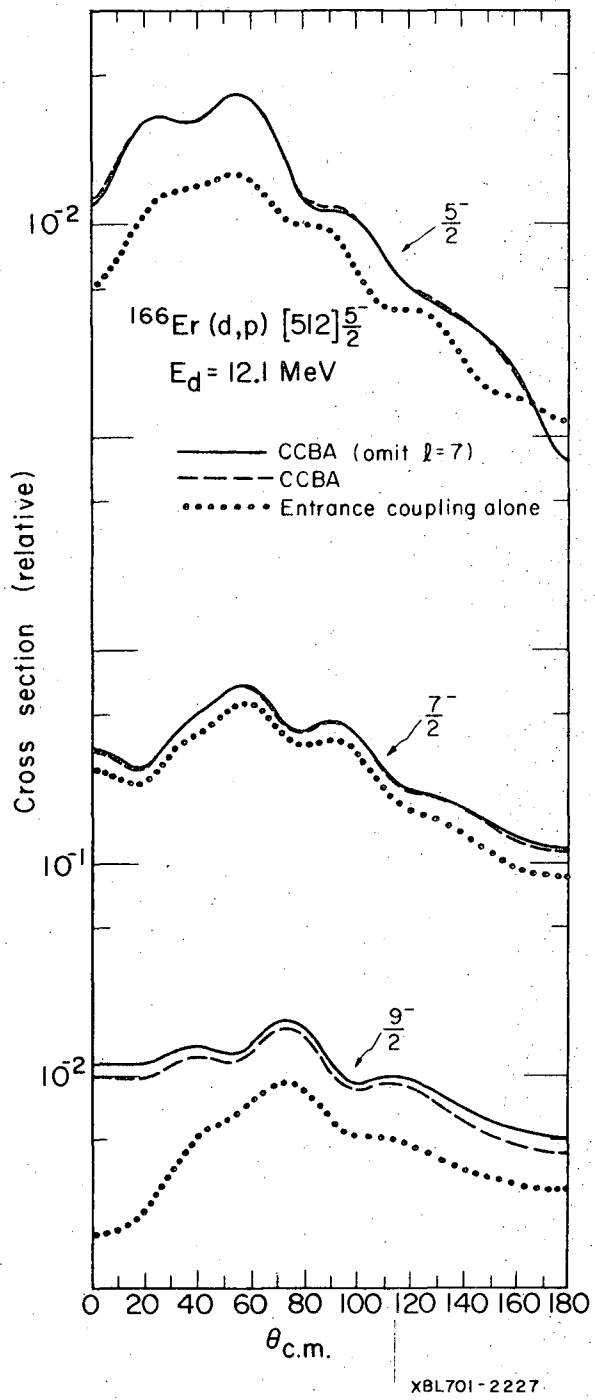
^{166}Er (d,p) [512]$\frac{5^-}{2}$
E_d = 12.1 MeV
CCBA (omit ℓ=7)
CCBA
Entrance coupling alone
$\frac{5^-}{2}$
$\frac{7^-}{2}$
$\frac{9^-}{2}$
10^{-2}
10^{-1}
10^{-2}
Cross section (relative)
0 20 40 60 80 100 120 140 160 180
$\theta_{c.m.}$
XBL701-2227

Fig. VIII.15

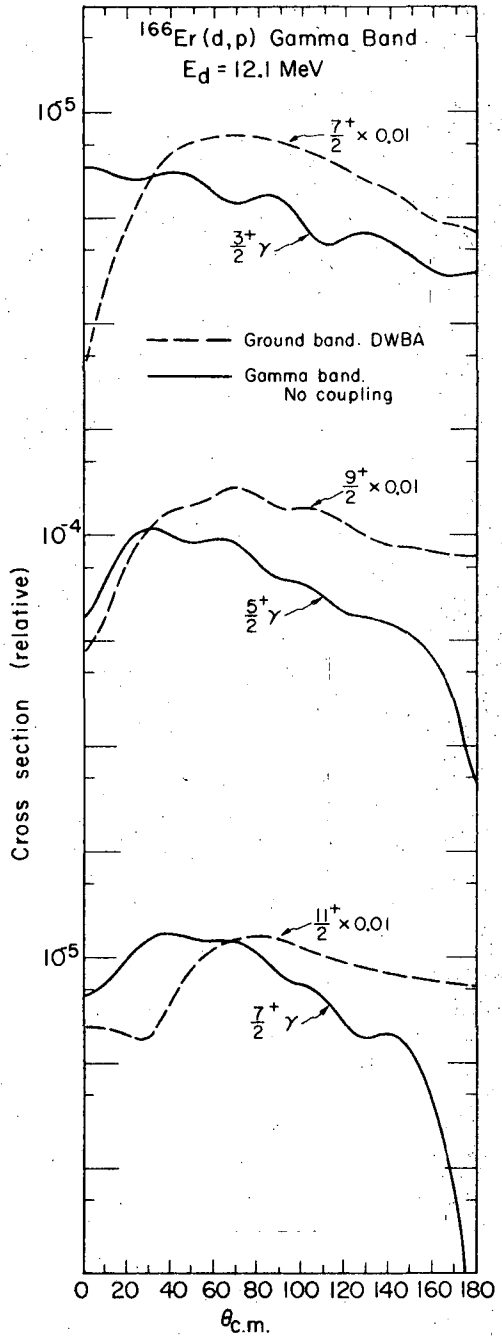
166Er(d,p) Gamma Band
Ed = 12.1 MeV
7+/2 × 0.01
3+/2 γ
Ground band. DWBA
Gamma band. No coupling
9+/2 × 0.01
5+/2 γ
11+/2 × 0.01
7+/2 γ
10-5
10-4
10-5
Cross section (relative)
0 20 40 60 80 100 120 140 160 180
θc.m.
XBL 701-2228

Fig. VIII.16

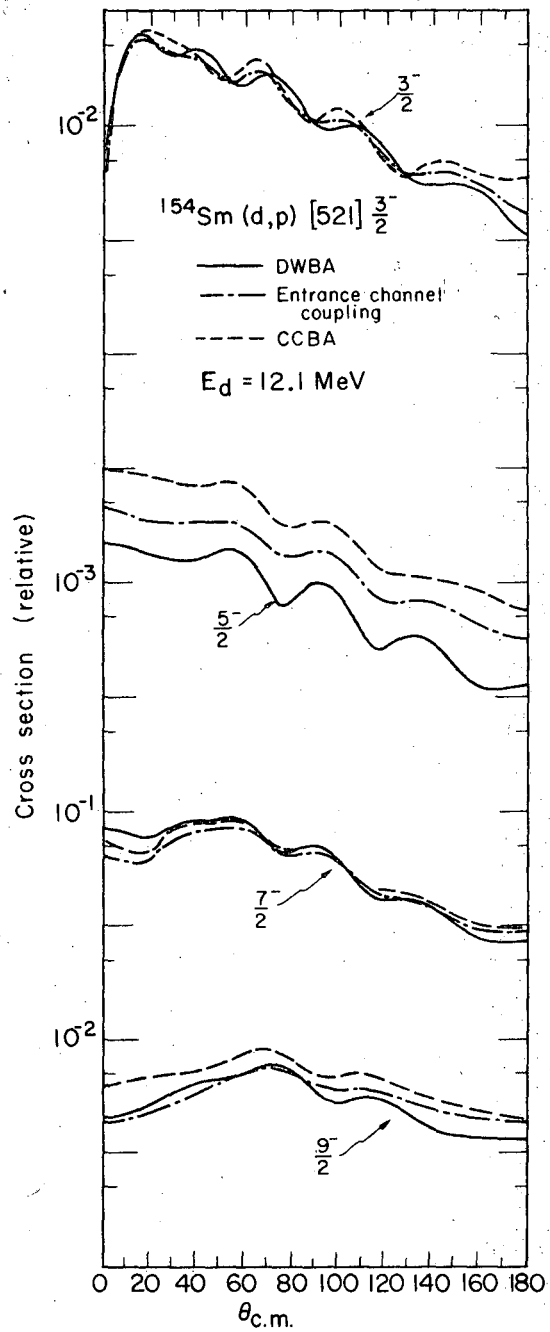

XBL701-2229

Fig. VIII.17

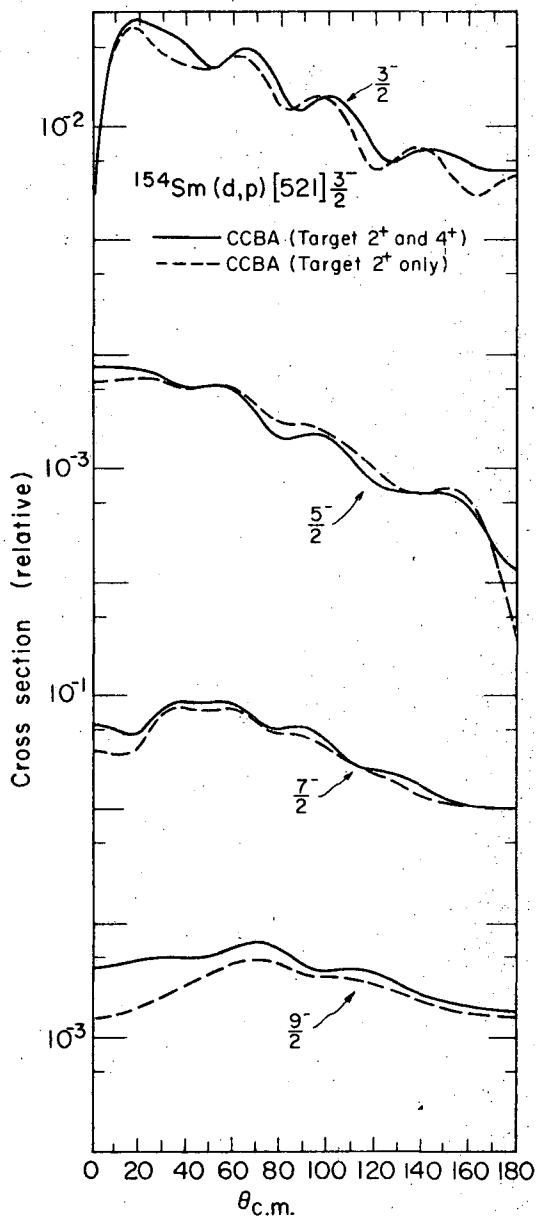

XBL701-2230

Fig. VIII.18

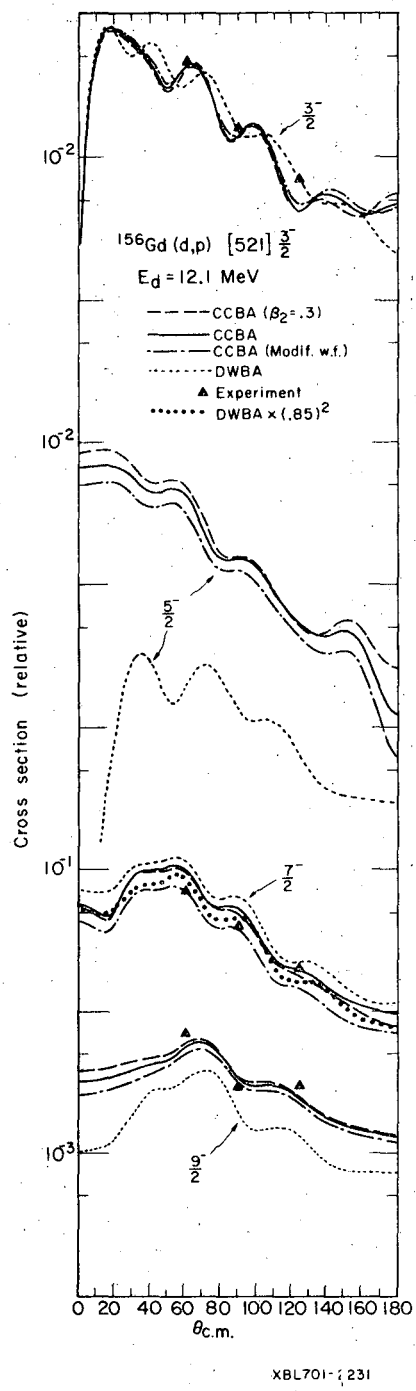
^{156}Gd (d,p) [521] 3/2⁻
E$_d$ = 12.1 MeV
CCBA (β$_2$=.3)
CCBA
CCBA (Modif. w.f.)
DWBA
Experiment
DWBA x (.85)^2
3/2⁻
5/2⁻
7/2⁻
9/2⁻
10^{-2}
10^{-2}
10^{-1}
10^{-3}
Cross section (relative)
0 20 40 60 80 100 120 140 160 180
θc.m.
XBL701-231

Fig. VIII.19

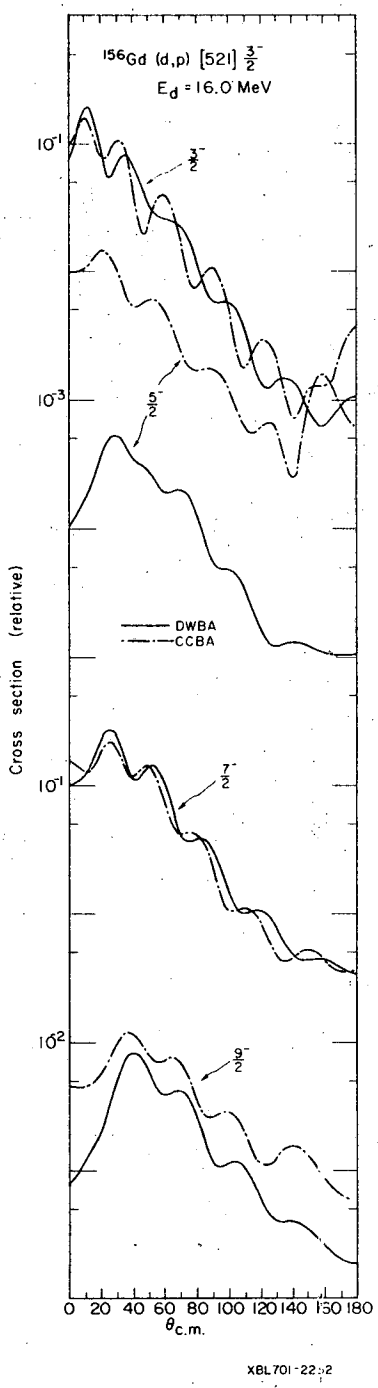
^{156}Gd (d,p) [521] $\frac{3}{2}^-$
E_d = 16.0 MeV
10^{-1}
10^{-3}
10^{-1}
10^{2}
$\frac{3}{2}^-$
$\frac{5}{2}^-$
$\frac{7}{2}^-$
$\frac{9}{2}^-$
DWBA
CCBA
Cross section (relative)
0 20 40 60 80 100 120 140 150 180
$\theta_{c.m.}$
XBL701-2252

Fig. VIII.20

IX. SUMMARY AND CONCLUSION

A. Summary

The customary theoretical analyses of stripping reactions ignore the possibility that the incoming deuteron and outgoing proton can excite the target or residual nucleus, although, if the nucleus is strongly deformed, the probability that a projectile (at typical stripping energies) will excite rotational transitions is quite large. There is now a large literature in which the conventional analysis of stripping reactions on deformed nuclei[1] has been employed to identify Nilsson states and measure the probabilities of j components within these states. In this work we have studied in detail, for magnesium and selected nuclei of A=155-167, the role that inelastic processes (specifically rotational excitations) play in stripping reactions, the extent to which they invalidate the customary analyses and the possibility that more refined spectroscopic information can be obtained if their effect is included in the calculations.

We have used the source term[4] approach which we have shown is equivalent to the natural generalization of DWBA that had previously been written down by Penny and Satchler.[3] We derive thislatter in a manner that exhibits the approximations that remain. We have discussed in some detail the calculation of the neutron bound state wavefunction and stress the sensitivity

of the results to the correctness of this procedure. In the course of determining suitable optical potentials, we fitted certain inelastic deuteron scattering data for samarium and erbium, getting slightly different deformation parameters from those appropriate to (α,α') experiments.[43]

B. Conclusions

At the end of Chapter II we listed possible consequences for stripping calculations on deformed nuclei of including inelastic processes. We shall now discuss these in the same order.

1. We have seen that it is no longer possible to factorize the angular distributions of various levels of arbitrary bands in the form $\sigma(\theta) \propto C_{j\ell}^2\, \sigma_\ell(\theta)$. There is a strong tendency for weak states of a band to be enhanced: the cross section of the strong levels in a band may be enhanced or reduced, and in principle this is important where the quasiparticle occupation factors, U^2, of several bands are to be compared, for example, or an absolute cross section calculation attempted. However, it is probable that even with stripping transitions through the target 2+ state included (or other inelastic processes) that a very strong state, I, will be fed mostly through the component j=I. In this case, there is approximate proportionality to c^2 in the restricted sense that over a limited range of c^2 the cross section of this particular state I will be roughly proportionate to c_I^2. This is not true for weaker levels, and the proportionality constant is different for

each state.

2. Certain distinctive features of the angular distributions in light ($A \sim 25$) nuclei can be explained, in particular the "j-dependence" of the $l=2$ levels in Mg. However other details such as the precise shape of the stripping peak or the large back angle cross section were not explained. This latter may be improved by decreasing W(deut) but this appears to be a fundamentally unmotivated artifice (but see the end of Chapter II, section C). The inelastic processes considered do not account for the difference between "stripping" and "scattering" optical potentials.

3. The angular distributions were often considerably altered, to the extent that a diffraction pattern might appear where none had been, or maxima and minima would interchange. The overall shape of the medium strength 5/2- level in erbium was changed to the point where it had more the appearance of an $l=1$ than of an $l=3$ transfer. For such levels more than four experimental points are necessary to set the scale or define the l-transfer unambiguously, unless, that is, a calculation including inelastic processes (and, where needed, coriolis mixing) had been performed. Even so, there are as yet no experimental grounds to assure us that our calculation is adequate for this. Unfortunately, we do not know precisely how an alternate deuteron optical potential (we say deuteron because of the particularly serious ambiguities that arise)

could affect the positions of the sometimes quite marked diffraction minima.

We have mentioned above how j-dependence comes out of the calculations for Mg. Little is known experimentally about this for the heavier deformed nuclei. In any case, for the heavier nuclei, we did not include a deuteron spin-orbit potential.

4. Our discussion in Chapter VII makes the finding of ref.[28] plausible, but we have not demonstrated it explicitly.

5. The speculations[30] concerning the probable effect of inelastic processes on the angular distributions have been shown to be untrue in general, except perhaps for the dominant member of a band.

General Comments

In our deformed rare earth calculations, we were not usually able to get perfect agreement with the experimental results. There was always a considerable improvement, however, and we were generally able to give plausible arguments about the discrepancies in terms of coriolis mixing (5/2- band in ^{167}Er) or perhaps an incorrect radial wavefunction (7/2+ band in ^{167}Er). The cross section is extremely sensitive to this latter, and our (in principle, readily remediable) lack of knowledge of the effect of pairing on the observed quasiparticle energy made the asymptotic form uncertain. In one case (^{157}Gd) we achieved good agreement with the data (except at back angles)

provided one j-component was scaled somewhat.

We have shown that inelastic processes are potentially, at least, as important as coriolis mixing, and suggest that these together might explain the very bad agreement with theory for the [512]5/2- band in ^{167}Er. In addition, we have used this theory to make it plausible that a previously unassigned level in the spectrum of ^{167}Er is the 11/2- level of [512]5/2- in spite of its strength. This suggests how our program might be used to deduce spectroscopic information. In the s-d shell too we have strengthened the claim[80] that ^{24}Mg is prolate and axially symmetric. Further, we have been led to speculate that the core in ^{25}Mg has a somewhat different structure to ^{24}Mg, although for reasons stated this is less certain. Our calculations did not seem to consistently underestimate or overestimate the importance of inelastic processes.

We claim that a "good" DWBA angular distribution should not necessarily lead to confidence in the theory; we have in mind the vibrational case[27] discussed in Chapter II. Angular distributions depend primarily on the l-transfer, and in some cases, the inelastic processes largely involve the same l, so that the overall cross section is scaled somewhat without much changing the angular distribution. This phenomenon occurs most markedly for a level in a rotational band that has most of the direct stripping strength.

Finally, we believe that we have demonstrated the utility

of the source term procedure[4] for the inclusion of inelastic processes in stripping reactions. We are still faced with a very big computing job (one calculation in the rare earth region can easily take an hour, filling the CDC6600) and it is not always possible to repeat calculations performed with too hastily chosen parameters.

Extensions of the present work are (a) a less modelistic study of energy dependence (see, "Experiments" below), (b) the inclusion of coriolis mixing, (c) a better treatment of the proton scattering problem: a program to study the inelastic scattering of protons for odd nuclei with spin-orbit interactions included should be written. Related to this is (d) the inclusion of transitions between bands. In the magnesium region in particular, the enhancement of collective transitions over single particle transitions is perhaps, ten. This corresponds to amplitude enhancement of about three, potentially a source of error where the effects of single particle transitions can act coherently.

We also recognize the desirability of printing out and examining some of the wavefunctions involved, especially perhaps the deuteron wavefunctions in the case where the l=3 transfer angular distribution was altered to look like an l=1 transfer reaction. It was postulated that the deuteron wavefunction component corresponding to excited target states was concentrated at the nuclear surface. It is to be understood that giving a

complete account of this might prove to be a substantial project, owing to the large number of degrees of freedom involved.

Experiments Needed

Most obviously, we have no assurance that our predicted angular distributions, which differ in many instances from DWBA results, are, in fact, good. Perhaps instead of 150 states at four angles, someone will measure 15 states at 40 angles? Preferably in a nucleus where the coriolis mixing is thought to be small, at least for one band, and specifically not tungsten.[28] An effort would be made to measure weak levels. The ground band of ^{157}Gd might be a good candidate. The measurements would be carried out for a series of energies, at each of which (d,d) and (d,d'(2^+,4^+)) angular distributions would be taken. If possible, (p,p') measurements would be taken at each corresponding energy. It would be interesting to carry out this program in an energy range straddling the coulomb barrier. A similar program is needed for A~25. Here, however, the seeming greater importance of the spin-orbit interactions makes desirable a full set of polarization measurements .

We have scarcely mentioned the deformed actinides. Unfortunately, the simultaneous increase in integration radius and number of partial waves make calculations with our program (in which the spins of the projectiles are treated correctly) prohibitive.

ACKNOWLEDGMENTS

This work would not have been possible without the contributions of many people. In particular, I am grateful to:

Dr. Norman Glendenning who suggested the project, who supplied the coupled channel programs from which the programs used herein evolved, and whose advice and criticism contributed much to this research project and to my education as a physicist.

Dr. Robert Ascuitto, who had a recent memory of studenthood, for friendship, encouragement in dark days, and for imparting information about nuclear reactions.

Dr. Bent Sørensen for kindness to me and for much insight into nuclear structure.

Dr. Martin Redlich, whose personal style of physics offers much as an example to students, for many enlightening discussions.

Dr. Gordon Struble, for many discussions on a variety of subjects.

Professor R. Sheline, for sending programs to us and for discussing experiments.

Professor K. Hosono, for kindly sending detailed experimental data.

Dr. D. Hendrie, for the use of programs and discussions.

Fellow graduate students Oliver Johns, Chin-Wa Ma and

Alan Goodman, for many useful discussions

Mr. Noel Brown, for help with programs.

My wife, Marjorie, for everything (and a heroic typing job).

This work was performed under the auspices of the U.S. Atomic Energy Commission.

REFERENCES

1. For a recent review article, see B. Elbek and P.O. Tjøm, Advances in Nuclear Physics, III, ed. Baranger and Vogt (Plenum Press, New York, 1969).
2. G.R. Satchler, Annals of Physics 3, 275 (1958).
3. S.K. Penny and G.R. Satchler, Nucl. Phys. 53, 145 (1964); P.J. Iano and N. Austern, Phys. Rev. 151, 53 (1966); P.D. Kunz, E. Rost and R.R. Johnson, Phys Rev. 177, 1737 (1969); P.J. Iano, S.K. Penny and R.M. Drisko, Nucl. Phys. A127, 47 (1969).
4. R.J. Ascuitto and N.K. Glendenning, Phys. Rev. 181, 1396 (1969).
5. N.K. Glendenning, in Ann. Rev. Nucl. Sci. 13, 1963.
6. G.R. Satchler, in Lectures in Theoretical Physics, Boulder, 1965, Vol. VIIIc.
7. N. Austern, R.M. Drisko, E.C. Halbert and G.R. Satchler, Phys. Rev. 133B, 3 (1964).
8. A. Bohr and B.R. Mottelson, monograph Nuclear Structure (W.A. Benjamin, New York, 1969).
9. A.R. Edmonds, Angular Momentum in Quantum Mechanics (Princeton University Press, Princeton, 1957).
10. N. Austern, R.M. Drisko, E.C. Halbert and G.R. Satchler, Phys. Rev. 133, B3 (1964).

11. J.K. Dickens, R.M. Drisko, F.G. Perey, G.R. Satchler, Phys. Lett. 15, 337 (1965).

12. F.G. Perey and D.S. Saxon, Phys. Lett. 10, 107 (1964).

13. W.R. Smith, Nucl. Phys. A94, 550 (1967).

14. P.J.A. Buttle and L.J.B. Goldfarb, Proc. Roy. Soc. 83, 701 (1964).

15. N. Austern, Phys. Rev. 137, B572 (1965).

16. L.L. Lee, J.P. Schiffer, B. Zeidman, G.R. Satchler, R.M. Drisko and R.H. Bassel, Phys. Rev. 136, B971 (1964).

17. R.C. Johnson, Nucl. Phys. A90, 289 (1967).

18. R.C. Johnson and F.D. Santos, Phys. Rev. Lett. 19, 364 (1967).

19. L.S. Rodberg, Nucl. Phys. 47, 1 (1963).

20. G.L. Strobel, thesis UCLA (1965).

21. J.P. Schiffer, G.C. Morrison, R.H. Siemssen, B. Zeidman, Phys. Rev. 164, 1274 (1967).

22. J.L. Alty, L.L. Green, R. Huby, G.D. Jones. J.R. Mires and J.F. Sharpey-Schafer, Nucl. Phys. A97, 541 (1967).

23. C.A. Pearson and M. Coz, Nucl. Phys. 82, 533 (1966); Later papers are referred to in C.A. Pearson and J.C. Wilcott, Phys. Rev. 181, 1477 (1969) where the reaction $^{12}C(d,p)$ is analysed.

24. G.H. Rawitcher, Phys. Rev. 163, 1223 (1967); G.H. Rawitcher and S.N. Mukherjee, Phys. Rev. 181, 1518 (1969).

25. W.R. Smith and E.V. Ivash, Phys. Rev. 131, 304 (1963).

26. K. Hosono, J. Phys. Soc. Japan, 25, 26 (1968).

27. P.J. Bjorkholm, W. Haeberli and B. Mayer, Phys. Rev. Lett. 22, 955 (1969).

28. R.H. Siemssen and J.R. Erskine, Phys. Rev. Lett. 19, 90 (1967), also Phys. Rev. 146, 911 (1966).

29. R.S. Mackintosh, Phys. Lett. 29B, 629 (1969). The uncharacteristically forward peaked second 4+ state must have considerable direct excitation.

30. D.G. Burke and P. Alford, private communication quoted in ref.[1]

31. M.L. Goldberger and K.M. Watson, Collision Theory (John Wiley and Sons, Inc., New York, 1964).

32. K.R. Greider and L.R. Dodd, Phys. Rev. 146, 675 (1966).

33. E. Brezin, Theory of Three-Particle Systems. Service de Physique Theorique CEN, Saclay (1967).

34. H. Feshbach, (a) Ann. of Phys. (NY) 5, 537 (1958); (b) Ann. of Phys. (NY) 19, 287 (1962).

35. N.K. Glendenning, UCRL-17503 and Proc. Int. Sch. of Phys. "Enrico Fermi" Course XL, ed. M. Jean (Academic Press, New York, 1969).

36. L.R. Dodd and K.R. Greider, Phys. Rev. 146, 675 (1966).

37. T.H. Rihan, Phys. Rev. 164, 1247 (1967).

38. G. Ripka, in Advances in Nuclear Physics, Vol. I, ed. M. Baranger and E. Vogt (Plenum Press, New York, 1968).

50. L. Rosen, J.G. Beary, A.S. Goldhaber and E.H. Auerbach, Annals of Physics (NY) 34, 96 (1965).

51. P.O. Tjøm and B. Elbek, Dan. Mat-fys. Medd. 36,8 (1967).

52. A. de-Shalit and I. Talmi, Nuclear Shell Theory (Academic Press, New York, 1963).

53. K. Kumar and M. Baranger, Nucl. Phys. A112, 273 (1968) and earlier references cited therein.

54. N.K. Glendenning and R.S. Mackintosh, Phys. Lett. 29B, 626 (1969).

55. C.A. Heras, S.M. Abecasis and H.E. Bosch, USAEC report NP-17506 (1968); see also, P.O. Lipas and J.P. Davidson, Nucl. Phys. 26, 80 (1961).

56. G.M. Crawley and G.T. Garvey, Phys. Rev. 167, 1070 (1968).

57. M.A. Preston, Physics of the Nucleus (Addison Wesley, Reading, Massachussets, 1962).

58. J. Sawicki, Nucl. Phys. 6, 575 (1958).

59. P.E. Hodgson, The Optical Model of Elastic Scattering (Oxford University Press, Oxford, 1963).

60. G.W. Greenlees, G.J. Pyle and Y.C. Tang, Phys. Rev. 171, 1115 (1968).

61. N.K. Glendenning, D.L. Hendrie and O.N. Jarvis, Phys. Lett. 26B, 131 (1968).

39. (a) S.G. Nilsson, in Lectures in Theoretical Physics, Vol. VIIIc, ed. P.D. Kunz et al (University of Colorado Press, Boulder, 1966).
(b) O. Nathan and S.G. Nilsson, in Alpha-Beta-Gamma-Ray Spectroscopy, ed. K. Siegbahn (North-Holland Publishing Co., Amsterdam, 1965).

40. R.A. Harlan and R.K. Sheline, Phys. Rev. 168, 1373 (1968).

41. S.G. Nilsson, Mat. Fys. Medd. Dan. Vid. Selsk. 29, no. 16 (1955).

42. A. Faessler and R.K. Sheline, Phys. Rev. 148, 1003 (1966).

43. D.L. Hendrie, N.K. Glendenning, B.G. Harvey, O.N. Jarvis, H.H. Duhm, J. Saudinos and J. Mahoney, Phys. Lett. 26B, 127 (1968).

44. R. deSwiniarski, C. Glasshauser, D.L. Hendrie, J. Sherman, A.D. Bacher and E.A. McClatchie, Phys. Rev. Lett. 23, 317 (1969).

45. J. Blomquist and S. Wahlborn, Arkiv for Fysik, 16, 545 (1960).

46. M.N. Vergnes and R.K. Sheline, Phys. Rev. 132, 1736 (1963).

47. A.L. Goodman, G.L. Struble and A. Goswami, Phys. Lett. 26B, 260 (1968); G.L. Struble, private communication.

48. We are indebted to Prof. Struble for private communications concerning this matter.

49. R.A. Kenefick and R.K. Sheline, Phys. Rev. 139, B1479 (1965).

62. P.E. Hodgson, Advances in Physics, 15, 329 (1966).

63. S. Mukherjee, Nucl. Phys. A118, 423 (1968).

64. J. Testoni and L.C. Gomes, Nucl. Phys. 89, 288 (1966).

65. N.K. Glendenning, private communication.

66. H. Sherif and J.S. Blair, Phys. Lett. 26B, 489 (1968).

67. H. Sherif and R. deSwiniarski, Phys. Lett. 28B, 96 (1968).

68. B. Cujec, Phys. Rev. 136, B1305 (1964).

69. T. Tamura, Rev. Mod. Phys. 37, 679 (1965).

70. C. Glasshauser, private communication.

71. G.M. Crawley and G.T. Garvey, Phys. Rev. 160, 981 (1967).

71a. Program MERCY adapted from SEEK by M.A. Melkanoff, J. Raynal, T. Sawada, UCLA report #66 - 10, Jan. 1966. We are grateful to D. Hendrie for allowing us to use this program.

72. P. Stoler, M. Slagowitz, W. Makofske and T. Kruse, Phys. Rev. 155, 1334 (1967).

73. P.H. Stelson and L. Grodzins, Nuclear Data 1A, 21 (1965).

74. R.J. Ascuitto and N. Brown, private communication.

75. J.K. Dickens and F.G. Perey, Phys. Rev. 138, B1080 and B1083 (1965); see also ref. 62

76. B. Buck and P.E. Hodgson, Nucl. Phys. 29, 496 (1962).

77. C. Mayer-Böricke, R. Santo and U. Schmidt-Rohr, Nucl. Phys. 33, 36(1962).

78. C. Mayer-Böricke and R. H. Siemssen, Z. fur Naturforsch. 21A, 958 (1966).

79. P.O. Tjøm and B. Elbek, Nucl. Phys. A107, 385 (1968).

80. E. Veje, B. Elbek, B. Herskind and M.C. Olesen, Nucl. Phys. A109, 489 (1968).

81. S. Watanabe, Nucl. Phys. 8, 484 (1958).

82. J.R. Rook, Nucl. Phys. 61, 219 (1965).

83. R. Middleton and S. Hinds, Nucl. Phys. 34, 404 (1962).

84. G.J. McCallum and B.D. Sowerby, Phys. Lett. 25B, 109 (1967).

85. B.R. Mottelson and S.G. Nilsson, Mat, Fys. Skr. Dan. Vid. Selsk. 1, no.8 (1959).

86. J.C. Parikh, Phys. Lett. 26B, 607 (1968).

87. B.E. Chi and A.E. Anderson, Phys. Rev. 185, 1594 (1969).

88. I. Kanestrøm and P.O. Tjøm, Nucl. Phys. A138, 177 (1969).

89. W.R. Smith, Nucl. Phys. A130, 657 (1969).

90. A.E. Litherland, H. McManus, E.B. Paul, D.A. Bromley and H.E. Gove, Canadian Journal of Physics 36, 378 (1958).

APOLOGY TO THE READER

To be perfectly intelligible,
one must be inaccurate;
to be perfectly accurate,
one has to be unintelligible.

Bertrand Russell

LEGAL NOTICE

TECHNICAL INFORMATION DIVISION
LAWRENCE RADIATION LABORATORY
UNIVERSITY OF CALIFORNIA
BERKELEY, CALIFORNIA 94720